To the Graduate Council:

I am submitting herewith a thesis written by John G. Bultman entitled “Structure, Stratigraphy, and Tectonics preserved of the Northwestern Bays Mountain Synclinorium, Greene and Hawkins Counties, Northeast Tennessee.” I have examined the final electronic copy of this thesis for form and content and recommend that it be accepted in partial fulfillment of the requirements for the degree of Master of Science, with a major in Geology.

Robert D. Hatcher, Jr. _____
Major Professor

We have read this thesis and
recommend its acceptance:

Don W. Byerly

Linda C. Kah

Peter J. Lemiszki

Accepted for the Council:

Anne Mahew_____
Vice Chancellor and
Dean of Graduate Studies

(Original signatures are on file with official student records.)

Structure, Stratigraphy, and Tectonics preserved of the Northwestern Bays Mountain Synclinorium, Greene and Hawkins Counties, Northeast Tennessee

A Thesis

Presented for the

Master of Science Degree

The University of Tennessee, Knoxville

John G. Bultman

December 2005

There are no great things, only small things with great love. Happy are those.
- Mother Theresa

Shall I refuse my dinner because I do not fully understand the process of digestion?
- Oliver Heaviside (1850-1925) English physicist

When we try to pick out anything by itself, we find it is tied to everything else in the universe.
- John Muir (1838-1914) U. S. naturalist, explorer

We learn geology the morning after the earthquake.
- Ralph Waldo Emerson

But the mountain falls and crumbles away, and the rock is removed from its place; the waters wear away the stones; the torrents wash away the soil of the earth; so you destroy the hope of mortals.
- Job 14: 18-19

ACKNOWLEDGMENTS

I am very grateful to Dr. Robert Hatcher, Jr., for his advice, support, and constant pursuit of good field-based science. I would also like to thank: Dr. Peter J. Lemiszki for his friendly advice and help in the field; Dr. Linda C. Kah for her support and striving to ask not only good questions, but also the right ones, Dr. Don W. Byerly for all his geologic mapping during the summers of 1963 and 1964 and for his help with this project; and lastly I would like to thank all the teachers who pushed me in a constructive way without deriding my efforts and questions. I would also like to thank the other Hatchery students who have given me help throughout my graduate studies at the University of Tennessee.

I would like to thank: Dr. Stan Finney, UCLB, for his identification of graptolites in the Sevier Shale, Dr. John Repetszki, USGS, for his identification of conodonts, and Dr. Robert Neuman for identification of fossils in the upper Sevier Shale. I am most grateful to my family for their love, support, and friendship.

This work was supported by a grant from the U. S. Department of Energy National Energy Technology Laboratory grant DOE DE-FC26-02NT15341.

ABSTRACT

The Bays Mountain synclinorium and surrounding area provide critical facies data to address Sevier-Bountian basin development. This area preserves the Middle Ordovician post-Knox unconformity, the Sevier-Blountian basin depositional sequence, overlying Bays Formation quartz arenite-redbed sequence, the Bays/Martinsburg unconformity, and the base of the overlying Caradocian Martinsburg clastic wedge. Detailed geologic mapping in the Northwestern half of the Sevier-Blountian basin has divided the Sevier Shale into three members: a lower thin-bedded, dark gray-black, graptolite-bearing shale overlain by dark gray-black micritic limestone; a middle silty-sandy limestone interbedded with light gray silty shale and calcareous sandstone; and an upper thick-bedded light gray shale grading upward into massive fossil-bearing sandy limestone. Detailed geologic mapping has also delineated previously unrecognized small and large displacement faults in part of the Bays Mountain synclinorium.

Total thickness of the Sevier Shale increases from 1006 m (3,300 ft) in the northernmost part of the study area, where entire unit thickness is measurable, to an estimated 1830 to 1981 m (6,000 to 6,500 ft) in the southern part (5,000 ft preserved and 1,500 ft estimated removed). These thickness changes are important not only for basin analysis but also should be considered when constructing geologic cross sections elsewhere in the Valley and Ridge.

Graptolites collected from the lower Sevier Shale lie in the *Nemagraptus gracilis* zone. This is slightly older than the Athens Shale. The Sevier Shale and lower portion of the Bays Formation have been given an age estimate of 461-454Ma (Llanvirnian-LLandeilian) based on the age of the conodont and graptolite zones, and the age of the Milbrig bentonite that occurs in the upper Bays Formation. The Bays/Martinsburg contact in this area likely represents an unconformity of ~ 9 m.y. duration and marks the transition from the Sevier-Blountian to Martinsburg basin deposition in the study area.

The study area is part of the Saltville-Carter Valley thrust sheet and is overlain by the Pulaski thrust sheet to the southeast. Detailed geologic mapping has delineated previously unrecognized faults in part of the Bays Mountain synclinorium. The Sevier Shale exhibits disharmonic folding between the stronger structural lithic units of the Knox Group and Bays Formation. Evidence for the recognized faults in the Sevier Shale included: noted deformation zones (small faults, dismembered slickensided calcite veins, slickensides, abundant cleavage), stratigraphic discontinuities, and seismic reflection profiles. The stratigraphic discontinuity and deformation zone noted between the lower Jonesboro Limestone and Sevier Shale mark the Pulaski fault along the northwestern edge of the Babbs Knobs flap.

A new model for basin dynamics was constructed to better conceptualize basin deposition during the Taconic orogeny. The model depicts the transition from a remnant ocean basin to the Sevier-Blountian phase of the Taconic orogeny due to a tectonic load emplaced onto the Laurentian margin. The prograding overthrust belt, zone of subsidence, basin axes, and flexural foreland bulge migrated west toward the foreland.

Sediments evolved from shallow marine to intertidal environments and prograded over the shelf sequence of the former passive margin. The Sevier-Blountian phase represents the rapid erosion of the highly elevated fold-thrust belt west of the approaching arc. Isostatic uplift (Bays Formation) was initiated in the inner parts of the foreland basin. This was then followed by the “Taconic” (Martinsburg) pulse and basin formation.

TABLE OF CONTENTS

CHAPTER PAGE

I. **INTRODUCTION** 1

Location and Extent of Area Studied 1
Geomorphology 6
Previous Geologic Mapping Investigations 6
Present Investigation 13

II. **STRATIGRAPHY** 14

General Statement and History 14
Knox Group 17
The Chickamauga Group 19
Lenoir Limestone 20
Sevier Shale 22
Lower Sevier 22
Middle Sevier 26
Upper Sevier 29
The Whitesburg Limestone 34
The Bays Formation 34
Martinsburg Formation 42
Biostratigraphic Correlation 45
Quaternary Units 48

III. **STRUCTURE** 52

Regional Setting 52
Map-Scale Structural Features 54
Saltville and Associated Faults 54
Town Knobs and Carter Valley Fault 56
Bays Mountain Synclinorium 56
Pulaski Fault 63
Mesoscale Structural Features 68
Cross Sections 83

IV. **SEVIER BASIN TECTONICS** 88

Tectonic Background 88
Previous Models 91
Current Model 98

V. **CONCLUSIONS** 103

REFERENCES CITED 106

APPENDIX 118

VITA 163

LIST OF FIGURES

FIGURE PAGE

1-1. Distribution of Taconic basins in the Appalachians 2
1-2. Locations of the Bays Mountain synclinorium and quadrangles with respective mappers in the compiled study area 4
1-3. Location of study area showing important structural features and Ordovician outcrop 5
1-4. Structural features outlined in the study area and digital elevation model depicting how topography is related to the underlying structure 7
1-5. Simplified version of Arthur Keith's geologic map of the study area 9
1-6. Simplified version of Rodgers' geologic map of the study area 10
1-7. Compiled geologic map without structural data 12
2-1. Generalized stratigraphic column of units in the northwestern portion of the field area near the Holston River 15
2-2. Generalized stratigraphic column of units in the southeastern portion of the field area south of the Mosheim anticline and north of the Pulaski fault 16
2-3. Massive and ribboned Jonesboro Limestone along Baileyton Pike in the hanging wall of the Pulaski fault 18
2-4. Nodular Lenoir Limestone near Hwy 70 Burem quadrangle 21
2-5. Weathered "whaleback" exposure of Mosheim Member of the Lenoir Limestone along the Holston River 23
2-6. Dark gray-black shale of the lower Sevier Shale on Baileyton Pike 24
2-7. Bedding-parallel calcite veins in the lower Sevier Shale along Baileyton Pike across road and along strike from Figure 2-6 25
2-8. Middle member of the Sevier Shale along Raccoon Branch Road 27
2-9. Photomicrographs from the middle Sevier Shale 28
2-10. Upper member of the Sevier Shale 30
2-11. Fossils of the upper member of the Sevier Shale 31
2-12. Cross beds of the Bays Mountain synclinorium 33
2-13. Bays Formation along Hwy 70 depicting interbedded clean sandstones and red mudstone-siltstone-sandstones 36

2-14. Burrow trace fossils (Fucoids) representing the *Camarocladia* zone in the Bays Formation 37
2-15. Bays Formation quartz arenite thin section with gypsum plate 39
2-16. Sevier basin thickness estimates based on measured sections in the study area 40
2-17. Milbrig bentonite and cleaved sandstones in the Bays Formation, TN Hwy 70 41
2-18. Contact between Bays and Martinsburg Formations on Hwy 347 likely representing the Rocklandian unconformity 43
2-19. Martinsburg Formation along Hwy 347 44
2-20. Selected graptolite specimens submitted to Prof. Stanley Finney (CSLB) for identification from the lower member of the Sevier Shale 46
2-21. Graptolite zonation and relative ranges of common species in Middle Ordovician shale of southern Appalachians 47
2-22. Upper Ordovician chronostratigraphic scale and preliminary chronostratigraphy for units in the study area as compared to Twenhofel et al., and Drake and others 49
3-1. Geologic map of the study area showing major structures and stratigraphic units 53
3-2. Faults recognized in the compiled study area 55
3-3. Profile in the upper Sevier Shale depicting folds faults, and contrasting cleavage 58
3-4. Disharmonic folding of the Sevier Shale between strong structural lithic units of the Bays Formation and Knox Group 60
3-5. Small backthrust in the Bays Formation at Lauderback Gap on Highway 347 61
3-6. Small fault and fold in the Bays Formation near Wattenbarger Gap Road likely associated with the Romeo fault zone 64
3-7. Past 100 years depicting the configuration of the Pulaski fault in the vicinity of the Babbs Knobs flap, Greeneville quadrangle 66
3-8. Trace of the Pulaski fault along Hwy 347-Spyder lane 67
3-9. Lower-hemisphere, equal-area stereographic projections of 1,712 poles to bedding in the Bays Mountain synclinorium, northeast Tennessee 69
3-10. Tight fold and hinge collapse zone from the compiled study area illustrating the difficulties with axial planar cleavage in the hinge that refracts and is fanned in the siltstone bed 71
3-11. Fanned fracture cleavage in an open fold of the Bays Formation 72
3-12. Lower-hemisphere, equal-area stereographic projections of 121 poles to cleavage in the Bays Mountain synclinorium 73

3-13. Seven stages of deformation in the Bays Mountain synclinorium during the Alleghanian orogeny 74
3-14. Photomicrographs of upper Sevier Shale 76
3-15. Lower-hemisphere, equal-area stereographic projection of 57 axial surfaces of mesoscale folds in the Bays mountain synclinorium 78
3-16. Conjugate and broken conjugate kink folds in the upper member of the Sevier Shale along Tob Cooter and Dru Haynes Roads 79
3-17. Photo taken from I-181 roadcut in the upper Sevier Shale displaying non-concentric parallel and similar folds 80
3-18. Geologic cross sections depicting the major structural features in the study area 84
3-19. Simplified 3-D fence diagram depicting the thickness increase to the southeast and generalized basin geometry in the vicinity of the study area 87
4-1. Schematic diagrams showing possible relationships between foreland-basin generation, infill, and deformational loading 89
4-2. Isopach map showing major depocenters for upper Middle-Upper Ordovician rocks in the Appalachian basin 90
4-3. Schematic Middle Ordovician Tellico-Sevier basin diagrams and locations from Walker et al. (1983) 92
4-4. Tectonic evolutionary stages of the Blockhouse-Sevier basin using a flexural bending model of basin subsidence 93
4-5. Sevier Basin as a back-bulge basin with the Murphy sediments as the foredeep 94
4-6. Block diagram using complex model of basin formation 95
4-7. Comparison with Ettensohn's generalized sequence of flexural events, accompanying sequence of lithologies, and transgressivev-regressive curve for early subduction-type orogenies on a continental margin 97
4-8. Model depicting the transition from a remnant oceanic basin to the Sevier-Blountian phase of the Taconic orogeny related to emplacement of the overthrusting tectonic load onto the Laurentian margin 99

LIST OF PLATES

I. Detailed Geologic Map of the McCloud, Stony Point, Baileyton, and portions of the Burem and Greeneville 7.5' quadrangles ..... In Pocket

II. Retrodeformed Geologic Cross Sections of the McCloud, Baileyton, Stony Point, Mosheim, and portions of the Burem and Greeneville 7.5' quadrangles ..... In Pocket

III. Station Locations in the McCloud, Stony Point, Baileyton, and portions of the Burem and Greeneville 7.5' quadrangles, northeast Tennessee ..... In Pocket

IV. Detailed Geologic Map of the northwestern Bays Mountain Synclinorium, northeast Tennessee ..... In Pocket

CHAPTER I

INTRODUCTION

The Sevier-Blountian and Martinsburg basins reflect timing, character, and distribution of lithospheric flexural responses during the Taconic orogeny (Fig. 1-1). The first phase of the Taconic orogeny is commonly called the Blountian tectophase (Llandeilian to Caradocian) (Rodgers, 1953b), which produced a westwardly prograding Sevier-Blountian clastic wedge from what is now Tennessee into Alabama (Rodgers, 1971; Pope and Read, 1998). Subsequently, the "Taconic phase" of deformation (Carodocian to Ashgillian) was concentrated more in the north and included the deposition of Martinsburg turbidites in the younger Taconic foreland basin.

Since Safford (1869) first outlined the geology of Tennessee, many interpretations have been made regarding the stratigraphy of the Sevier-Blountian basin. This project seeks to interpret stratigraphic and structural relationships in the Bays Mountain synclinorium in order to better understand Sevier-Blountian to Martinsburg basin dynamics. Detailed geologic maps were made at 1:12,000 scale in the McCloud quadrangle and 1:24,000 in Baileyton, Stony Point, and portions of Burem and Greeneville quadrangles to delineate lithologies and identify structural nuances within the synclinorium. An adequate geometric reconstruction and tectonic interpretation could then be reached with proper stratigraphic and structural data.

Location and Extent of Area Studied

Rodgers (1953a, p. 14) divided the Valley and Ridge in Tennessee into the hills and knobs of the south versus several peaks in the northern part of the Valley and Ridge called mountains coming out of Virginia. This study area encompasses ~ 648 km^2

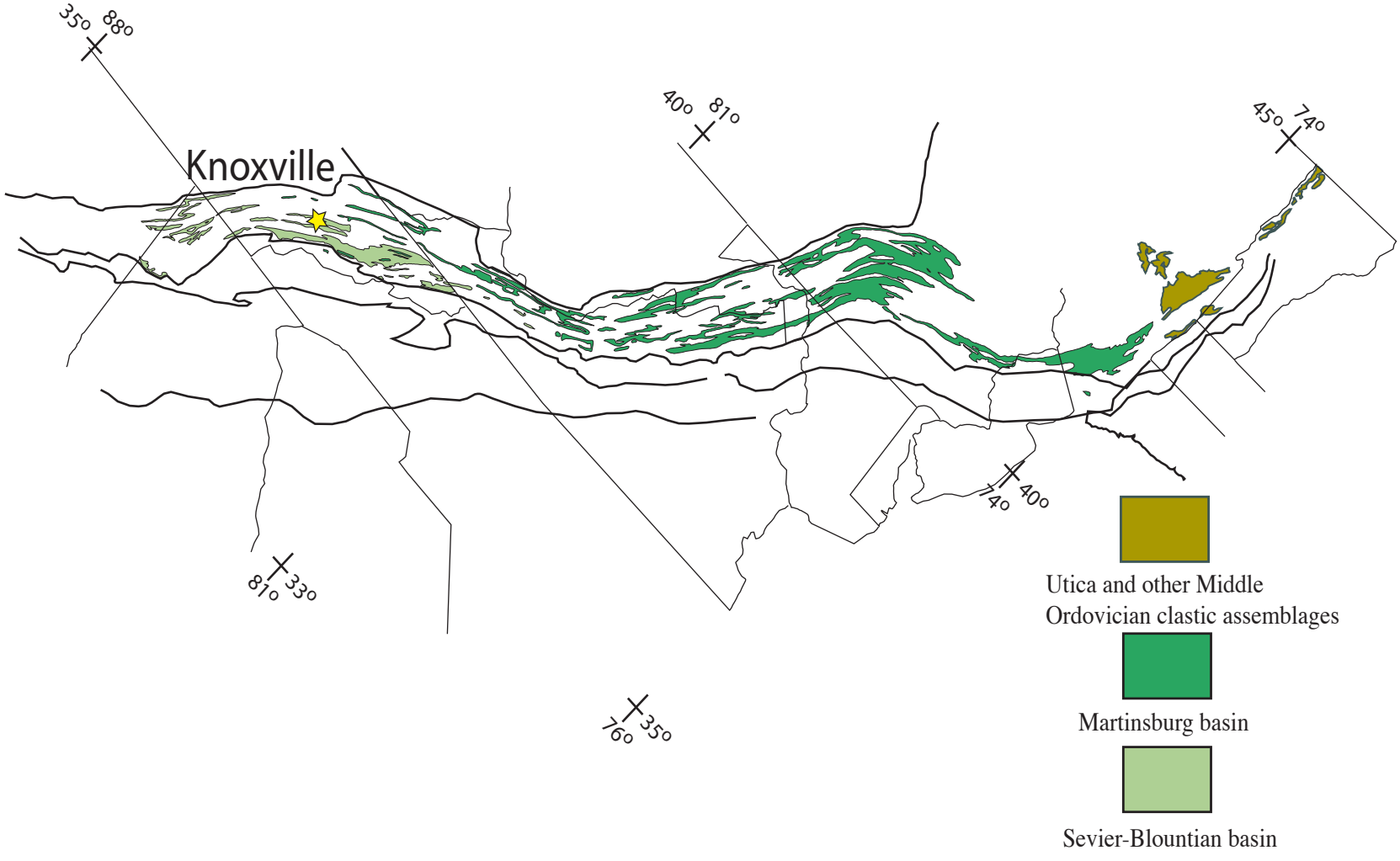

Figure 1-1. Distribution of Taconic basins in the Appalachians (modified from Hatcher, 1990).

(200 mi^2) and extends northward across five 7 1/2-minute quadrangles (1/24,000 scale): Baileyton, McCloud, Stony Point, and portions of Burem, and Greeneville (Fig. 1-2). The McCloud quadrangle was entirely mapped whereas Baileyton, Burem, Greeneville, and Stony Point were partially mapped and compiled from other work (Cummings, 1962; Haney, 1966; Byerly, 1966, 1969, 1996). There are no major cities in the study area, only small towns such as Rogersville, Surgoinsville, and Baileyton. The closest city, Greeneville, is located approximately 4 mi. southeast of the southernmost border of the study area. Major roads that transect the area include Interstate 81, U.S. 11-E, and Tennessee Highway 70.

The study area encompasses a portion of the Bays Mountain synclinorium (Fig. 1-3), northern Greene County and southern Hawkins County. The Bays Mountain synclinorium has been considered as a broad wavelength (2-3 km) open-folded synclinorium with adjacent thrust sheets on either side (Campbell, 1894; Rodgers, 1953b; Cummings, 1962; Ohlmacher, 1991). The Pulaski and Cliffs faults (southeast) and the Carter Valley, Town Knobs, and Saltville faults (northwest) bind the area (Fig. 1-3).

The study area was chosen for the following reasons:

1. The limy Sevier slope, basinal sequences, and proximal/distal facies relationships are exposed.
2. With elevations that exceed 950 m (3,100 ft) and no cities in the study area, some of the greatest outcrop potential exists here.
3. Rodgers (1953a, 1953b) concluded that folding in the Bays Mountain synclinorium is fairly simple and unbroken by faults. If this conclusion is viable, a relatively unbroken section would be preserved in the area.

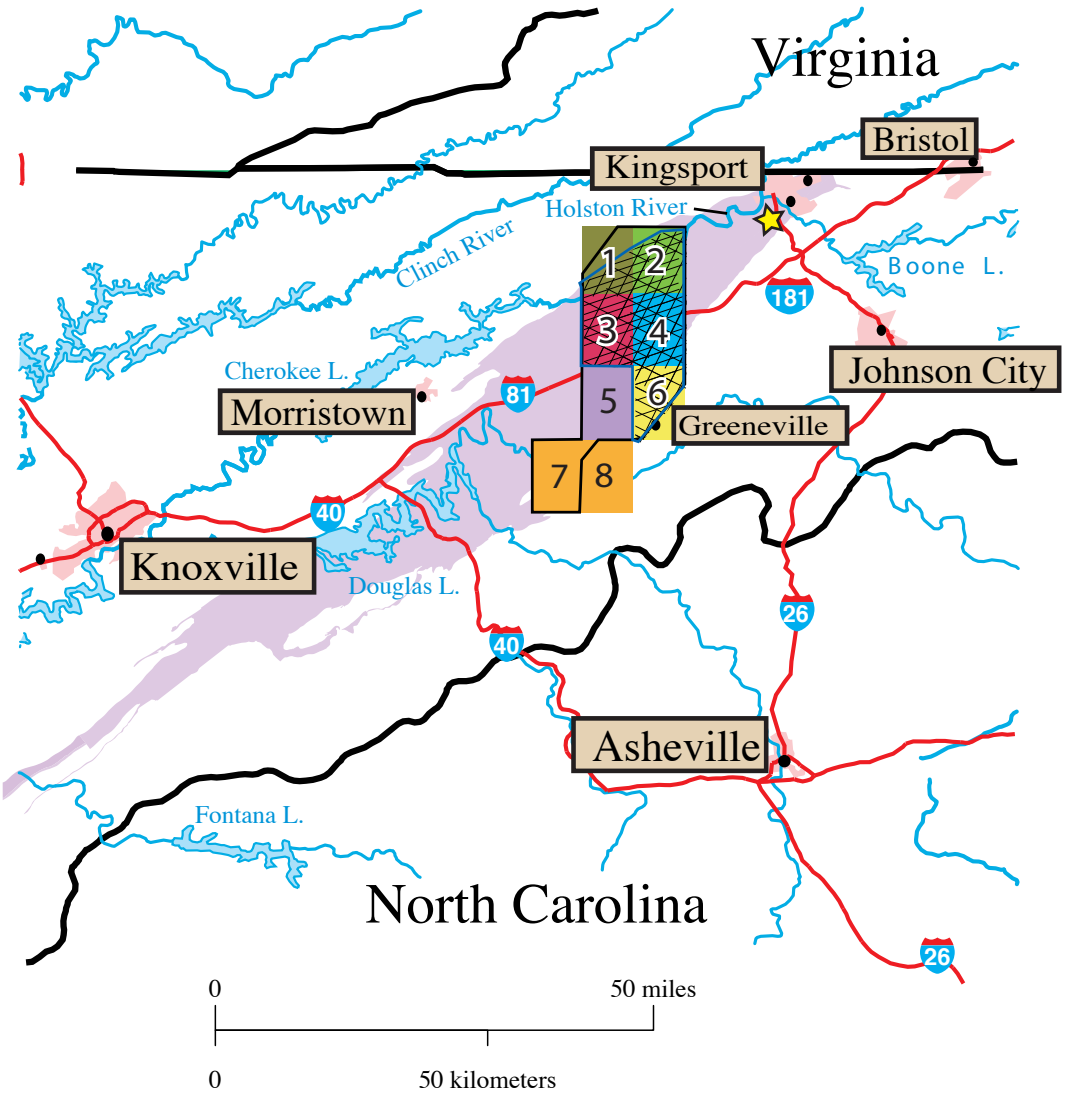

Figure 1-2. Location of the Bays Mountain synclinorium (lavender) and mapped quadrangles with respective mappers in the compiled study area (outlined): (1) Burem (Haney, 1966), (2) Stony Point, (3) McCloud, (4) Baileyton (Byerly, 1969), (5) Mosheim (Lemiszki, 2003), (6) Greeneville (Byerly, 1996), (7) Parrotsville, and (8) Cedar Creek (Whitmer, 2005) quadrangles. This study area (cross-hatched) includes the Baileyton, McCloud, and portions of the Burem, Greeneville, and Stony Point quadrangles. The heavily studied I-181 roadcut (star) northeast of the study area was used as an analog for many structures noted in the study area.

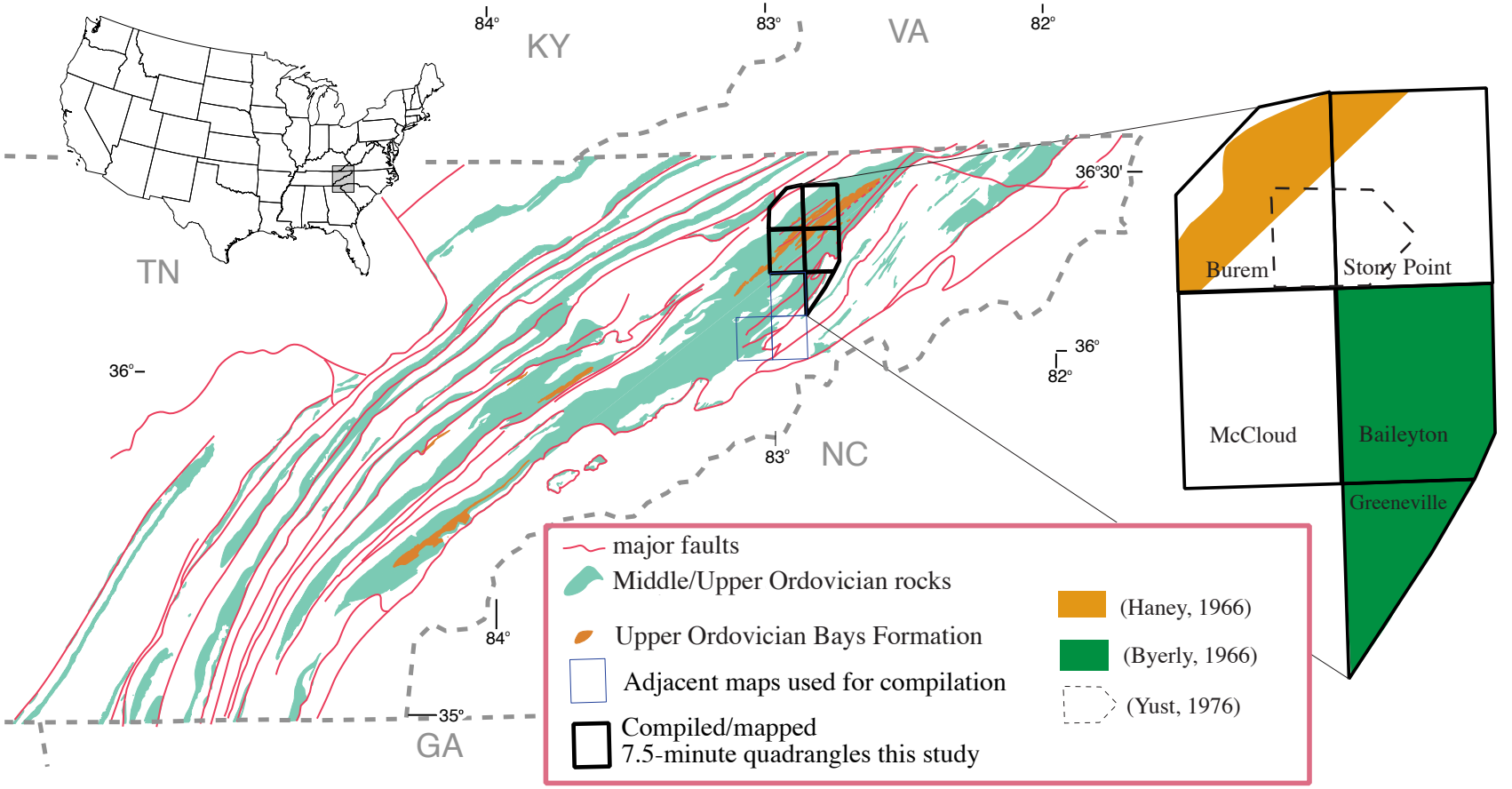

Fig. 1-3. Location of study area (in bold) showing important structural features and aereal extent of Ordovician outcrop. Previous University of Tennessee - Knoxville graduate work used for the compilation map indicated by color.

Geomorphology

The topography of the study area conforms to the general northeast-southwest trend of the Valley and Ridge physiographic province. Elevations in the study area range from 300 m (~1,000 ft) to 950 m (3,100 ft) (Chimneytop Mountain). High, linear ridges capped by the resistant sandstones of the Bays Formation or upper Sevier Shale represent the mountains in the synclinorium. The valleys contain linear ridges of the middle and lower Sevier or the knobby rounded hills of the Martinsburg Formation.

The stream pattern is dendritic where broad valleys are underlain by shale and display a trellis within ridges of the northwest synclinorium. Stream flow is generally south and east. Terrace deposits are present along the Holston River. The erosion patterns are directly related to underlying structure and may be noted from the digital elevation models (Fig. 1-4). Features such as doubly plunging anticlines and synclines of the Bays Mountain synclinorium, the Knox Group anticlines of the southeastern portion of the study area, and the faults throughout are outlined by erosional differences of contrasting lithologies. Along some of the ridges landslide deposits were noted and commonly occur where carbonates of the upper Sevier Shale are eroded and undercut slopes, bringing down Bays Formation sandstone. Karst topography was noted not only in the Knox Group but also along the upper Sevier ridges.

Previous Geologic Mapping Investigations

Previous regional geologic maps of the study area were made by Keith (1905a, 1905b), Rodgers (1953a, 1953b), and Cummings (1962). Byerly (1966), and Haney (1966) made detailed (1/24,000 scale) geologic maps of parts of the study area. Safford (1869) indicated the major stratigraphic relationships including recognition of the Lenoir Limestone, Knoxville (Holston) Marble, and Sevier Shale including the Gray Knobs (Keith 1905a) (middle Sevier Shale).

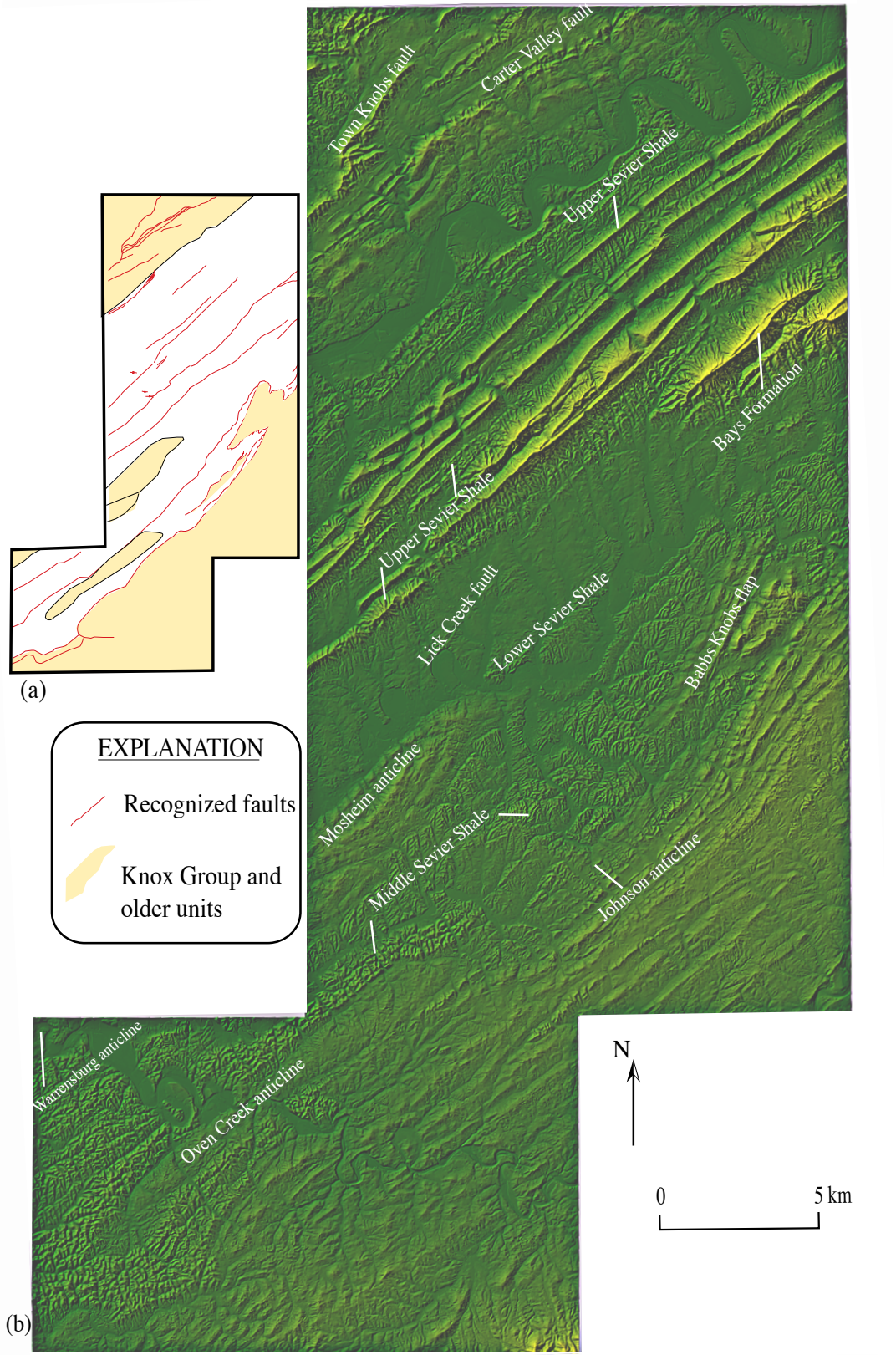

Figure 1-4. (a) Structural features outlined in the study area and (b) digital elevation model depicting how topography is related to the underlying structure. See Plate III for descriptions.

Keith's (1905a, 1905b) geologic maps of the area are some of the most spectacular considering the lack of topographic base maps (he made his own), or knowledge of stratigraphy (Fig. 1-5). Keith's geologic maps revealed nuances within the undivided Sevier Shale such as the presence of the Athens Shale (lower Sevier Shale equivalant) and Tellico Sandstone (middle Sevier Shale equivalent). Keith's (1896) earlier attempt to divide the basin stratigraphy as described in the present study may have prevented some of the later structural and stratigraphic misinterpretations. Ulrich (1911) and Butts (1933) later corrected stratigraphic errors in Keith's mapping, i.e., the correlation of the Middle Ordovician Bays Formation with the Upper Ordovician Juniata Formation on Clinch Mountain (Rodgers, 1953a).

Rodgers (1953a) resolved some of the problems with stratigraphy and adequately addressed several major structural issues (Fig. 1-6). He was first to recognize facies relationships between the units in the Rome, Conasauga, Knox, Shady, and Chickamauga. He did not subdivide the Sevier Shale and stated that individual units within the Sevier Shale did not appear to be consistent or mappable.

Cummings' (1962) study of the Bays Mountain synclinorium included most of the present study area (Fig. 1-3). His work included stratigraphic descriptions of the Bays Formation, but he did not make detailed geologic maps and was unable to address tectonics and Sevier-Blountian basin dynamics. He suggested that: (1) the Bays Formation formed under deltaic conditions; (2) clastic material was derived from the east and southeast (both grain size and unit thickness increase to the southeast); (3) heavy minerals identified in the Bays Formation were essentially the same as those found in the crystalline complex that now comprise the Blue Ridge; (4) the synclinorium is essentially doubly plunging; (5) the Bays Formation deformed visco-elastically, while

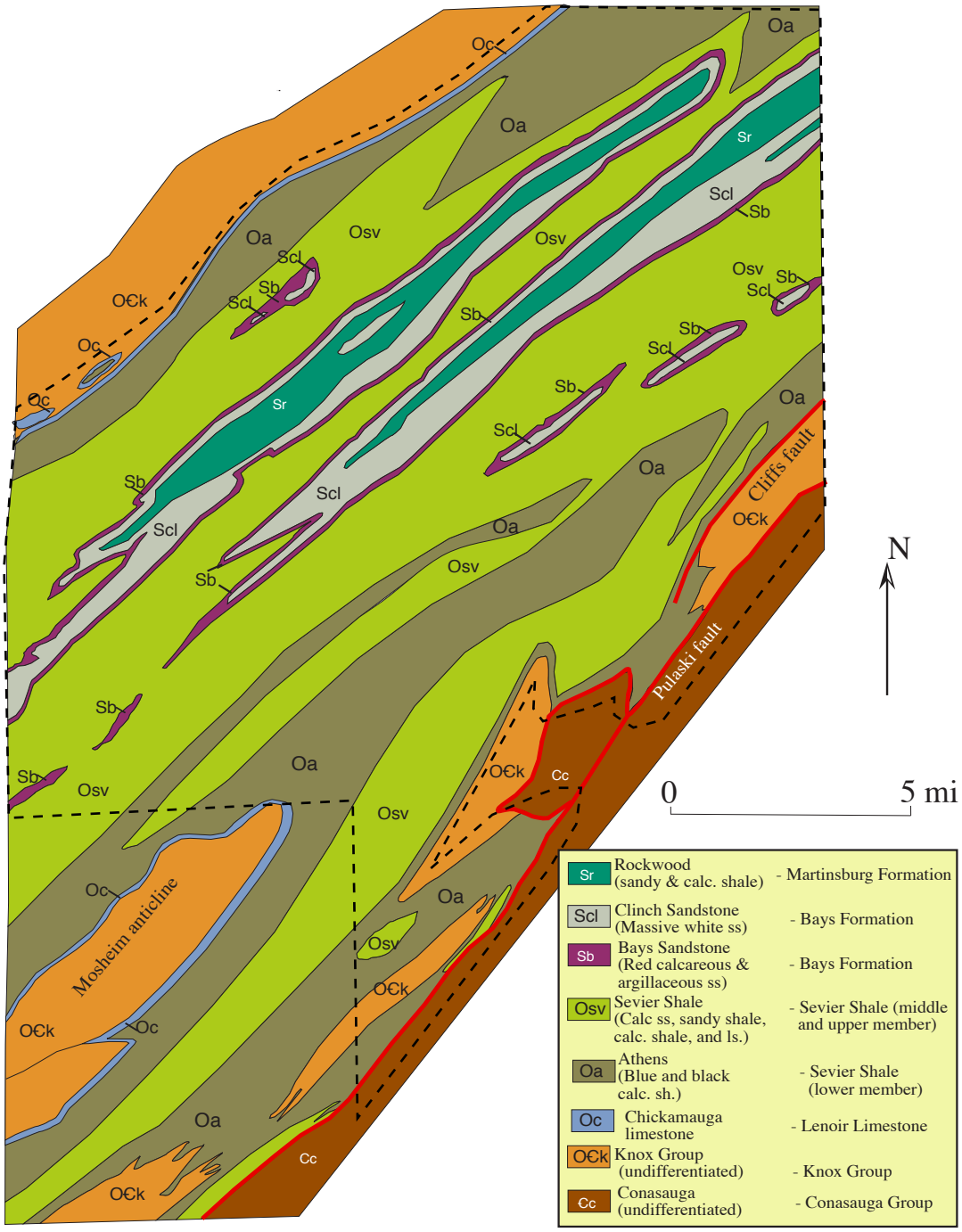

Figure1-5. Simplified version of Arthur Keith's (1905a) geologic map of the study area (dashed line). The present relative equivalents to Keith's mapped units are indicated. Keith's geologic map incorrectly subdivided the Bays Formation into the redbeds and clean sandstones indicating that the redbeds were confined to the lower portion and the arenites to the upper portion. Biostratigraphic correlation by Ulrich (1911) and others would disprove the Silurian ages given for the Bays and Martinsburg Formations.

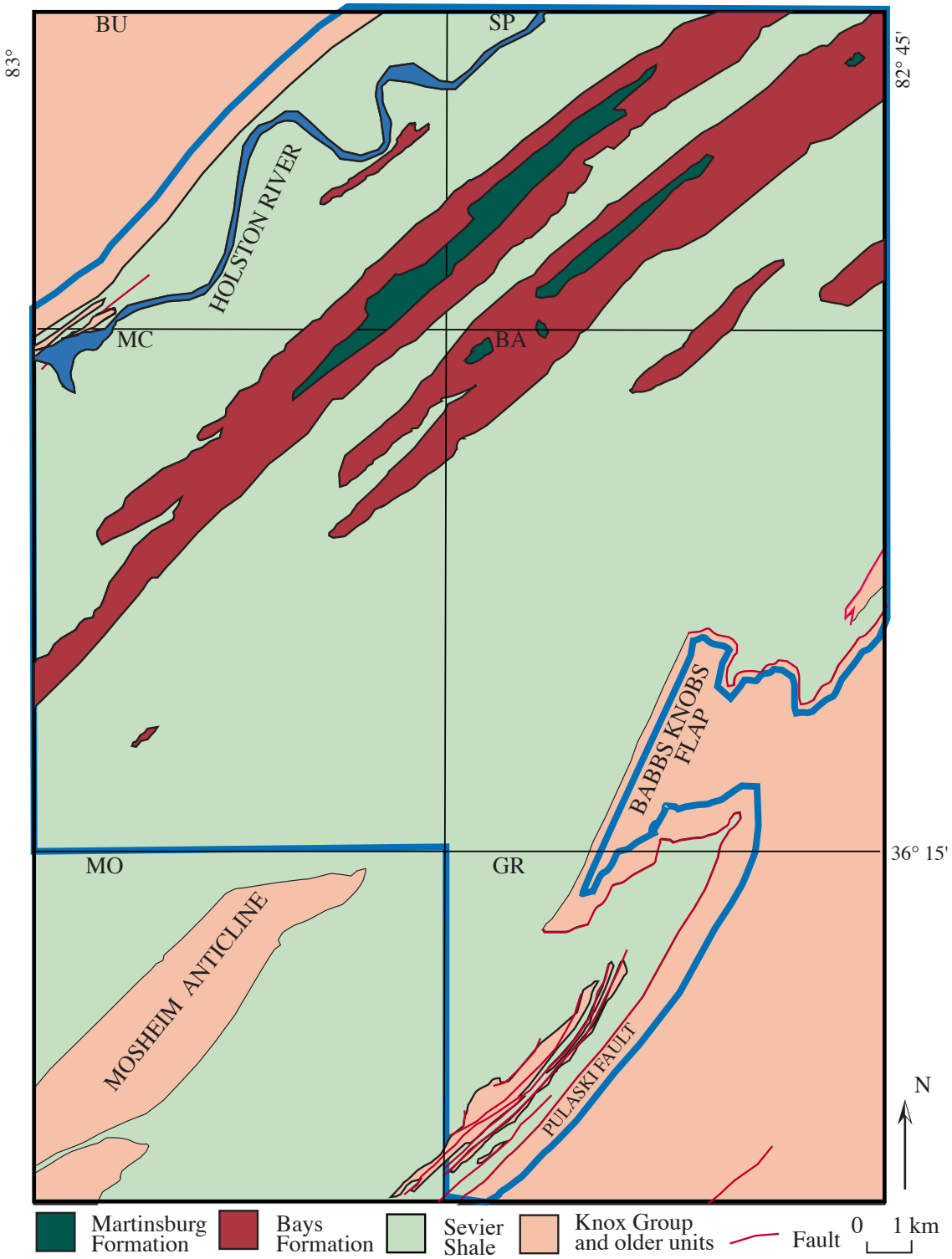

Figure1-6. Simplified version of Rodgers' (1953a) geologic map of the study area (heavy blue line). BU - Burem, SP - Stony Point, MC - McCloud, BA - Baileyton, MO - Mosheim, GR - Greeneville 7 1/2 - minute quadrangles.

the Sevier Shale underwent plastic deformation; and (6) the Bays Formation correlates with the Bowen Formation (upper member), the Witten Formation, Moccasin, and Eggleston Formations.

Contrary to Cummings' (1962) conclusions, the Sevier Shale and Bays Formation underwent brittle deformation. The only known correlative of the Bays Formation is the Moccasin Formation to the northwest (Harris and Repetszki, 1982), not the Bowen, Witten, or Eggleston Formations as Cummings (1962) suggested. Cummings' geologic mapping was reconnaissance mapping, eliminating the possibility of understanding details of stratigraphy, 3-D basin geometry, and dynamics.

Byerly (1966) constructed detailed geologic maps of the Baileyton and Greeneville 7 1/2-minute quadrangles (Fig. 1-3). Much of his work focused on the Pulaski fault around the Babbs Knobs flap. Byerly's (1969, 1996) structural measurements were compiled into this study, were digitized, and included in the compilation map (Fig. 1-7; Plate III).

Haney (1966) mapped the northeastern portion of a large reentrant of the Saltville fault in Hawkins County, Tennessee (Fig. 1-3). He attributed the origin of the Saltville fault to thrusting across a large syncline-anticline complex. The reentrant parallels and lies just northwest of the Bays Mountain synclinorium. The older rocks in Haney's area are notably more folded than in other areas of the Saltville fault belt and involve rock units from the Rome Formation (Lower Cambrian) to the Sevier Shale. Since his mapping joined the study area to the northwest, his map was digitized and compiled, although no stratigraphic and structural analysis was made of that area.

Two other investigations are presently being carried out in the Sevier-Blountian basin. Lemiszki (2003) mapped the 7-1/2 minute Mosheim quadrangle and the Camelot quadrangle (not included but stratigraphic information gathered from the study pertaining to the Sevier Shale and Martinsburg Formation was included) located

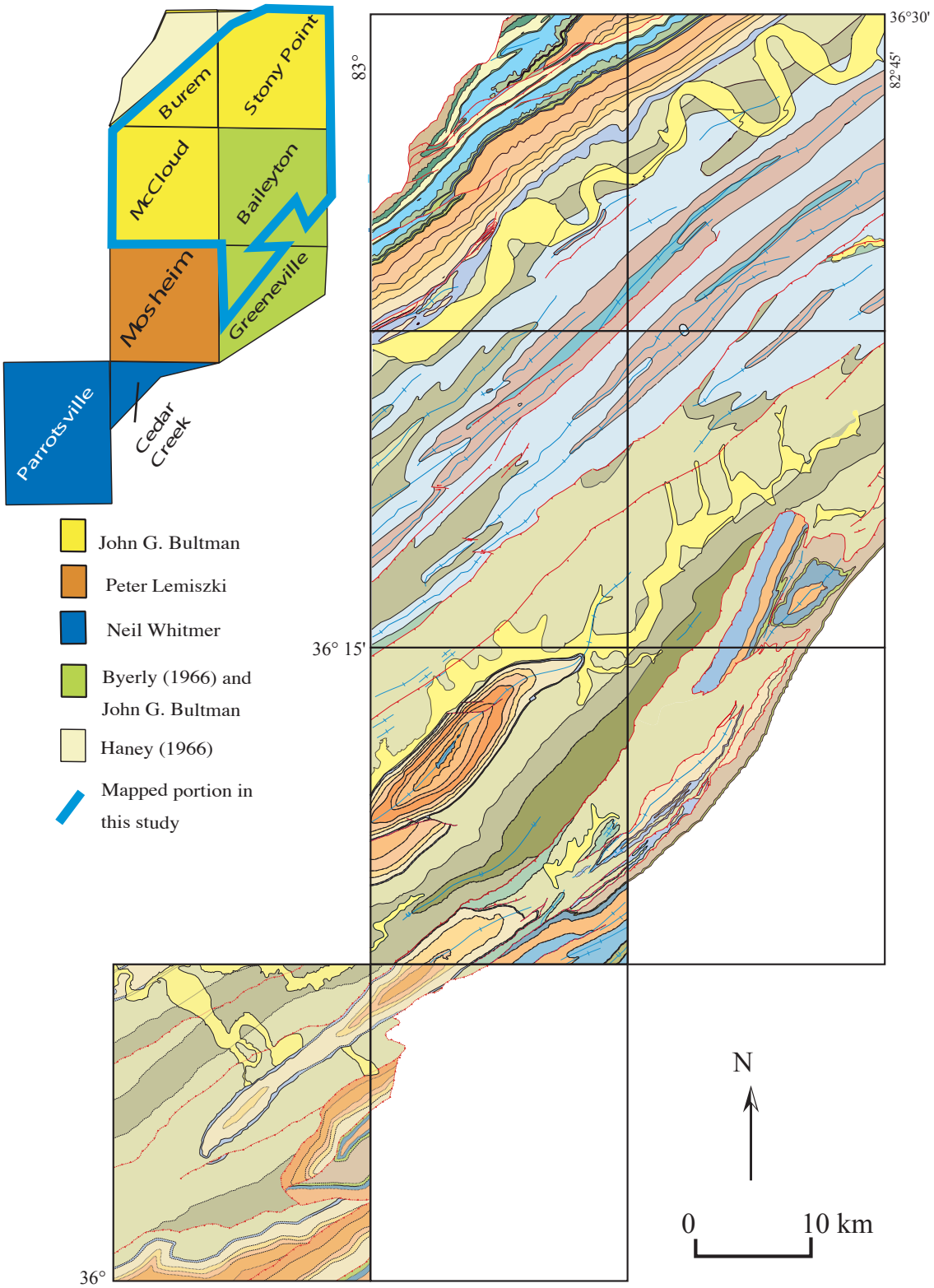

Figure 1-7. Compiled geologic map without structural data. For explanation of geologic map units, see Plate III.

northwest of the study area. The Mosheim quadrangle conveniently adjoins my study area and Neil Whitmer's (2005) study area (Fig. 1-7). The Mosheim quadrangle and Neil Whitmer's study area (Parrotsville and a portion of the Cedar Creek quadrangle) were digitized and included in the compilation (Fig. 1-7, Plate IV) to better understand the dynamics of the basin.

Present Investigation

In the northeastern part of the Bays Mountain synclinorium where a complete section of Sevier is present, this study for the first time divided the Sevier Shale into three parts. It includes analysis of the northern and southern parts of the Sevier basin, and a discussion of the Middle-Upper Ordovician unconformity (Bays and Martinsburg Formations).

The northeast portion of the Sevier-Blountian basin has never been studied in great detail. My work is based primarily on detailed geologic mapping and compilation and, to a lesser extent, subsurface data from the region (Plate I). The field studies for this thesis were conducted in the winter, spring, and summer of 2003 and 2004. Over 1,700 structural data stations (including measurements of strike and dip of bedding surfaces, cleavage, mesoscale folds, slickensides, fractures, and crossbedding) were collected using a Brunton compass (Appendix, Plate II). The structural data, along with rock unit contacts (many of which were gradational), were then plotted on topographic base maps at 1:12,000 scale in the McCloud quadrangle and 1:24,000 scale in Baileyton, Burem, Greeneville, and Stony Point quadrangles. Finally, data were compiled into digital format using Adobe Illustrator™ 10 software on digital raster graphic maps and were georeferenced by aligning latitude and longitude across a standardized grid using MaPublisher™ software. Much of the information concerning the stratigraphy of the surrounding area was obtained from the literature (Fig. 1-3).

CHAPTER II

STRATIGRAPHY

General Statement and History

The thickest section of the Middle Ordovician rocks in East Tennessee occurs in and around the Bays Mountain synclinorium in Sullivan, Hawkins, and Greene Counties and extends southwestward along the east side of the Valley and Ridge to McMinn County (Rodgers, 1953a). The rocks exposed in this study area range from Lower Ordovician (Tremadocian) Knox Group units to Upper Ordovician (Caradocian) Martinsburg Formation (Drake et al., 1989), and contain both the Sevier-Blountian and Martinsburg clastic wedge sediments. Stratigraphy in the Sevier-Blountian basin generally conforms to traditional Valley and Ridge stratigraphy recognized by Keith (1905a, 1905b) and Rodgers (1953a, 1953b), but now includes three new subdivisions of the Sevier Shale. These units closely resemble Neuman's Sevier Shale (lower and middle members) and Bacon bend member (upper), and Keith's originally identified Athens, Tellico, and Sevier units.

Stratigraphy in the study area changes from the northwest to the southeast (Figs. 2-1, 2-2). Facies changes are common in the Bays Mountain synclinorium: many previous workers felt the southwestern part could be divided whereas the northern portion should remain undivided (Rodgers, 1953b; Neuman, 1955; Cummings, 1962; Byerly, 1966; Shanmugam, 1978). Detailed mapping and subdivision of the Sevier Shale have resolved earlier structural simplifications because of the earlier lack of subdivisions of the Sevier Shale.

Although the compiled map includes units from the Rome (Lower Cambrian) to the Martinsburg Formations, this study is focused primarily on Sevier-Blountian basin

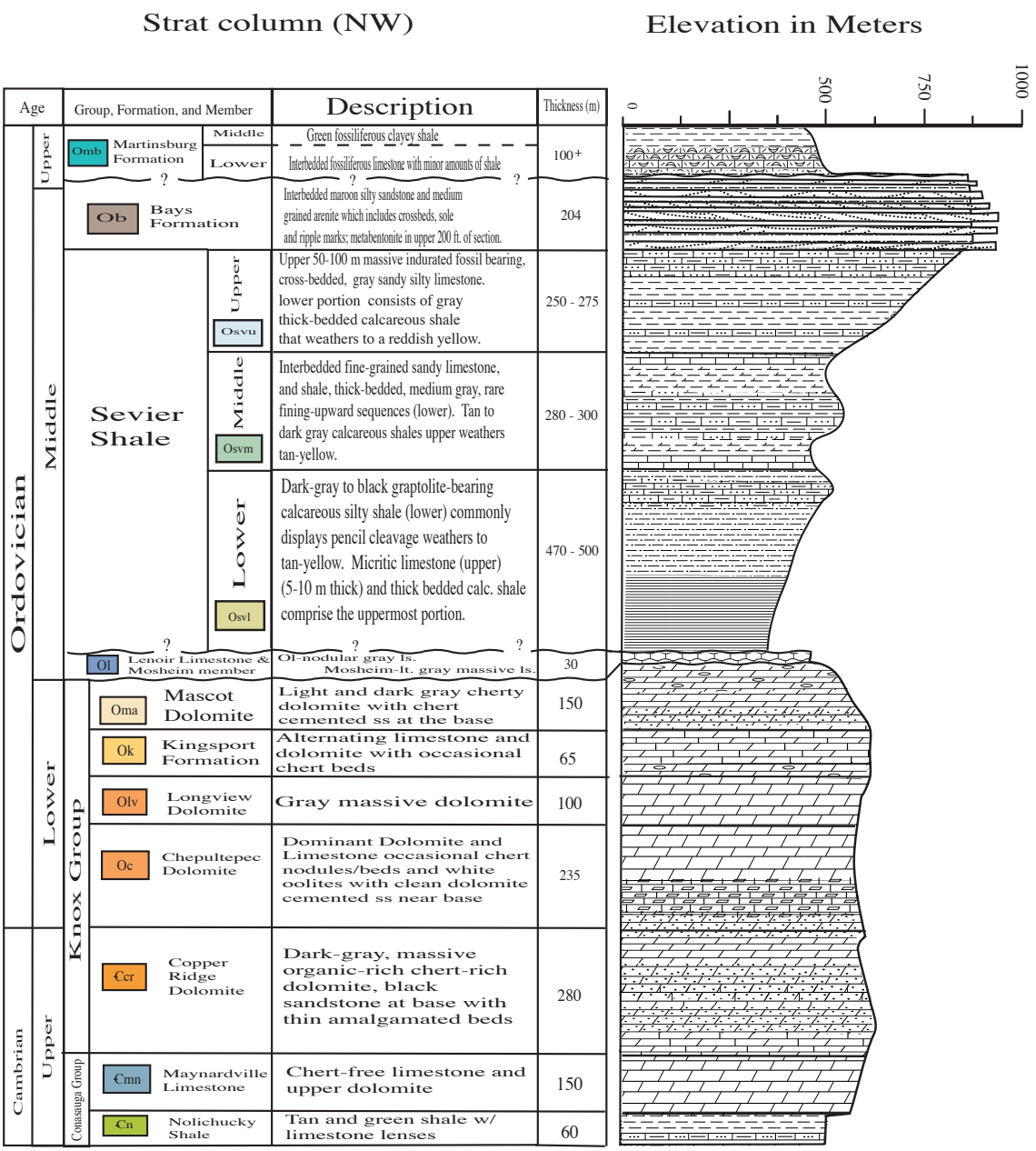

Figure 2-1 . Generalized stratigraphic column of units in the northwestern portion of the field area near the Holston River. Righthand column shows rock type, relative resistance of units, and average elevations.

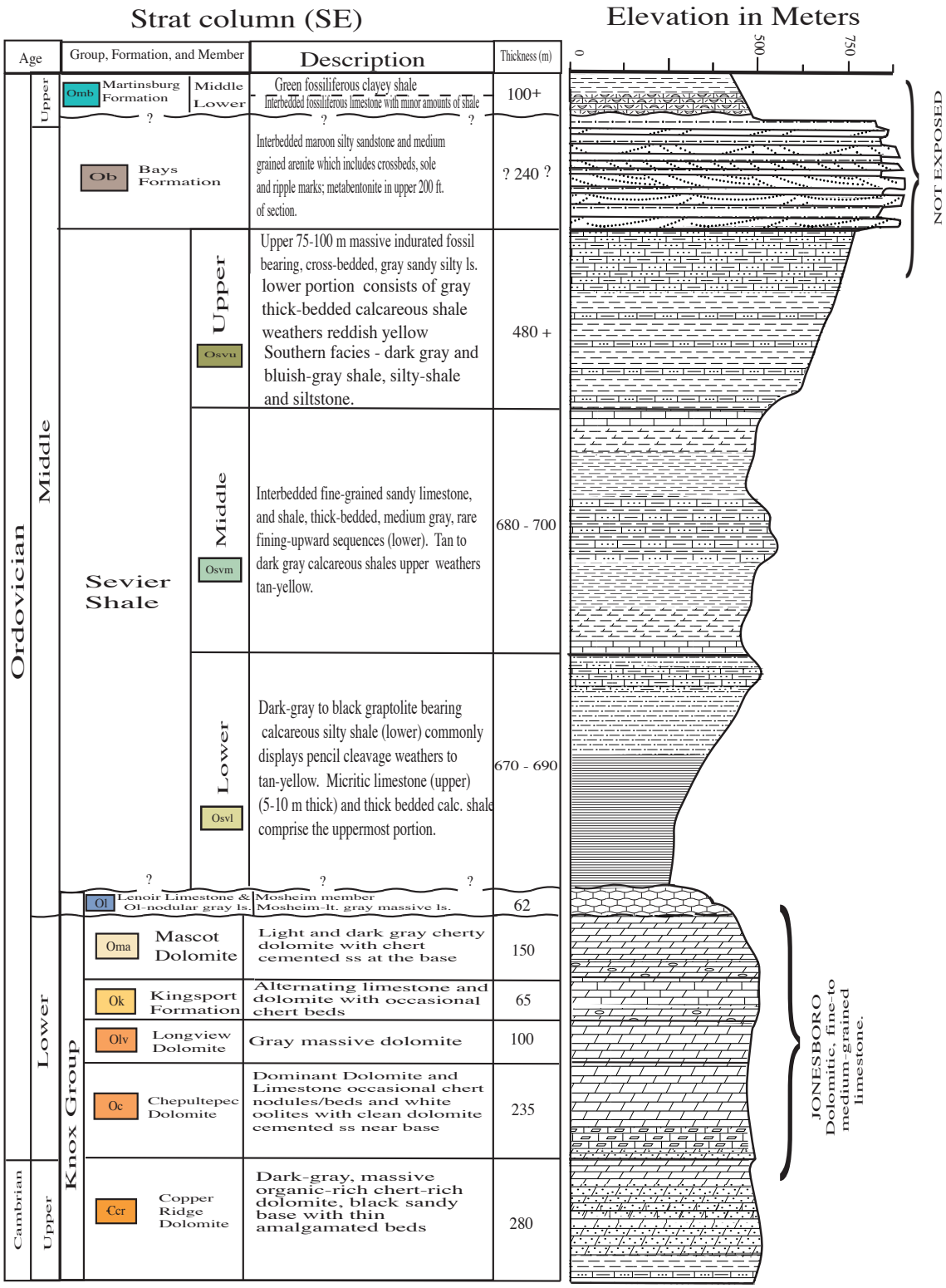

Figure 2-2. Generalized stratigraphic column of units in the southeastern portion of the field area south of the Mosheim anticline north of the Pulaski fault. Righthand column shows rock type, relative resistance of units, and average elevations.

dynamics and therefore includes an analysis of basin sedimentation directly affected by the Taconic (Blountian) orogeny. Units investigated for this study include: Mascot and Jonesboro Formations (Knox Group); Lenoir Limestone and Mosheim Member; lower, middle, and upper members of the Sevier Shale; Bays Formation; and the lower and middle members of the Martinsburg Formation.

Knox Group

The Knox Group consists of all strata above the Maynardville Limestone (Conasauga Group) and below the pre-Middle Ordovician unconformity. The Jonesboro Limestone (Fig. 2-3) of this report refers to a medium-bedded, dark bluish-gray, dolomitic, fine-to medium-grained, limestone that weathers medium bluish-gray and roughly correlates with (in ascending order) the Chepultepec and Longview Dolomite, Kingsport Formation, and Mascot Dolomite. For this study the Jonesboro Limestone was not mapped in sufficient detail to distinguish separate units but this could likely be done in the hanging wall of the Pulaski fault in the Babbs Knobs flap. The upper portion of the unit includes arenaceous dolomite beds and thin sandstone layers. The Jonesboro Limestone is approximately 610 m (2,000 ft) thick (Byerly, 1966). The basal 61-91 m (200-300 ft) of the Jonesboro contain numerous layers of cross-bedded sandstone, ranging up to 0.5 m (19 in). The base of the lowermost thick sandstone bed in this zone is mapped as the base of the Jonesboro. This sandy section, commonly traced in residuum, likely corresponds to the basal sandy member of the Chepultepec Dolomite (Rodgers, 1953a, 1953b).

The entire Knox Group was not mapped in the study area; only the Mascot Dolomite and younger units were mapped. The Mascot Dolomite at the top of the Knox Group (named after outcrops in Mascot, Tennessee) is a light-to medium-gray, fine-grained, thick-bedded dolomite (Rodgers, 1953a, 1953b; Brokaw et al., 1966).

(a)

(b)

Figure 2-3. Massive (a) and ribboned (b) Jonesboro Limestone along Baileyton Pike in the hanging wall of the Pulaski fault (Babbs Knobs flap) (compass ~ 7 cm).

.

The upper part of the formation exhibits yellow and pinkish-red weathering. The contact with the underlying Kingsport is marked by several thin layers of chert-matrix-cemented sandstone. The thickness of the Mascot Dolomite is approximately 150 m (650 ft) thick (Rodgers, 1953b).

The Middle Ordovician (Knox) unconformity, first recognized by Rogers (1838) on the Delaware and Hudson Canal, lies at the top of the Knox Group and separates Lower and Middle Ordovician age rocks. The unconformity has been suggested by Rodgers (1971), Wiener (1979), Mussman and Read (1986), and Pope and Read (1998) to mark the beginning of the collision of an island arc and creation of the Sevier-Blountian basin. In the study area the unconformity represents a duration of approximately 10 m.y. (Rodgers, 1953b; Pope and Read, 1998) with the thickness of strata removed increasing from the northeast to the southwest, from 0 m in Pennsylvania, Maryland and Northern Virginia (Suter and Tillman, 1973; Read and Tillman, 1977) to greater than 140 m in southern Virginia and Tennessee (Webb, 1959).

The Chickamauga Group

The Chickamauga Group (Swingle, 1962) was originally called the Chickamauga Limestone by Hayes (1891). The Middle Ordovician Chickamauga in the study area consists of sandy, micritic, and fossiliferous limestone, arenite, hematite-rich sandstone, siltstone, and shale. It was first examined by Safford (1869) and later studied by Keith (1905a, 1905b), Rodgers (1953a, 1953b), Cummings (1962), Haney (1966), Byerly (1969), Shanmugham and Walker (1978), and others; the Chickamauga Group has continuously presented stratigraphic continuity problems. The names of the units change from quadrangle to quadrangle more than the facies actually do. The three main units in the Chickamauga Group described in the study area include in ascending order:

(1) Lenoir Limestone, including the Mosheim Member; (2) Sevier Shale, with lower, middle and upper members; and (3) the Bays Formation.

Lenoir Limestone

The Lenoir Limestone (Fig. 2-4), named by Safford and Killebrew (1876) for exposures near Lenoir City, Tennessee, consists of thick to thin bedded, irregular to nodular, fine-grained, light to dark-gray limestone. Three distinct lithologies exist: (1) gray to bluish-gray argillaceous nodular limestone, weathering dark blue; (2) gray to bluish-gray, dense calcarenite that weathers blue gray; and (3) the Mosheim Member, a dense, aphanitic, gray to blue-gray limestone weathering dull gray and characteristically containing "birdseye" of calcite (Cummings, 1962).

The Lenoir Limestone commonly breaks into small, irregularly rounded nodules and forms a series of low knolls in the proximity of the Holston River (northwest part of the study area) and around the Knox anticlines (southern part of the study area). These thin carbonate units onlap the unconformity and represent a transgression from peritidal shelf environments (Benedict and Walker, 1978; Finney et al., 1996). The presence of fine-grained insoluble residue and abundance of micrite suggest turbid water during the formation of the Lenoir Limestone (Benedict and Walker, 1978). Based on the algal reappearance and disappearance above and below where sufficient sunlight is present such that photosynthesis prevails over respiration, Benedict and Walker (1978) placed the Lenoir Limestone in the euphotic zone (0 to 150 m).

The Lenoir Limestone and Mosheim Member (Ulrich, 1911), a massively bedded, light-gray micritic limestone, contain the gastropod *Maclurites magnus* (Neuman, 1955). Rip-up clasts of Mascot chert and dolomite from the Middle Ordovician unconformity (Knox unconformity) have been observed in the basal 5 cm

Figure 2-4. Nodular Lenoir Limestone near Hwy 70 Burem quadrangle (hammer head ~ 20 cm long).

(2 in.) of the Mosheim Member. The Mosheim Member may represent a unique facies marginal to the shaly *Christiania* limestone facies in Virginia and Alabama (Rodgers, 1953b) but here it likely interfingers and is correlated with part of the Lenoir Limestone (Rodgers, 1953b) (Fig. 2-5).

Sevier Shale

The name Sevier Shale was first coined for exposures of shale lying between the Tellico Sandstone and the Bays Sandstone immediately northwest of Chilhowee Mountain in Sevier County (Keith, 1895). Keith (1905a, 1905b) attempted to subdivide the synclinorium basin sediments into the Sevier Shale, Tellico Sandstone, and the black Athens Shale for the northern and southern sections. In this study the Sevier Shale consists of lower, middle, and upper members. Similarities for this study may be found with Safford's (1869), Keith's (1905a, 1905b) and Neuman's (1955) stratigraphic descriptions of the basin sediments, but mappable facies were not identified in the previous studies.

Lower Sevier. The lower Sevier Shale lies directly above the Lenoir Limestone and consists of gray-black, graptolite-bearing carbonaceous shale (Fig. 2-6, 2-7). The yellowish-tan weathering lower member commonly exhibits pencil cleavage, is very thinly bedded, and is typically more fissile than the rest of the unit. The uppermost part of the member contains a dark-gray to black, micritic limestone that varies in thickness. This capstone was used as a marker bed throughout the basin but may be most easily found approximately 0.5 km (1/4 mi) north of Interstate 81 on Hwy 70 (UTM 17 327220E 4016341N [WGS84/NAD83] Lat. 36.27702° and Long. 82.92611°).

Figure 2-5. Weathered "whaleback" exposure of Mosheim Member of the Lenoir Limestone along the Holston River (Burem quadrangle) (Open compass ~ 14 cm).

Figure 2-6. Dark gray-black shale of the lower Sevier Shale on Baileyton Pike (Baileyton quadrangle). Field guru ~ 6 ft 4 in (1.92 m).

Figure 2-7. Bedding-parallel calcite veins in the lower Sevier Shale along Baileyton Pike across road and along strike from Figure 2-6 (Baileyton quadrangle).

This limestone in the uppermost portion of the lower member of the Sevier Shale may be further noted in geophysical logs by indication of low gamma ray and higher resistivity spike compared to the shale (Eastern American Energy Corp. permit # 7822 and 7864 [UTM 17 335300E, 4025222N, lat. 36.35°N, long. 82.86°W]; Capital East Ventures permit # 9862 [UTM 17 320438E, 4023337N, lat. 36.33°N, long. 83.00°W]; and Longyear Drilling Co. DDR Summary sheet [UTM 17 324548E, 4013503N, lat. 36.25°N long. 82.95°W]). The lower member of the Sevier Shale is approximately 472-676 m (1549 to 2218 ft) thick (north to south). Graptolites were found only in the lower dark-gray to black shale.

Middle Sevier. The middle member of the Sevier Shale consists of interbedded gray calcareous shale, siltstone, and sandstone (Fig. 2-8). The shale and sandstone weather yellowish-tan. Thin sections from the middle Sevier Shale indicate that it is composed of carbonated cemented fine-medium grained quartz sandstone with poorly sorted angular quartz (40%) and feldspar (10%) and minor fossil fragments (brachiopods, bryozoans, crinoids, etc.). Detrital biotite and muscovite are also present, some of which is kinked (Fig. 2-9). Heavy minerals represent 2-5% of the total rock mass (Cummings, 1962).

The middle member holds up a line of small ridges that extend across the southern part of the study area and may most easily be found approximately 1 km (0.6 mi) south of I-81 along Baileyton Pike (UTM 17 336303E 4018337N [WGS84/NAD83] lat. 36.30º, long. 82.79º). The middle member of the Sevier Shale also exemplifies the decrease in grain size from southeast to the northwest. The northwestern facies is more difficult to distinguish from southeastern facies because the grain size of the southeastern sandstone beds is much more coarse than the northwestern facies, but may be defined as

Figure 2-8. Middle member of the Sevier Shale along Racoon Branch Road (Baileyton quadrangle). Graded beds and cleavage to bedding relationships indicate that they are upright.

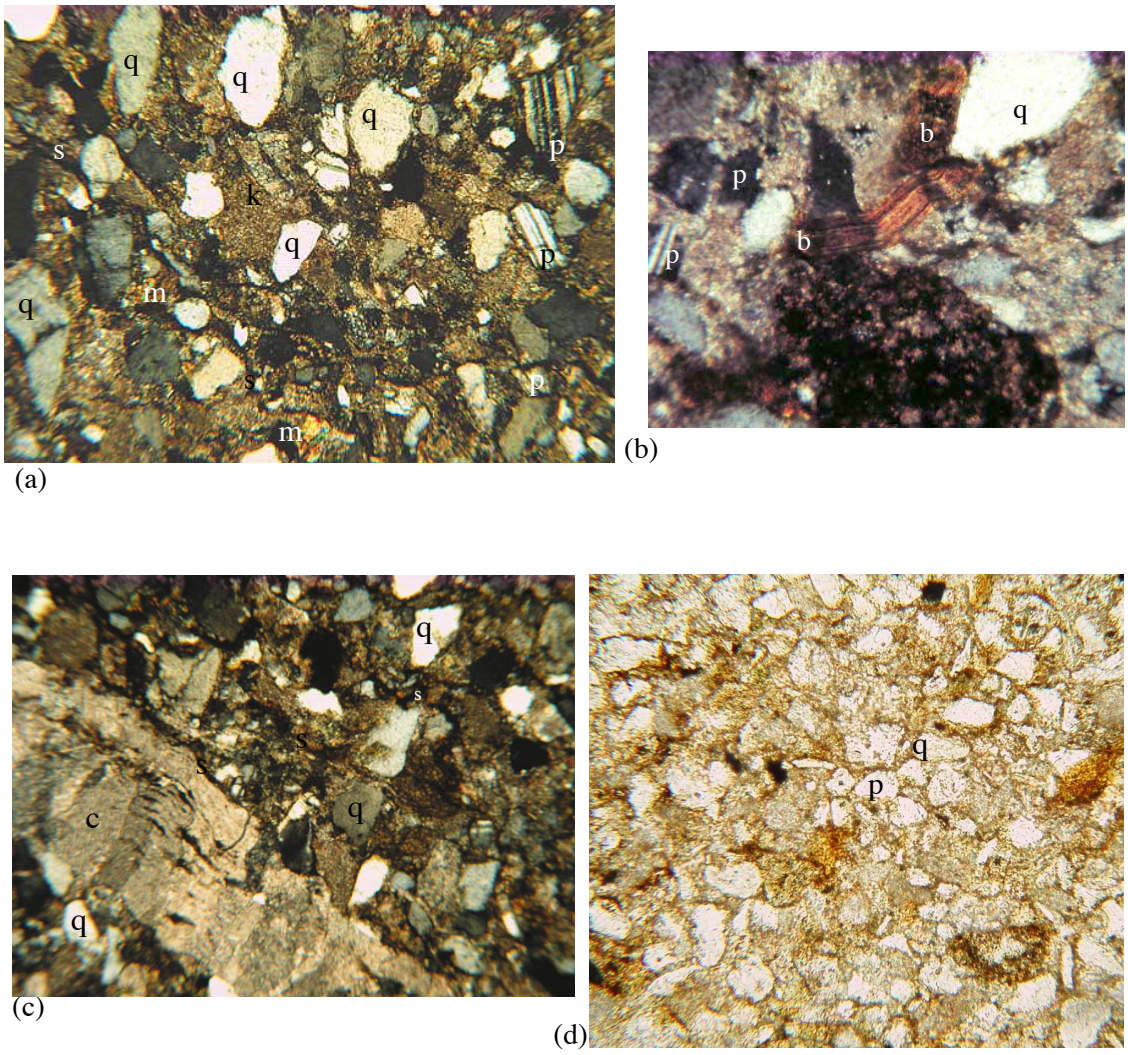

Figure 2-9. Photomicrographs from the middle Sevier Shale: b = biotite, c = calcite, m = muscovite, p = plagioclase feldspar, q = quartz, s = stylolite. a) Poorly sorted angular quartz sandstone with plagioclase and minor k-spar, and carbonate cement, hornblende and quartz, b) kinked muscovite grown around quartz, c) kinked muscovite along stylolite, d) graded bed (top to upper left). Images are imaged under crossed nicols (a, b, c) and plain polarized light (d) (Field of view in a, c, d ~10.2 mm; b ~ 2mm).

the unit between the micritic limestone in the uppermost portion of the lower member (observable in the north and south) and the silty to sandy limestone of the upper member. The middle member is approximately 283-680 m (929 to 2,230 ft) thick north to south.

Upper Sevier. The upper member of the Sevier Shale holds up many ridges (Brokenback Mountain, Bluff Mountain, Short Mountain, Big Mountain, Louderback Mountain, Pilot Knobs [McCloud quadrangle], and Pups Knobs [Stony Point quadrangle]). It consists of gray, thick-bedded, calcareous shale and siltstone in the lower part that grades into gray thick-to massively-bedded silty and sandy limestone in the upper part (Fig. 2-10). It may be correlated with the Bowen Limestone (Cooper and Prouty, 1943; Cummings, 1962), Bacon Bend member (Neuman, 1955), and possibly the Whitesburg Limestone. However, the Bacon Bend member is thinner and contains soft sediment deformation features not observed in this study area. The most easily accessible and heavily studied section of the upper Sevier Shale lies northeast of the study area southeast of Kingsport, Tennessee, on I-181 (UTM 17 358684E 4042965N [WGS84/NAD83] lat. 36.52743º, long. -82.580138º).

Based on exposed outcrop, siliciclastic grain size and thickness of the upper member become greater to the south and southeast. These sandy limestones frequently have herringbone cross beds in the southern section of the synclinorium and likely indicate a shallow-water, medium to high-energy beach environment (Cummings, 1962; Einsele, 2000). Fossiliferous lenses also exist locally (Fig. 2-11).

Cross bed measurements were collected where there was a near 3-D face exposed. Since the strata in the area are deformed their trends were corrected for the

Figure 2-10. Upper member of the Sevier Shale. (a) Abandoned quarry in the northern part of the study area along Old Hwy 70N in McCloud, Tennessee. (b) Lower in the section the upper Sevier Shale becomes thinner bedded. (c) Inset depicts tight fold breaking into fault (bottom right) along Wattenbarger Gap Road.

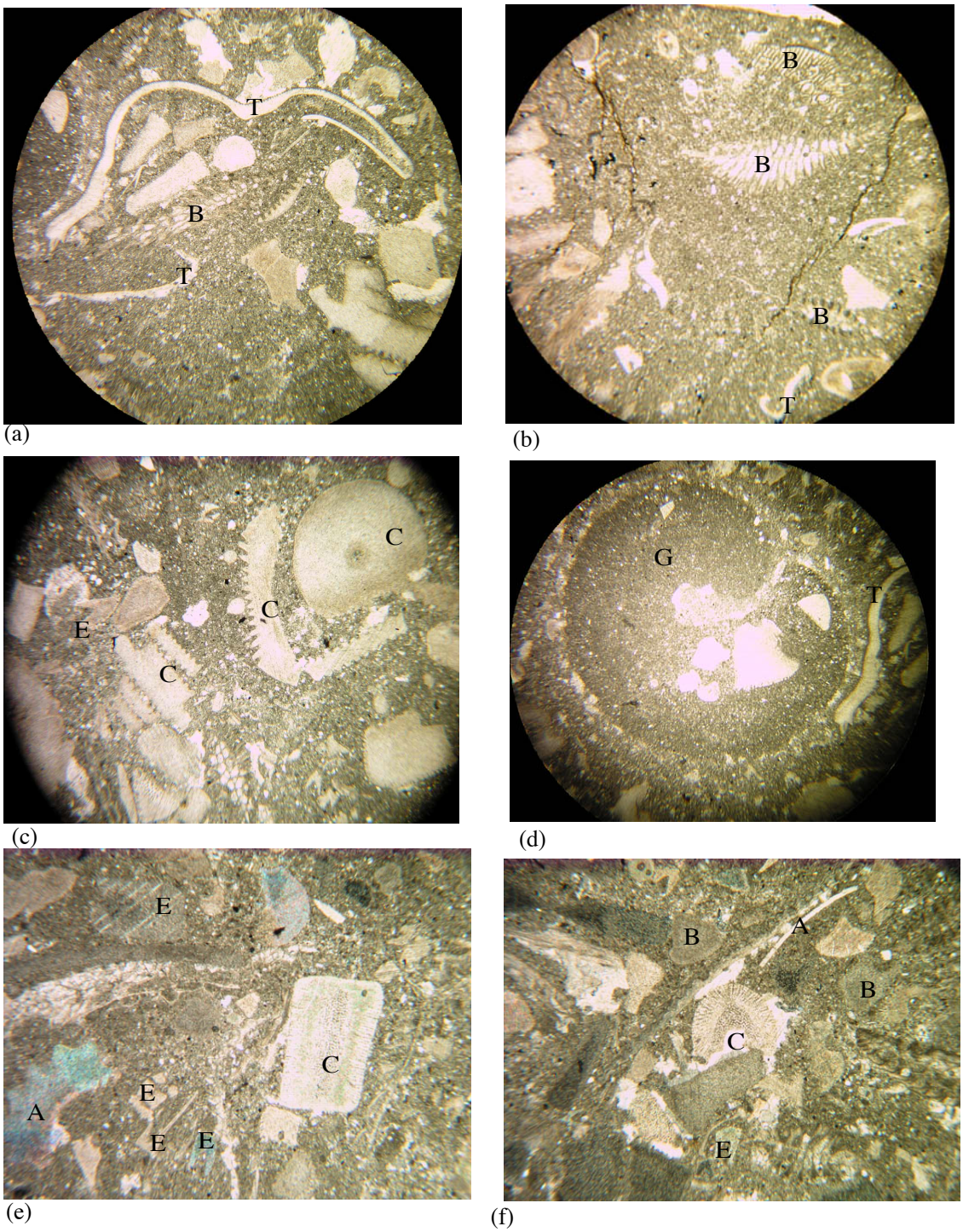

Figure 2-11. Fossils of the upper member of the (sparry calcite) Sevier Shale. T - trilobite; B - bryozoan; G - gastropod mold; E - echinoderm (crinoid) fragment; A - brachiopod; C - crinoid stem, Field of view (a, b, c, e, f ~ 5 mm, d ~ 10 mm).

deformed bedding (Prothero and Schwab, 1999, p. 48-49). First, the dipping plane of bedding is represented as a great circle on a piece of tracing paper. The paper is then rotated to place the strike of the great circle along the north-south axis. The angle (rake) between the cross bed and the strike line is plotted along the great circle giving an apparent paleocurrent direction. Next, the bedding plane is rotated back to horizontal. The intersection between the paleocurrent and plane of the bedding were also rotated along one of the small circles to the edge of the stereonet (horizontal). Finally, the true trend of the crossbed may be made in the horizontal bedding plane, the difference between corrected and uncorrected paleocurrents is so slight that it is not necessary to correct at all. After the corrections were made the cross beds indicate an east by northeast to west by southwest paleocurrent indication (Fig. 2-12). Cross bed measurements in the upper Sevier Shale indicate a bidirectional orientation with the source perpinducular to the shoreline and were likely caused by onshore-offshore tidal currents (Prothero and Schwab, 1999).

Sevier Shale thickness varies northwest to southeast from a maximum estimated 1,837 m (6,024 ft) (southern limb of the Mosheim anticline) to a minimum thickness of 792 m (2,600 ft) (southeast of Surgoinsville in the northern portion of the study area). The upper Sevier Shale is approximately 251–480 m (825 to 1,576 ft) thick north to south. The maximum estimate includes 457 m (1500 ft) of upper Sevier Shale that was likely removed by erosion. This estimated removed section is based on the average increase (1.91) in thickness of the other preserved units (middle and upper Sevier Shale) across the study area from northwest to southeast.

(a)

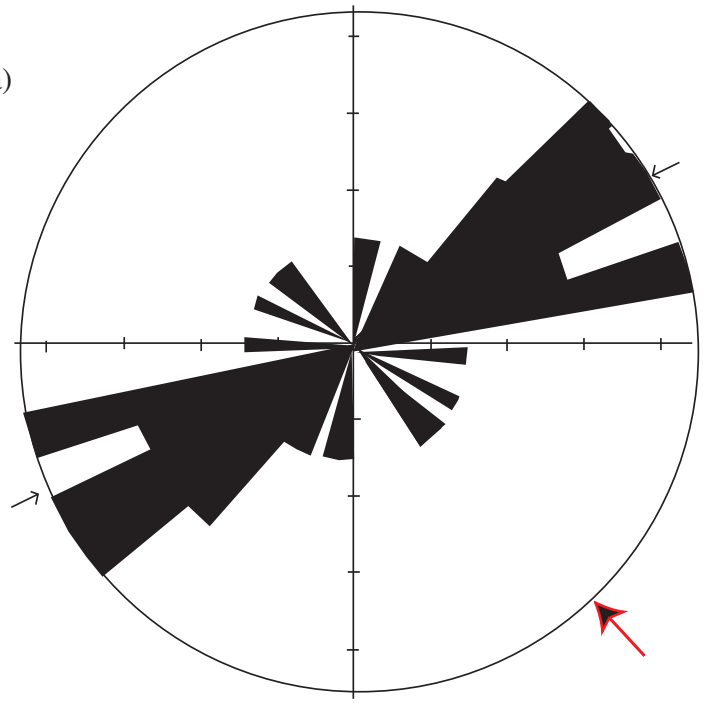

(b)

Figure 2-12. Cross beds of the Bays Mountain synclinorium. a) Rose diagram of 21 cross-bed measurements from the upper Sevier Shale. Note the bimodal shoreline paleocurrent trend from the northeast to southwest. The grain size and stratigraphic thickness increase indicate the source was likely from the southeast (red). Plot made using GeoOrient © v. 9.2.6 by Rod Holcombe, 2005, University of Queensland, AU. b) Cross beds in the upper Sevier Shale at Bluff Mountain exhibit high relief in the quartz-rich layers (1) compared to the carbonate layers (2).

The Whitesburg Limestone

Originally Ulrich (1930) stratigraphically "sandwiched" the Whitesburg Limestone between the underlying Lenoir Limestone and overlying basinal deposits of the Sevier Shale. The Whitesburg Limestone has been placed from the base of the Chickamauga to the base of the Bays Formation by various authors. The name is taken from Whitesburg, Hamblen County, but the type locality is 3 km (2 mi) southeast of the Whitesburg anticline (Knox Group) (Rodgers, 1953b). Rodgers (1953b) stated that the trilobite-rich Whitesburg Limestone appears to form a mappable unit within Hamblen, Hawkins, and Greene Counties. Based on lithology, stratigraphic and structural position in this portion of the study area, the Whitesburg Limestone is preliminarily correlated with the upper member of the Sevier Shale. The type locality Whitesburg Limestone may be viewed near Hwy 66 in Whitesburg, Tennessee. There are likely more complex structural issues to be resolved (due to the observed map pattern and its proximity with other units near the type locality) regarding the Whitesburg Limestone in the Bull's Gap quadrangle west of the study area. Since the type locality is outside the study area and no biostratigraphic samples were submitted, a comprehensive correlation and structural analysis of the Whitesburg Limestone was not done, but this is an area recommended for further study.

The Bays Formation

The upper-middle Ordovician Bays Formation was first defined as the formation that holds up the large peaks of the Bays Mountains (Campbell, 1894). The stratigraphy of the Bays Formation in the synclinorium was studied in several measured sections by Cummings (1962, 1965). In and around the synclinorium the Bays Formation consists of interbedded arenite, originally correlated with the Clinch Sandstone (Silurian) by

Campbell (1894) and Keith (1905a, 1905b), and locally cleaved maroon mudstone, siltstone, and sandstone (some of which have a calcareous component higher in the section and northwestward) (Fig. 2-13). Although some of the different lithologies likely interfinger within the Bays Formation (Cummings, 1962), many of the prominent sandstone beds outline the major structures of the area and may be traced along ridges and valleys across entire quadrangles.

Primary sedimentary features include cross bedding, ripple marks, rill marks (small dendritic channel, groove, or furrow formed on the surface of a beach mud or sand by wave-generated rill or by a retreating tide), and an overall decrease in grain size from southeast to northwest. Cross-bed measurements were similar to the cross bed measurements of the upper Sevier (Fig. 2-12). Rill marks found in the Bays Formation have a southwest trend. Cummings (1962) suggested the Bays Formation formed in a coalesced delta. Heavy minerals identified in his study indicated that the source material was derived from a combination of reworked sediments from an igneous and metamorphic terrane containing numerous heavy minerals (zoisite, fluorite, and augite, andalusite, apatite, augite, calcite, corundum, epidote, garnet, gold, hornblende, ilmenite, leucoxene, magnetite, pyrite, rutile, spinel, topaz, tourmaline, zaratite, and zircon) (Cummings, 1962).

Based on the distribution of a *Camarocladia* zone (marine worm burrow traces) (Fig. 2-14) Cummings (1962) correlated the Bays Formation with the Moccasin Formation, the Witten Formation, the upper portion of the Bowen Limestone, and part of the Eggleston Formation. Using conodont biostratigraphy, Neuman (1955), Walker (1980, 1985) and others resolved the correlation incompatibility, indicating that the Moccasin Formation is the only known correlative to the Bays Formation.
This correlation is supported extends into Virginia where the Eggleston overlies the

(a)

(b)

(c)

Figure 2-13. a) Bays Formation along Hwy 70 (McCloud quadrangle) depicting interbedded clean sandstone and red mudstone-siltstone-sandstone. b) Cross beds and (c) ripple marks in Bays Formation sandstone (Stony Point quadrangle).

Figure 2-14: Burrow trace fossils (Fucoids) representing the *Camarocladia* zone (Cummings, 1962) in the Bays Formation. Sample found along Bear Hollow road (McCloud quadrangle).

Moccasin, which pinches out to the east, but underlies the Martinsburg Formation to the west, whereas the Bays Formation underlies the Martinsburg Formation in the synclinorium.

In thin section the arenite has quartz overgrowths (Fig. 2-15). The Bays Formation has a greater siliciclastic component to the southeast (Cummings, 1962) and changes thickness from 183 m (600 ft) in the northwestern part of the study area to 274 m (900 ft) where preserved in the midsection of the study area. If the Sevier Shale increases thickness to the southeast and the average increase of the Sevier (thickness of middle mapped portion x 1.91 or average increase of the other units) is applied to the Bays Formation, the estimated thickness in the southeasternmost part of the study area is 350 m. This agrees with the thickness estimates from Neuman (1955) and Whisner (2005). Although evidence has been eroded, the Bays Formation may also double its thickness by the time it reaches the present southern limb of the Mosheim anticline (Fig. 2-16).

The Millbrig bentonite bed (5-7 cm) (Big Bentonite, Sweden) occurs in the upper Bays Formation (UTM 17 323271E 402419N [WGS 84/NAD 83]; Lat. 36.3423514 Long –82.949615) (Fig. 2-17). The bentonite was dated using U-Pb (Edwards et al., 1959; Huff et al., 1992) yielding an age of 454 $\pm$ 10 m.y. An estimated 1,140 km^3 of ash were expelled during this massive explosive eruption. The eruption was situated between the southern Appalachians and Sweden (Huff et al., 1992). It was an estimated 8 on volcanic index (1-9 with a 9 never being recorded), and was similar in size to the eruption at Yellowstone 630,000 years ago (Huff et al., 1992). From analysis of light rare earth elements (LREE) in the T-4 bentonite (Millbrig) Huff et al. (1992) indicated that it was continental-crust derived.

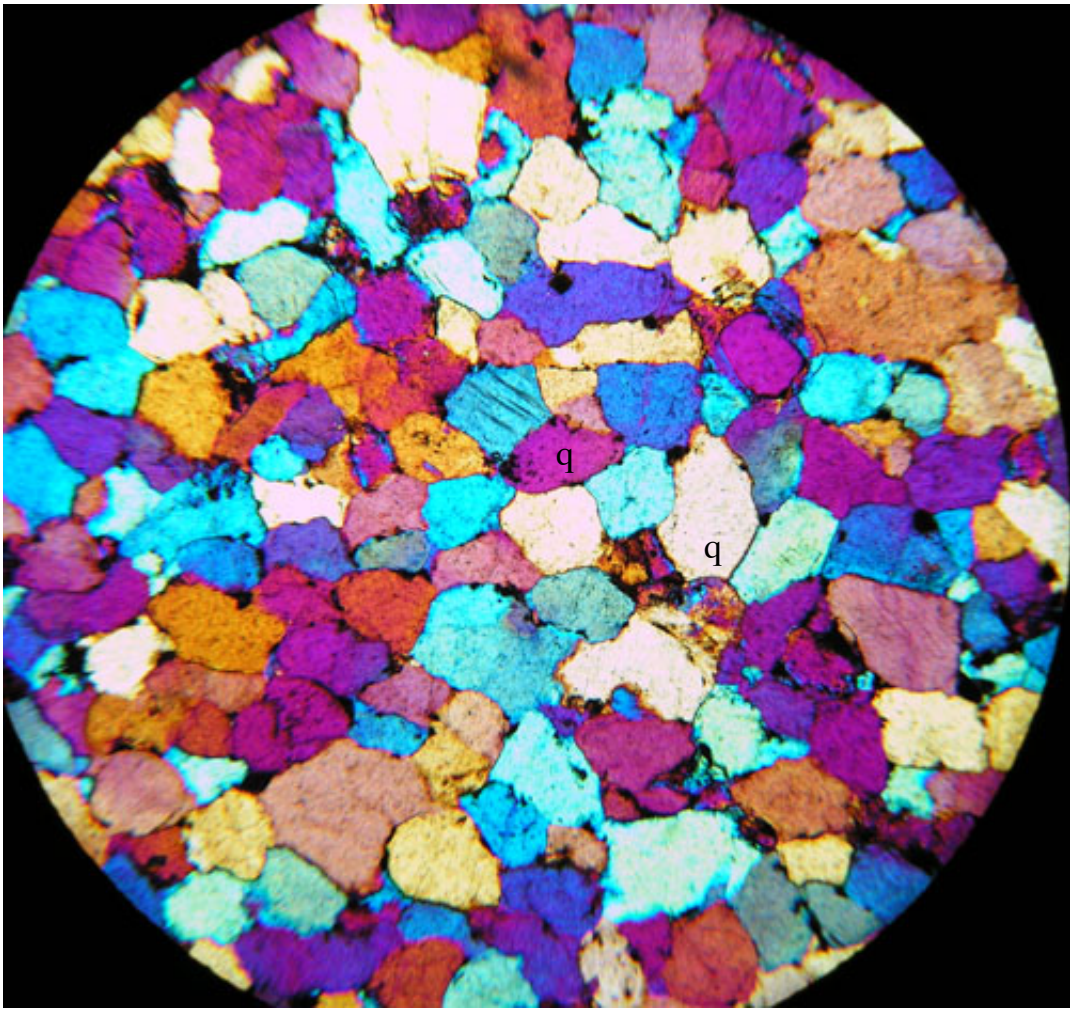

Figure 2-15. Bays Formation quartz arenite thin section with gypsum plate. Quartz displays nearly all undulatory extinction (q), and quartz overgrowths (field of view ~ 10.2 mm).

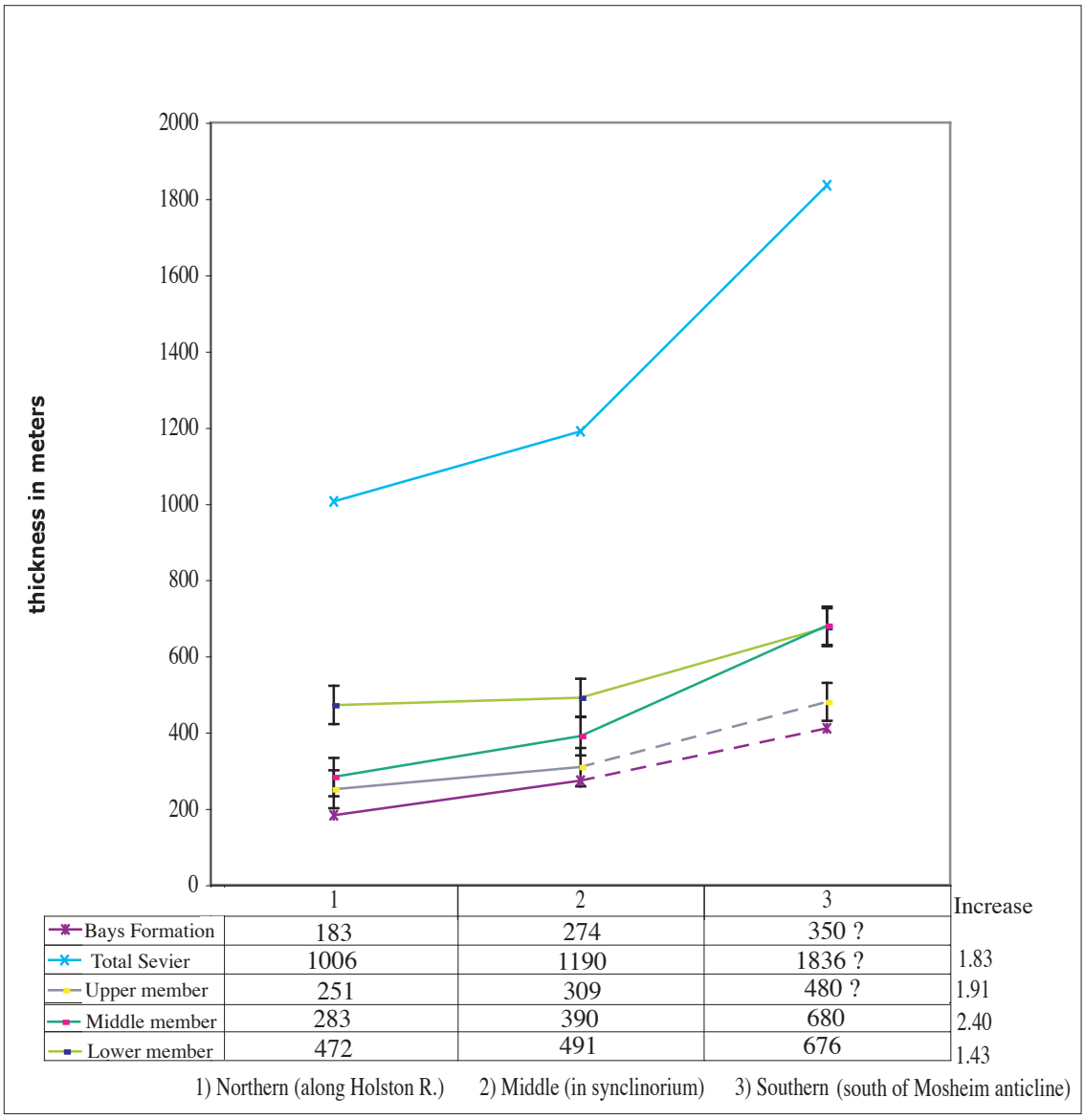

	1	2	3	Increase
Bays Formation	183	274	350 ?	
Total Sevier	1006	1190	1836 ?	1.83
Upper member	251	309	480 ?	1.91
Middle member	283	390	680	2.40
Lower member	472	491	676	1.43

1) Northern (along Holston R.) 2) Middle (in synclinorium) 3) Southern (south of Mosheim anticline)

Figure 2-16. Sevier basin thickness estimates based on estimated sections in the study area. The thickness estimates of the upper member of the Sevier Shale and the Bays Formation are based on averaged increased thickness of other exposed units. Lines are dashed where extrapolated. Because thicknesses are extrapolated, basin structure may only be interpreted.

Figure 2-17. Millbrig bentonite (white) and cleaved sandstones in the Bays Formation, TN Hwy 70 (McCloud quadrangle).

Rodgers (1953b) and Cummings (1962) concluded that the Bays Formation formed in a marginal marine tidal flat. It is possible that interbeds of arenites and red (sometimes carbonate rich) sandstones represent episodic transgression and regression. A tremendous change in depositional environment may be encountered at the contact between the Bays Formation and the Martinsburg Formation. This contact is exposed at a quarry on Tennessee Hwy 347 (UTM 17 332687E 402994 [N WGS 84/NAD 83], Lat. 36.3990463, Long. –82.863395) (Fig. 2-18) and may represent the Rocklandian unconformity (Ettensohn, 2004). The presence of the worm burrows found in the Bays Formation suggest that it was formed in a shallow marine environment.

Martinsburg Formation

The Martinsburg Formation, originally named by Geiger and Keith (1891), is the youngest Middle Ordovician formation in the Bays Mountain synclinorium. It represents the second (type Taconian) tectophase of Ordovician foreland basin formation (Shanmugam and Lash, 1982; Pope and Read, 1998). Here it consists of greenish-blue gray, fossiliferous, calcareous, shale and limestone. Thin layers of altered volcanic ash occur in the formation in other parts of the Valley and Ridge, but were not found in the study area. The lower part of the Martinsburg Formation consists of interbedded fossiliferous limestone and shale with increasing shale content toward the middle of the formation (Walker, 1980; Lemiszki, personal communication 2004) (Fig. 2-19). This is consistent with what was observed in the study area and what is described in the intensely studied portion of the Thorn Hill section (Walker, 1985).

The top of the Martinsburg Formation is eroded, but approximately 122 m (400 ft) of the formation is preserved. Fossils identified by the U. S. Geological Survey (Cummings, 1962) in the formation include: *Oniella fertilis; Rafinesquina aff.,*

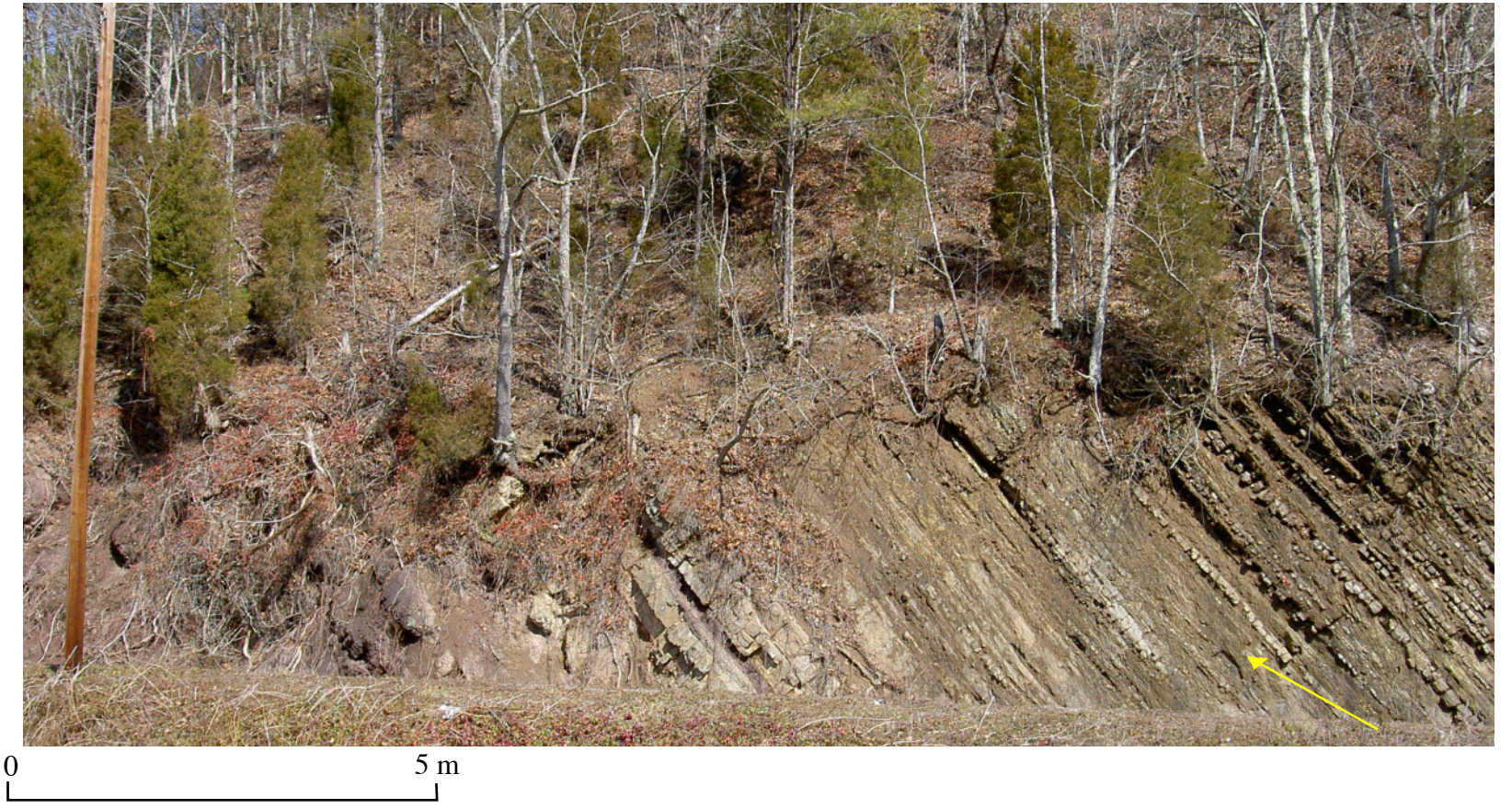

Figure 2-18. Contact between Bays and Martinsburg Formations (yellow arrow) on Hwy 347 (Stony Point quadrangle) possibly representing the Rocklandian unconformity (~ 2 m.y. removed) (Holland, 2003). (UTM 17 332687E 402994 [N WGS 84/NAD 83], Lat. 36.3990463, Long. - 82.863395.

(a)

(b)

(c)

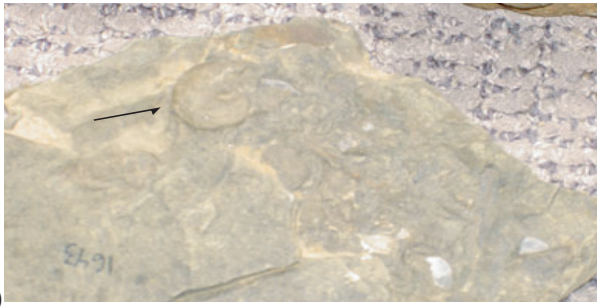

(d)

Figure 2-19. (a) Martinsburg Formation (middle member) along Highway 347 (Stony Point quadrangle). Fossils include: brachiopods (b,c), *Rafinesquina aff., Trentonensis sp.,* and *Sowerbyella sp*. and (d) a gastropod (~3 cm).

Trentonensis sp.; *Ceraurus aff. C. pleurexanthemus; Sowerbyella sp.; Modiolopsoid (clams Whiteavesia); Raymondites cf. R. ingalli*; and *Encrinurid* trilobites.

Biostratigraphic Correlation

Graptolites occur in the lower member of the Sevier Shale. Samples were collected from the lowermost part of the lower member of the Sevier Shale (Station #853)(UTM 17 330963E 4014079N [WGS84/NAD83]) and were sent to Prof. Stan Finney, CSU Long Beach (Fig. 2-20). Identified fossils include *Thamnograptus sp., Didymograptus sp., Glossograptus ciliatus, Cryptograptus sp., Nemagraptus gracilis, Dicellograptus gurleyi, Dicellograptus bispiralis, Climacograptus meridionalis*, and *Dicranograptus nicholsoni* (Fig. 2-21).

The occurrence of *Dicranograptus nicholsoni* places the lower Sevier member in the uppermost portion of the *Nemagraptus gracilis* zone (lower Llandeilo). Generally, the Athens may be a correlative with the lower member of the Sevier Shale. Since this locality is younger than the zone correlated with the Athens to the southwest, further sampling throughout the Sevier Shale in this portion of the basin may provide evidence for northeasterly basin depocenter migration.

Conodonts are small, variously shaped, calcium phosphate toothlike fossils from small vagile (mobile) marine organisms. These fossils provide an excellent opportunity to correlate local stratigraphic sections with standard conodont zones and subzones.

Two samples were collected by Dr. John Repetszki, U.S.G.S., for biostratigraphic analysis. One sample was collected from the upper member of the Sevier Shale and the other from the Bays/Martinsburg Formation contact. The sample (JR7-17-03G [USGS fossil location number 11955-CO]) was collected from a silty,

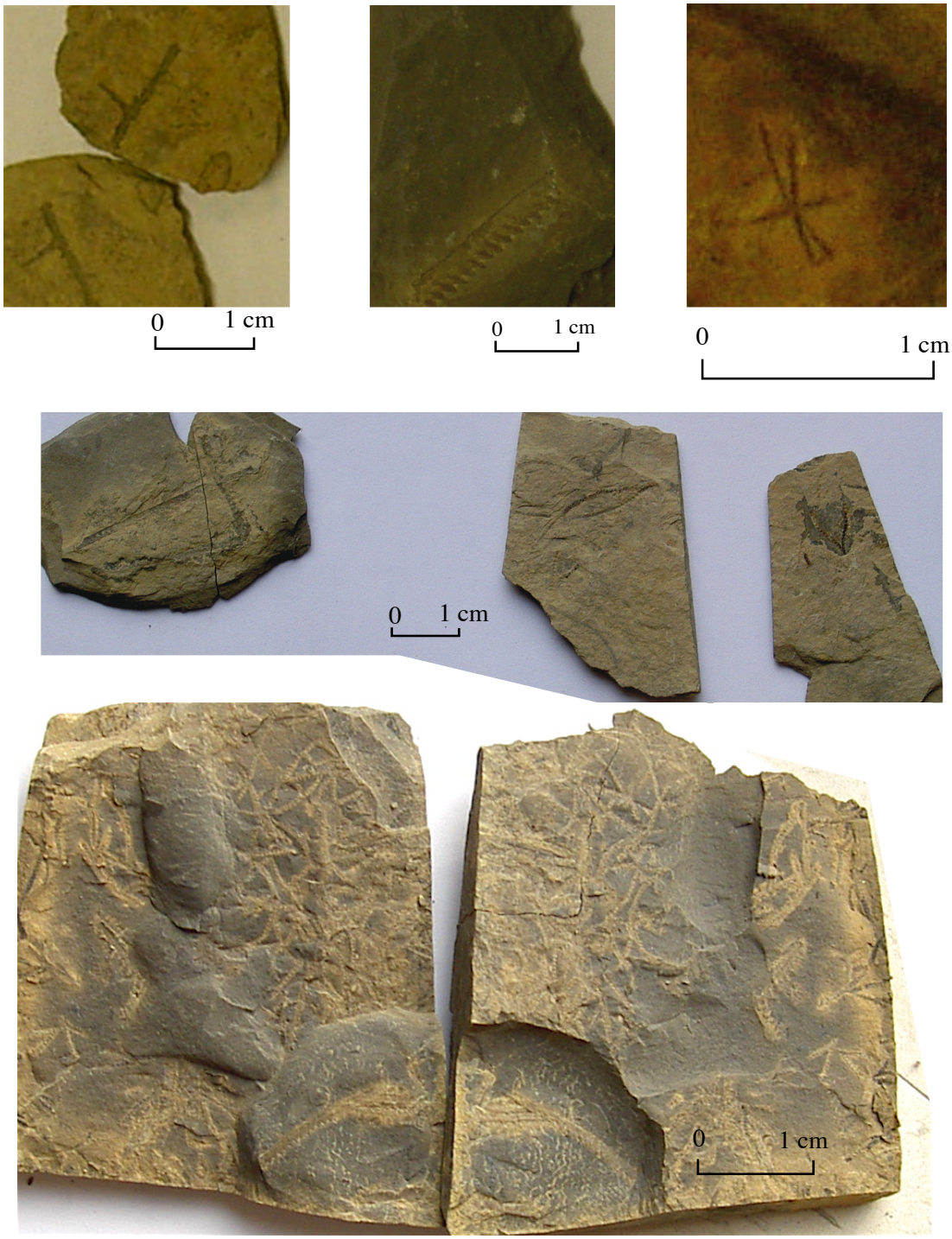

Figure 2-20. Selected graptolite specimens submitted to Prof. Stanley Finney (CSLB) for identification from the lower member of the Sevier Shale. Identified graptolites confined the age to the uppermost *Nemagraptus gracilis* zone include: *Thamnograptus, Didymograptus, Glossograptus ciliatus, Cryptograptus, Nemagraptus gracilis, Dicellograptus gurleyi, Dicellograptus bispiralis, Climacograptus meridionalis, Dicranograptus nicholson.*

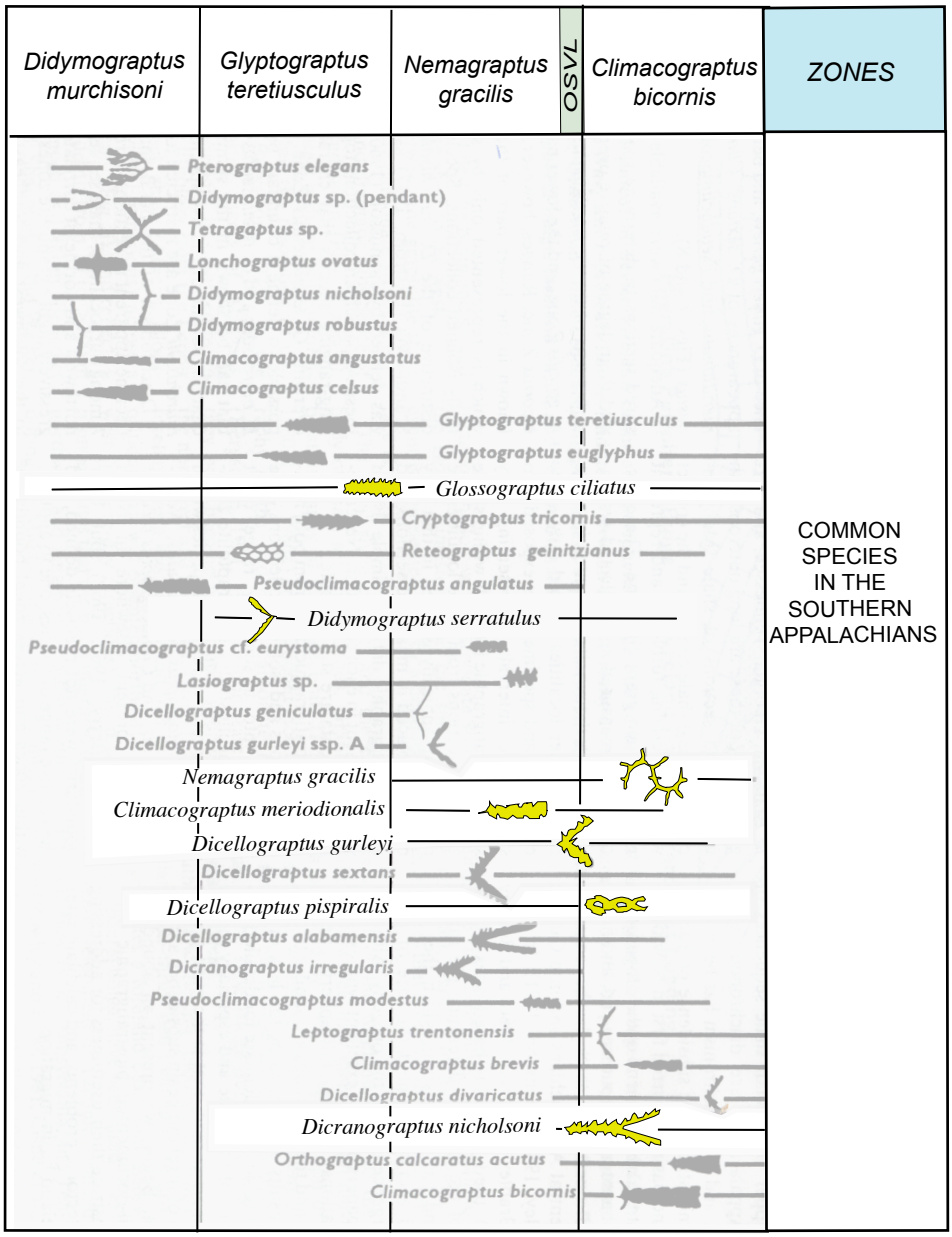

Figure 2-21. Graptolite zonation and relative ranges of common species (light gray) in Middle Ordovician shale of southern Appalachians (50 localities) (Finney et al., 1996). Samples collected from the lower member of the Sevier Shale from this study (yellow) indicate they are from the uppermost portion of the *Nemagraptus gracilis* zone (green)(Finney et al., 1996).

medium-gray, bryozoan-rich limestone at Station # 668 along Bear Hollow Road (UTM 17 330241E 4023396N [WGS84/NAD83], 36.3407°N, 82.8916°W). A 9.5 kg sample was processed for conodonts. Approximately 4.52 kg of insolubles were discarded with no identifiable macrofossils seen. Then 180 g of 20 to 170-mesh insolubles were processed by heavy liquid separation. The conodonts recovered from the upper member of the Sevier Shale include: *Drepanoistodus suberectus, Panderodus gracilis, Plectodina sp.,* and 2 unassigned oistodontiform elements (J. Repetszki, written com., 2005). Other findings of note include numerous short fragments of graptolites preserved in 3-D and a conodont alteration index between 2 to 2.5, indicating that the host rocks were heated to between 60° to 140° C (J. Repetszki, written com., 2005).

All of the conodont taxa are relatively long-ranging at the level that they could be confidently identified. They indicate a Middle to end-Ordovician total possible age range, and is likely in the age of the *Amorphoganthus tvaerensis* zone or younger (Fig. 2-22). Based on biostratigraphic data collected from this study and from the literature, the age constraints for the Sevier Shale and Bays Formation are from 461 ± 2 m. y. to 453 ± 2 m. y. This agrees with the ages presented by Twenhofel et al., (1954) and Holland (2003) and is approximately 10 - 15 m. y. younger than that proposed by Drake and others (1989).

Quaternary Units

Late Tertiary - Quaternary colluvium, alluvium, and landslide deposits lie unconformably above the Paleozoic rocks. Alluvium was identified along the major and some minor streams throughout the study area. Major alluvial and terrace deposits were found along the Holston River and Lick Creek. The alluvium contained scattered cobbles, dominantly comprised of vein quartz and microcrystalline chert.

Figure 2-22. Upper Ordovician chronostratigraphic scale (modified from Holland, 2003) and preliminary chronostratigraphy for the units in the study area (yellow) as compared to Twenhofel et al., (1954) (blue), and Drake and others (1989) (lavender). The lower member (light green) of the Sevier Shale is fairly well delimited in the upper portion of the *Nemagraptus gracilis* zone (Finney et. al., 1996; Finney, pers. comm.). The Millbrig bentonite (orange) in the upper Bays Formation (Red) yielded U-Pb ages of 454 ± 10 m.y. (Edwards et al., 1959; Huff et al., 1992). The conodonts sampled from the upper Sevier Shale (blue) indicate that they are in the *Amorphoganathus tvaerensis* zone or younger. Conodonts sampled, the Milbrig bentonite and previous work (Twenhofel et al., 1954) helped to constrain the timing of Sevier-Blountian deposition. CSS—composite standard reference section (measures time in terms of rock accumulation), RO.—Rocklandian, KI.—Kirkfieldian.

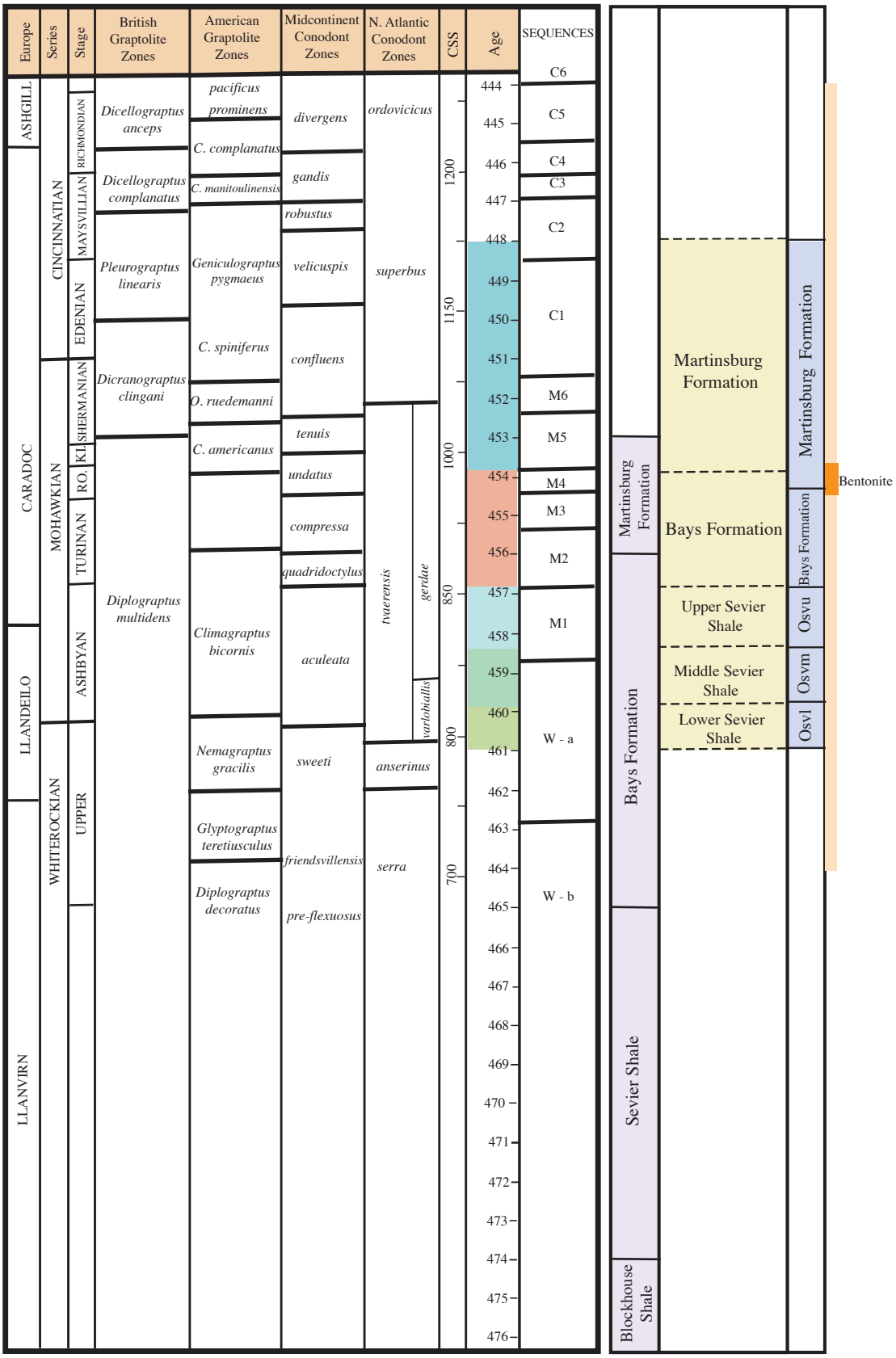
Europe
Series
Stage
British Graptolite Zones
American Graptolite Zones
Midcontinent Conodont Zones
N. Atlantic Conodont Zones
CSS
Age
SEQUENCES
ASHGILL
CARADOC
LLANDEILO
LLANVIRN
CINCINNATIAN
MOHAWKIAN
WHITEROCKIAN
RICHMONDIAN
MAYSVILLIAN
EDENIAN
SHERMANIAN
KI.
RO.
TURINAN
ASHBYAN
UPPER
Dicellograptus anceps
Dicellograptus complanatus
Pleurograptus linearis
Dicranograptus clingani
Diplograptus multidens
pacificus
prominens
C. complanatus
C. manitoulinensis
Geniculograptus pygmaeus
C. spiniferus
O. ruedemanni
C. americanus
Climagraptus bicornis
Nemagraptus gracilis
Glyptograptus teretiusculus
Diplograptus decoratus
divergens
gandis
robustus
velicuspis
confluens
tenuis
undatus
compressa
quadridoctylus
aculeata
sweeti
friendsvillensis
pre-flexuosus
ordovicicus
superbus
tvaerensis
gerdae
variabialis
anserinus
serra
1200
1150
1000
850
800
700
444
445
446
447
448
449
450
451
452
453
454
455
456
457
458
459
460
461
462
463
464
465
466
467
468
469
470
471
472
473
474
475
476
C6
C5
C4
C3
C2
C1
M6
M5
M4
M3
M2
M1
W - a
W - b
Martinsburg Formation
Bays Formation
Upper Sevier Shale
Middle Sevier Shale
Lower Sevier Shale
Martinsburg Formation
Bays Formation
Sevier Shale
Blockhouse Shale
Martinsburg Formation
Bays Formation
Osvu
Osvm
Osvl
Bentonite

Several (recent) landslide deposits were also found in the Bays Mountain synclinorium. These were likely due to erosion of the underlying upper Sevier sandy limestone member beneath the Bays Formation. Landslides are frequently the result of clear-cutting. Cobble-to-boulder-size blocks of overlying Bays Formation sandstones slid down small areas (usually perpendicular to strike) toppling trees and infilling small valleys previously marked on the topographic maps.

CHAPTER III

STRUCTURE

Regional Setting

The Valley and Ridge of East Tennessee is characterized by parallel northeast-striking thrust blocks (Safford, 1856). The study area is bounded to the northwest by the Saltville fault and Pulaski fault to the southeast. It consists of lower Cambrian to upper Ordovician age rocks that were deformed during the Alleghanian orogeny (Pennsylvanian-Permian) caused by collision of Laurentia with Gondwana (Hatcher, 1989).

Throughout the Valley and Ridge, the Rome Formation (Lower Cambrian) serves as the basal décollement with other detachments located in the Conasauga (Rodgers, 1953b), Chickamauga (shale and sandy limestone), and Upper Devonian - lower Mississippian Chattanooga Shale (Rich, 1934). As the foreland fold thrust belt (FFTB) formed, the already wedge shaped sedimentary package developed a critically tapered wedge with the thickness decreasing westward (Chapple, 1978; Davis et al., 1983).

The study area (Fig. 3-1; Plate I) is part of the Saltville-Carter Valley thrust sheet, overlain by the Pulaski thrust sheet to the southeast. Alleghanian faulting is thought to have occurred in-sequence from east to west with some local out-of-sequence and opposite verging faults (Woodward and Gray, 1985; Hatcher, 2004). The combination of folding and faulting has accumulated over 250 km of shortening (Hatcher, 1989). The study area differs strikingly from the rest of the Valley and Ridge

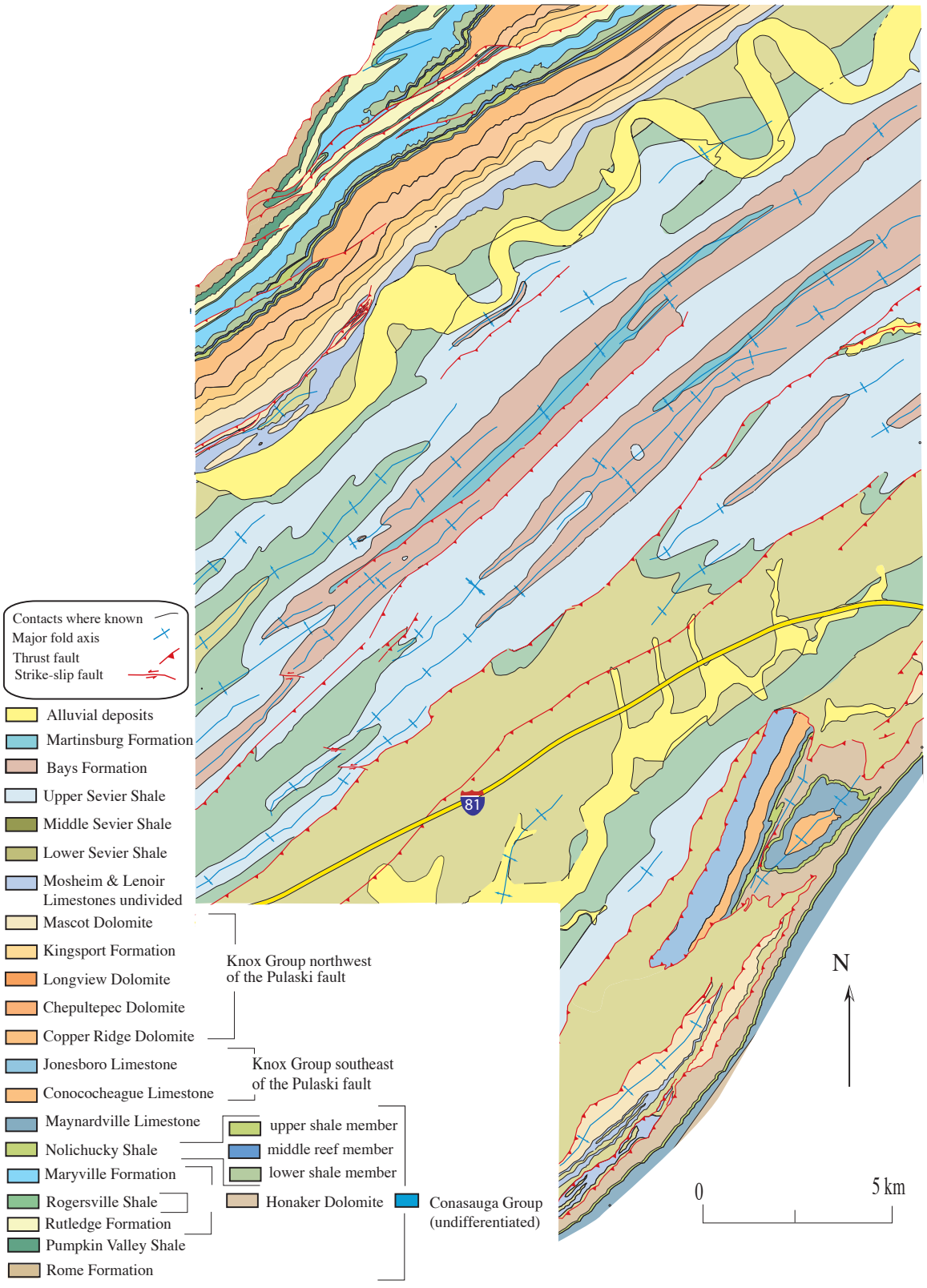

Figure 3-1. Geologic map of the study area showing major structures and stratigraphic units. See Plate I for details.

province in that it preserves: (1) a large northeast-striking, faulted synclinorium that extends more than 200 km to the southwest; (2) a large areal extent of Sevier-Blountian basin sediments; and (3) the highest topography in the Valley and Ridge in Tennessee.

One of the most important structures to be considered when addressing the stratigraphy in the area is bedding-plane faults (Rich, 1934; Yust, 1976) because their presence thickens stratigraphy and convolutes further structural and stratigraphic interpretations. While established thrust sheets exposing the Knox Group and older rocks bound the study area, many smaller thrusts are located in the Sevier Shale. Many small faults in the core of the synclinorium were mapped based on structural data collected and discontinuities in the stratigraphy outlined in the previous chapter.

Map-Scale Structural Features

Saltville and Associated Thrusts

The Saltville fault (Stevenson, 1885) and associated thrusts extend northwest of the study area (Fig. 3-2) and stretch from the valley of Sinking Creek, Craig County, Virginia across Tennessee into Georgia where they are known as the Rome fault (Hayes, 1891). It is bounded to the northwest of the study area by the overturned Greendale syncline (Haney, 1966).

Displacement varies along the trace of the Saltville fault and estimates for this area range from 6.5 km (4 mi) (Haney, 1966) to 110 km (Whisner, pers. com.). My estimate for total displacement of the Saltville thrust is a minimum of 21 km (13 mi) for this study determined from the Tennessee Division of Geology [T.D.G.] seismic reflection profile (TC-2) . The displacement greatly exceeds this, but this is the minimum measurable displacement. This estimate generally agrees with the previously accepted minimum of 20 km (Roeder et al., 1978; Milici et al., 1979; House and Gray, 1982).

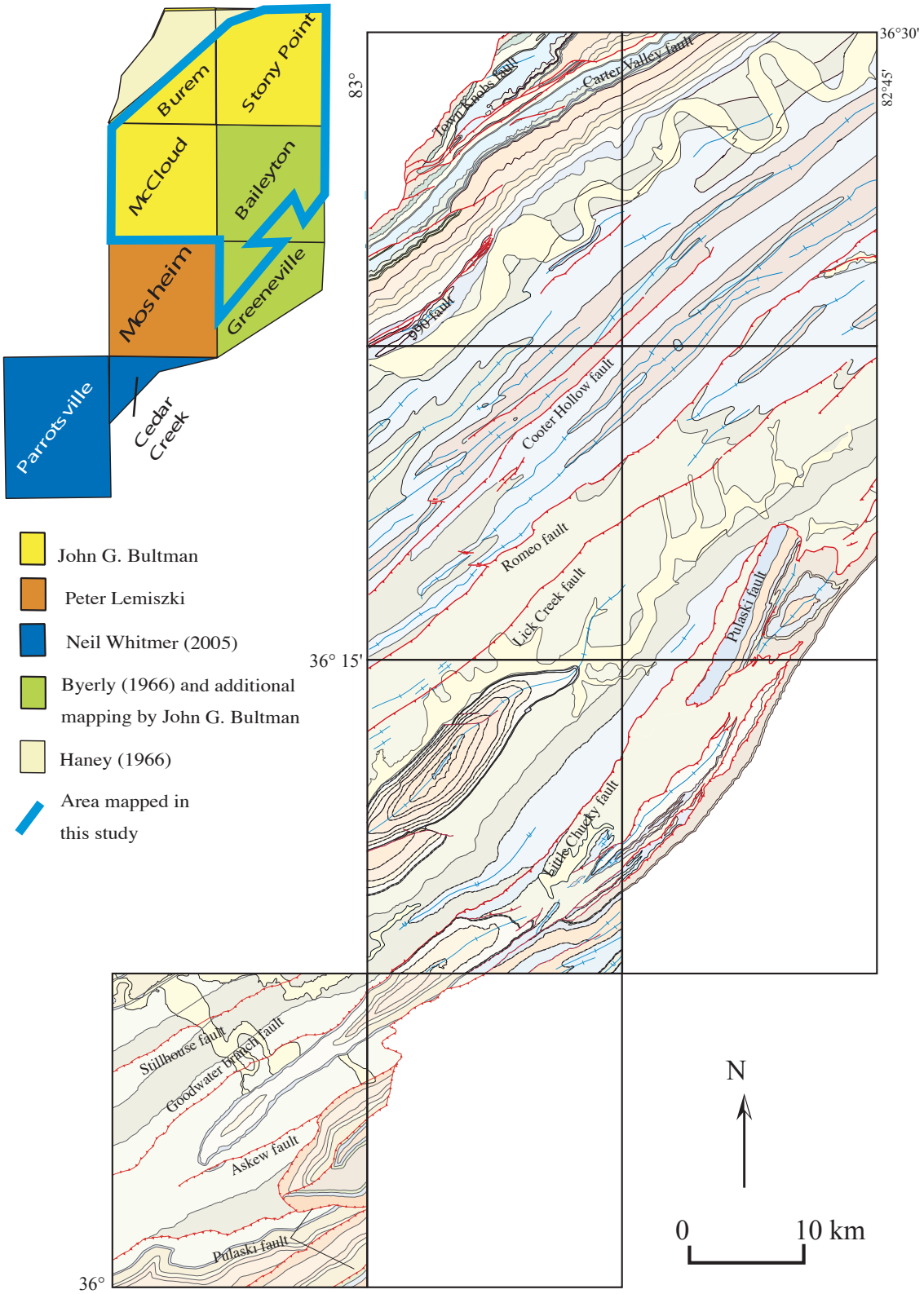

Figure 3-2. Faults recognized in the compiled study area. Names of faults are in the hanging wall. See Plate I for explanation of rock units.

Town Knobs and Carter Valley Faults

The Town Knobs fault (Fig. 3-2) and 990 fault (Milici et al., 1979) thrust Rome Formation onto Conasauga and Knox Groups footwall rocks. It extends northeastward from Hamblen Knob near Cherokee Lake through the northwestern border of the study area. The configuration of the Town Knobs fault closely parallels and is likely a splay of the Saltville fault. Evidence for the fault exists in the seismic reflection profile acquired by T.D.G. (Milici et al., 1979). Differences in lithology exist in the Maryville Limestone between the footwall and hanging wall of the Town Knobs fault (i.e., ~ 150 m of dolomite in hanging wall not found in the footwall) (Haney, 1966). Seismic reflection data further indicate a large displacement on the fault. The dip of the fault surface (calculated using the three-point method) ranges from 10° to 30° near the surface through the northern part of the study area (Haney, 1966). The Town Knobs fault joins the Saltville décollement under the Bays Mountain synclinorium making the minimum estimated displacement 12-13 km (8 mi).

The Carter Valley fault branches from the Town Knobs fault near Striggersville, Tennessee, and extends into Virginia where it merges with the Saltville fault (Rodgers, 1953a). Stratigraphic displacement ranges from near zero on the ridge east of Striggersville, Tennessee, where the fault zone originates, to 1.7 km (5,500 ft) in Carter Valley at the northeast boundary of the study area. The fault is not exposed, so evidence for the fault is stratigraphic discontinuity (Haney, 1966).

The Bays Mountain Synclinorium

The major structure of the study area is a doubly plunging synclinorium with doubly and singly plunging anticlines and synclines outlined by the Bays Formation

and Sevier Shale (Rodgers, 1953a, 1953b; Cummings, 1962). Many of the large structural features recognized in the Bays Formation may also be inferred from the topography (Plate II).

Large individual folds of the Bays Formation in the synclinorium have been described in detail by Cummings (1962). A more in-depth look at the deformation may be observed when comparing the map-scale folding in the Bays Formation (Fig. 3-1; Plate II) to the mesoscopic folding of the Sevier Shale (Fig. 3-3; Plate II).

Cummings (1962) mistakenly thought the Sevier Shale, because of its highly contorted and fractured nature, would not be useful for addressing structural problems. Although this may be true related to some of the major map-scale structures in the study area, the Sevier Shale (since it is structurally weaker) absorbed most of the deformation throughout the area and subsequently reveals many previously overlooked structural features. This may most easily be illustrated at a roadcut along I-181 (Fig. 1-2) northeast of the study area where tight overturned folds and several thrusts in the Sevier Shale underlie the open folds (outcrop scale) of the Bays Formation preserved on the ridges above the roadcut. Here it is clear that the structure in the Sevier Shale is disharmonic with the overlying structure in the Bays Formation.

In many ways the contrast in lithology between strong and weak units directly relates to the scale of the study. The study area may be divided in this manner (increasing in the total amount of shortening and decreasing in lithologic competency):

1) Map-scale structural features – Knox Group and Bays Formation
2) Mesoscale-microscale structural features – Martinsburg Formation and Sevier Shale

Figure 3-3. Profile in the upper Sevier Shale depicting folds, faults, and contrasting cleavage. The fault in the northwest portion of the segment continues more than 25 m to the northwest.

The strong structural-lithic unit in the study area is the Knox Group. The Bays Formation is mixed but generally strong compared to the incompetent units of the Sevier Shale. The key to understanding the structure of the study area is understanding the delicate nature between the structural features at all scales. Many previous workers approached this portion of the study area by looking only at the large structural features that are commonly outlined by the topography (Fig. 1-4). It is essential when constructing a geologic map that the details of the weaker units be taken into account.

The major folds of the study area behave in the manner described above. The Bays Formation was deformed into parallel-concentric folds. Generally, Bays Formation folds are more open than those in the Sevier Shale and are predominantly doubly plunging. The overall package of rocks in the study area exhibits disharmonic folding (Fig. 3-4). As a result of the relative movement of the competent units, the incompetent layers were subjected to inhomogeneous simple shear. In many cases there was likely a rotational component to the stress (Yust, 1976; Ohlmacher, 1991; Ohlmacher and Aydin, 1995, 1997). Strain was manifested in the incompetent layer as shearing, folding, or cleavage. Local change in the plunge direction is related to undulations in the map-scale folds and a likely pivoting of the fold axes (as a result of local faulting) (Fig. 3-5) (Cummings, 1962).

Detailed geologic mapping has delineated previously unrecognized faults in part of the Bays Mountain synclinorium (Fig. 3-2). The Cooter Hollow, Romeo, and Little Chucky faults have relatively small displacements. The Lick Creek fault, a splay of the Saltville, is the detachment for the Mosheim anticline and has an estimated minimum displacement of 12 km based on T-2 seismic reflection line (Milici et al., 1979). Four fault zones have been recognized and named in the study area (Fig. 3-2):

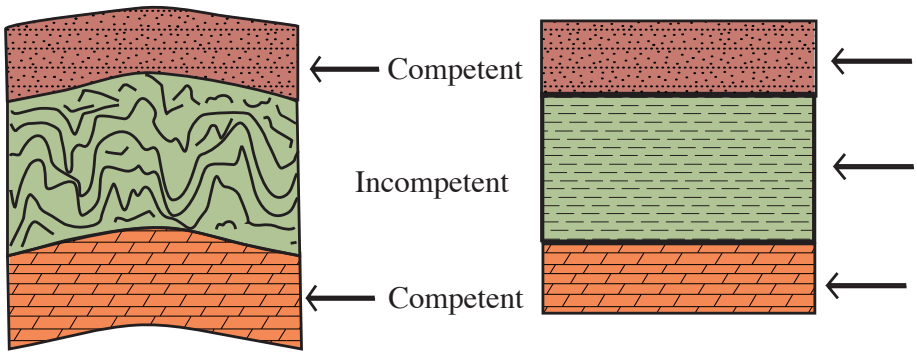

Figure 3-4. Disharmonic folding of the Sevier Shale (green) between strong structural lithic units of the Bays Formation (red) and Knox Group (orange).

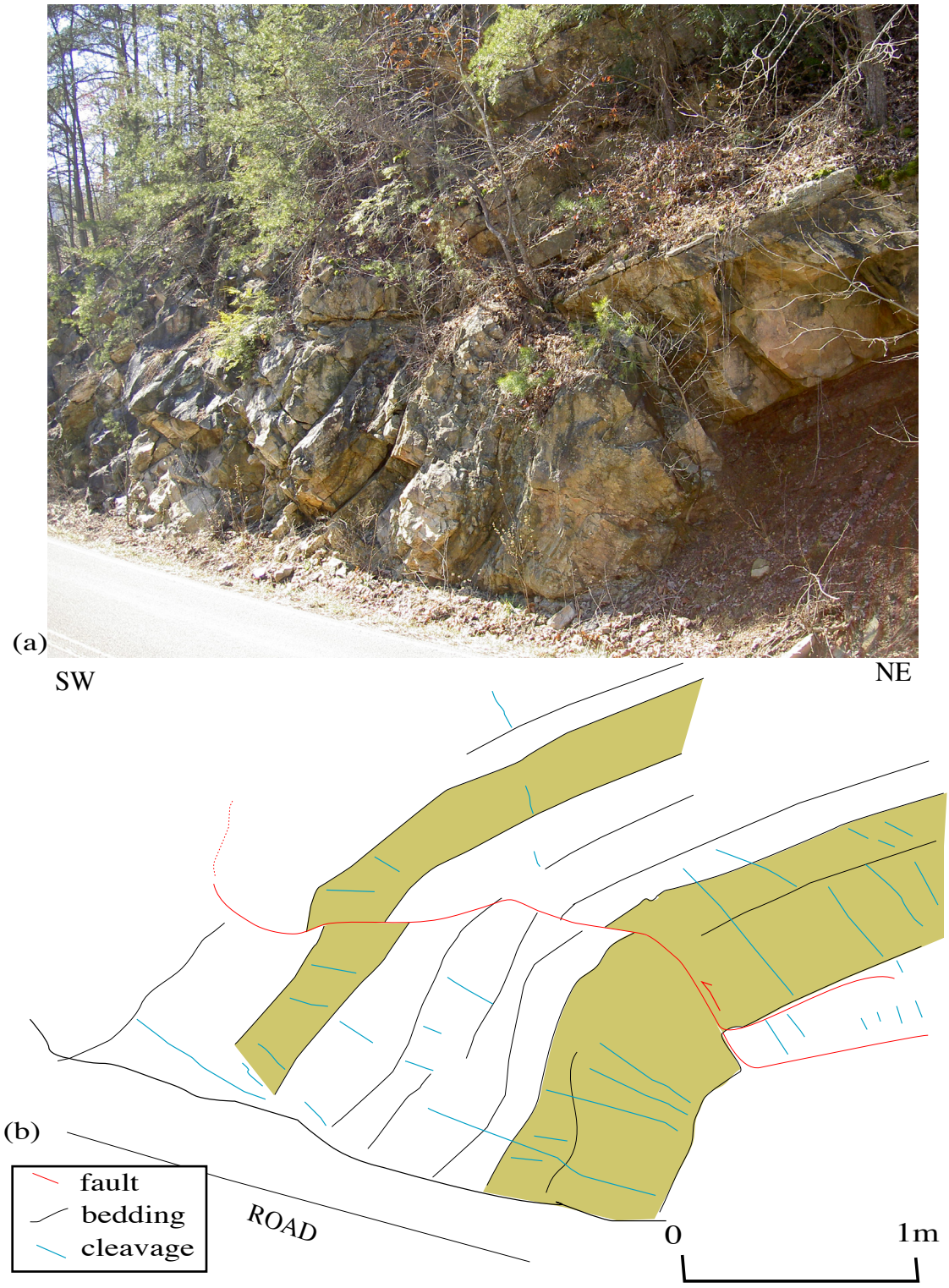

Figure 3-5. Small backthrust in the Bays Formation at Lauderback Gap on Highway 347 (Stony Point quadrangle)(a). Slip occurs along beds in the red siltstone as well as on the fault plane (b). Displacement decreases to the southwest.

1) The Cooter Hollow fault trends parallel to Cooter Hollow and Butcher Valley at the base of Brushy Mountain and associated ridgeline (Stony Point and McCloud quadrangles). More shearing and slickensided calcite veins, and missing units provide evidence for the fault. Previous authors also recognized a similar fault in the synclinorium. Cummings (1962) depicted a thrust in the same vicinity and Yust (1976) depicted the fault in his cross section (breaking the Knox Group but not surfacing).

2) The Romeo fault (trending NE-SW) lies at the southeast base of Short and Bluff Mountains. Evidence for this fault may be found from the abundance of outcrop scale faults along the base of these ridges, slickensided dismembered calcite veins in soil (calcite chips), repetition of units (Fig. 3-2), and intense pressure solution cleavage; This is indicated by zones of slickensides, mesoscale faulting, and intense cleavage with highly varied dips. This, coupled with the stratigraphic discontinuity, provides evidence for the placement of a fault.

3) The Lick Creek fault lies northwest of the Mosheim anticline and strikes NE-SW. Evidence for this fault may be found in T-2 seismic reflection profile (Milici et al., 1979), repetition of units (Fig. 3-2), intense pressure solution cleavage, and greater deformation of the footwall relative to the hanging wall. This is indicated by zones of slickensides, mesoscale faulting, and intense cleavage with highly varied dips. This, coupled with the stratigraphic discontinuity, provides evidence for the placement of a fault.

4) The Little Chucky fault extends the length of the study area and to the southwest is basal décollement for the northeastern part of the Oven Creek anticline. This portion of this fault was previously interpreted as

the northwestern boundary of the Babbs Knobbs flap of the Pulaski fault (Hardeman, 1966; Byerly, 1969). The remaining southwestern portion of the present fault configuration extends through the southeastern portion of the Mosheim quadrangle (Fig. 3-2) (Lemiszki, 2003). Evidence for this fault consists of the stratigraphic discontinuity (Fig. 3-2), slickensided calcite veins in soil (calcite chips), intense pressure solution cleavage and increased deformation indicating a fault zone. In the Mosheim quadrangle Lemiszki (2003) truncated the fault against a backthrust.

Many mesoscopic scale thrusts exist in the study area. These smaller faults were observed in individual exposure often representing portions of anastomosing faults, or en echelon thrusting (Fig. 3-6) (Aydin, 1988; Ohlmacher, 1991; Olmacher and Aydin, 1997) within a larger fault system like that seen at the I-181 roadcut. Quite frequently the Knox Group acts as "basement" and the dark gray lower member of the Sevier Shale acts as the weak basal detachment (Cummings, 1962).

Pulaski Fault

The Pulaski fault (Fig. 3-2) is one of three major faults in the Valley and Ridge of East Tennessee (Hatcher, 1989). Minimum horizontal displacement along the Pulaski fault in the study area is as little as 5 km (3 mi) (Byerly, 1969), and as much as 100-110 km (Bartholomew, 1987). The minimum displacement may be as much as 100 km based on seismic reflection profiles (Milici et al., 1979). Since this study focused more on the footwall rocks of the Pulaski fault, minimum displacements were not calculated for this area.

The extent of the Pulaski fault, originally recognized by Campbell (1925) and later by Butts (1933), is over 575 km (350 mi) from Rockingham County, Virginia,

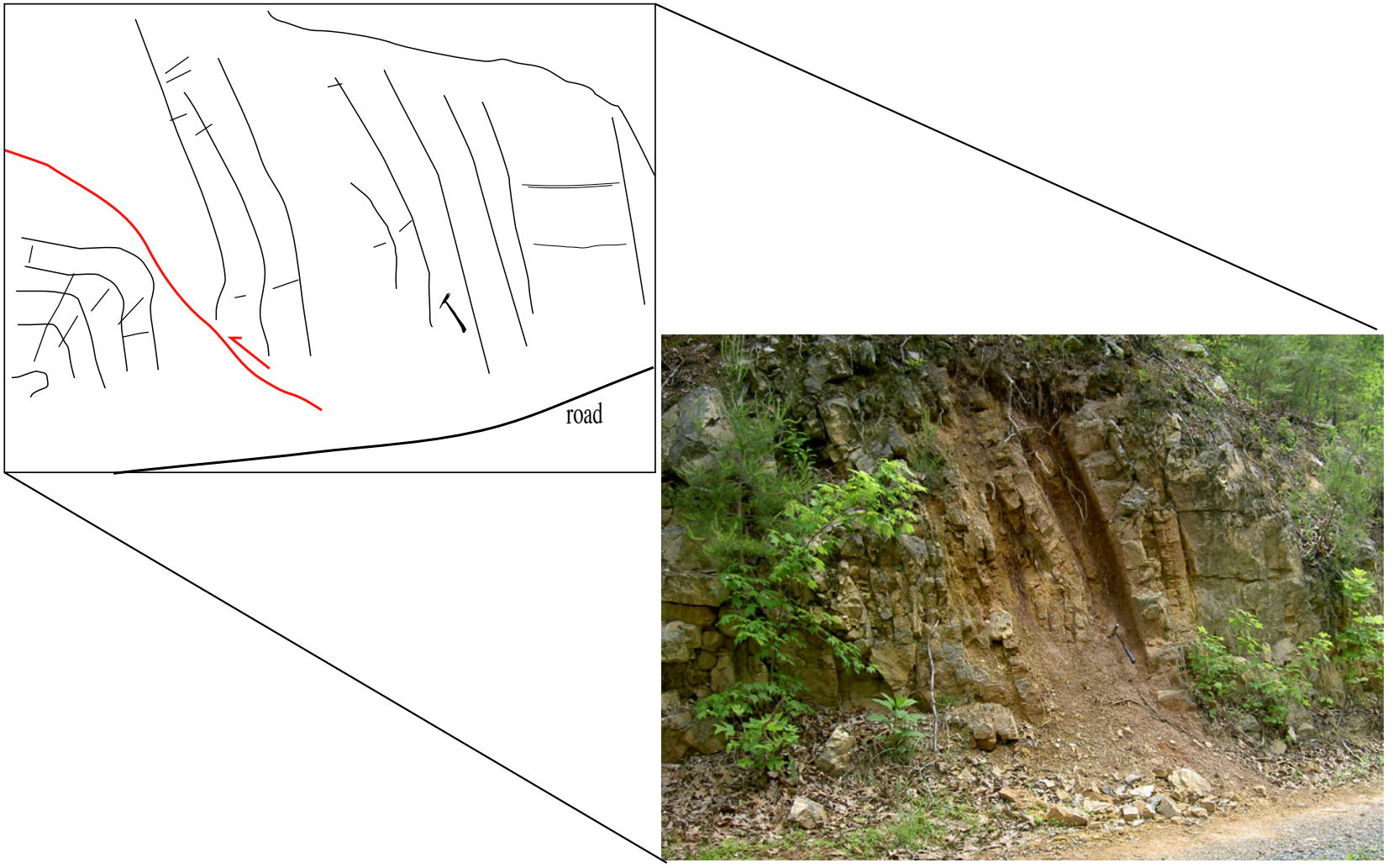

Figure 3-6. Small fault and fold in the Bays Formation near Wattenbarger Gap Road (hammer head ~ 25 cm) likely associated with the Romeo fault zone. Joints are normal to bedding.

through Cocke County, Tennessee (and plausibly further southwest beneath the Great Smoky fault). The fault was mapped by Byerly (1969), Lemiszki (2003), and Whitmer (2005) throughout the southeastern portion of the study area and is the boundary for this part of the study. The dip of the Pulaski fault around the Babbs Knobs flap is 0 to 20° (Byerly, 1969).

Rodgers' (1953a, 1953b), and Byerly's (1969) work on the Pulaski fault were instrumental for this part of the study area (Fig. 3-7). The only segment of the Pulaski fault in contention is located on the northwestern extremity of the Babbs Knobs flap. Byerly (1969) noted that it would seem logical for the fault trace on the northwest edge of the Babbs Knobs flap to be mapped along the Jonesboro-Sevier contact. Byerly (1969) did not separate the Lenoir Limestone on his map but instead included it as a basal unit of the Sevier.

Byerly (1969) and this author mapped a fault zone in the Sevier Shale northwest of the Babbs Knobs flap defined by an intense zone of deformation. This fault zone, however, is now called the "Little Chucky fault," which Lemiszki (2003) mapped in the Mosheim quadrangle. This fault was already identified by stratigraphic discontinuity (Fig. 3-2), an intense zone of deformation, and was mapped less than a mile southwest of Byerly's configuration (Lemiszki, 2003). The Little Chucky fault is continuous along the previously recognized deformation zone; the Pulaski fault was moved to the Jonesboro-Sevier contact and merges with the Little Chucky fault at the northernmost edge of the Babbs Knobs flap (Fig. 3-8). The suspect Lenoir lithology was found only once along the Sevier-Jonesboro contact (along Baileyton Pike). Here the "Lenoir" did not display the typical nodular appearance, and contained approximately 5 m total outcrop. Elsewhere, better evidence exists where ribboned basal limestone in the Jonesboro was found adjacent to the Sevier Shale along Baileyton Pike indicating that the absence of upper Jonesboro, Lenoir,

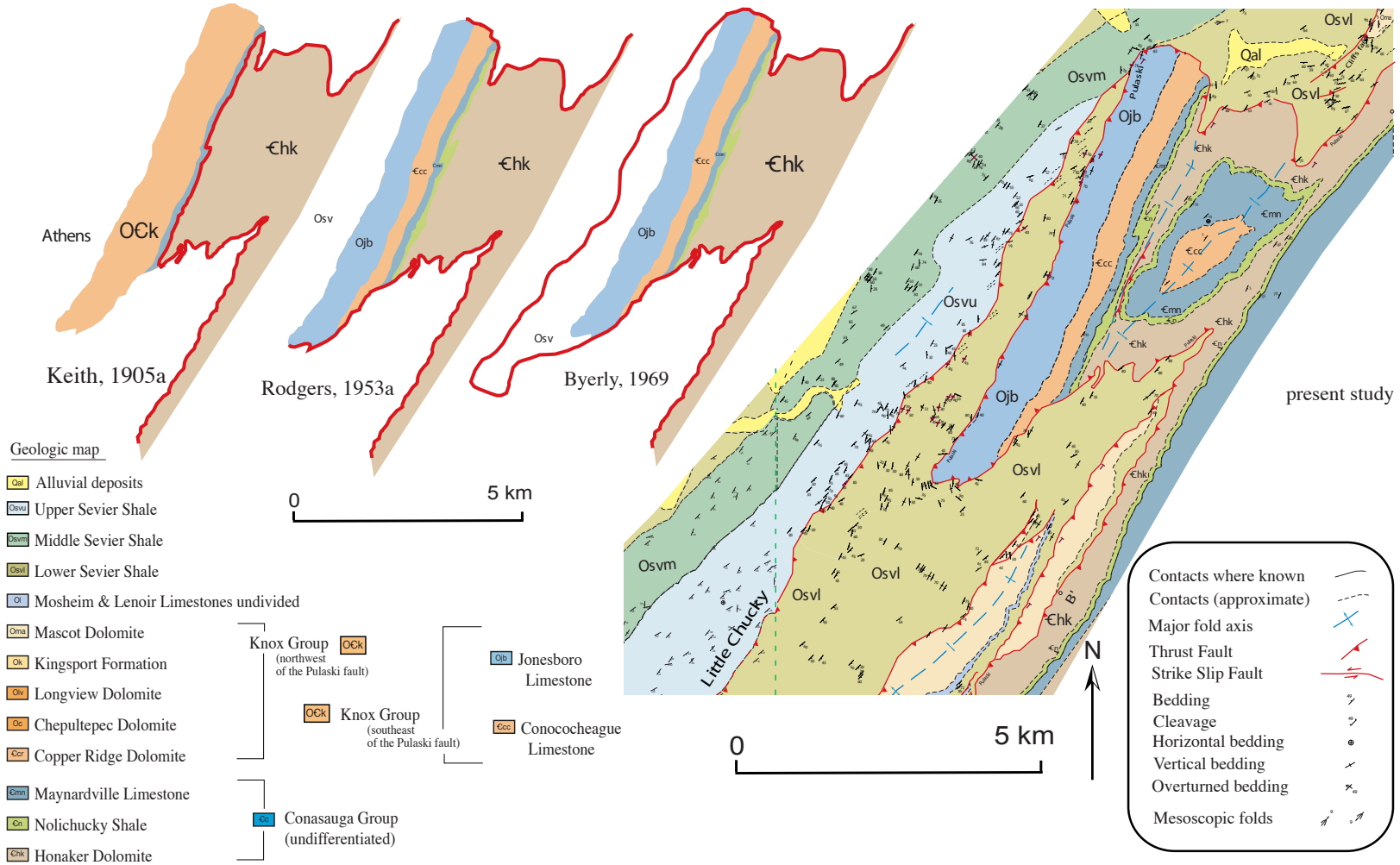

Figure 3-7. Past 100 years depicting the configuration of the Pulaski fault in the vicinity of the Babbs Knobs flap, Greeneville quadrangle. Little Chucky fault connected to Byerly's previous configuration at quadrangle boundary (dashed green line).

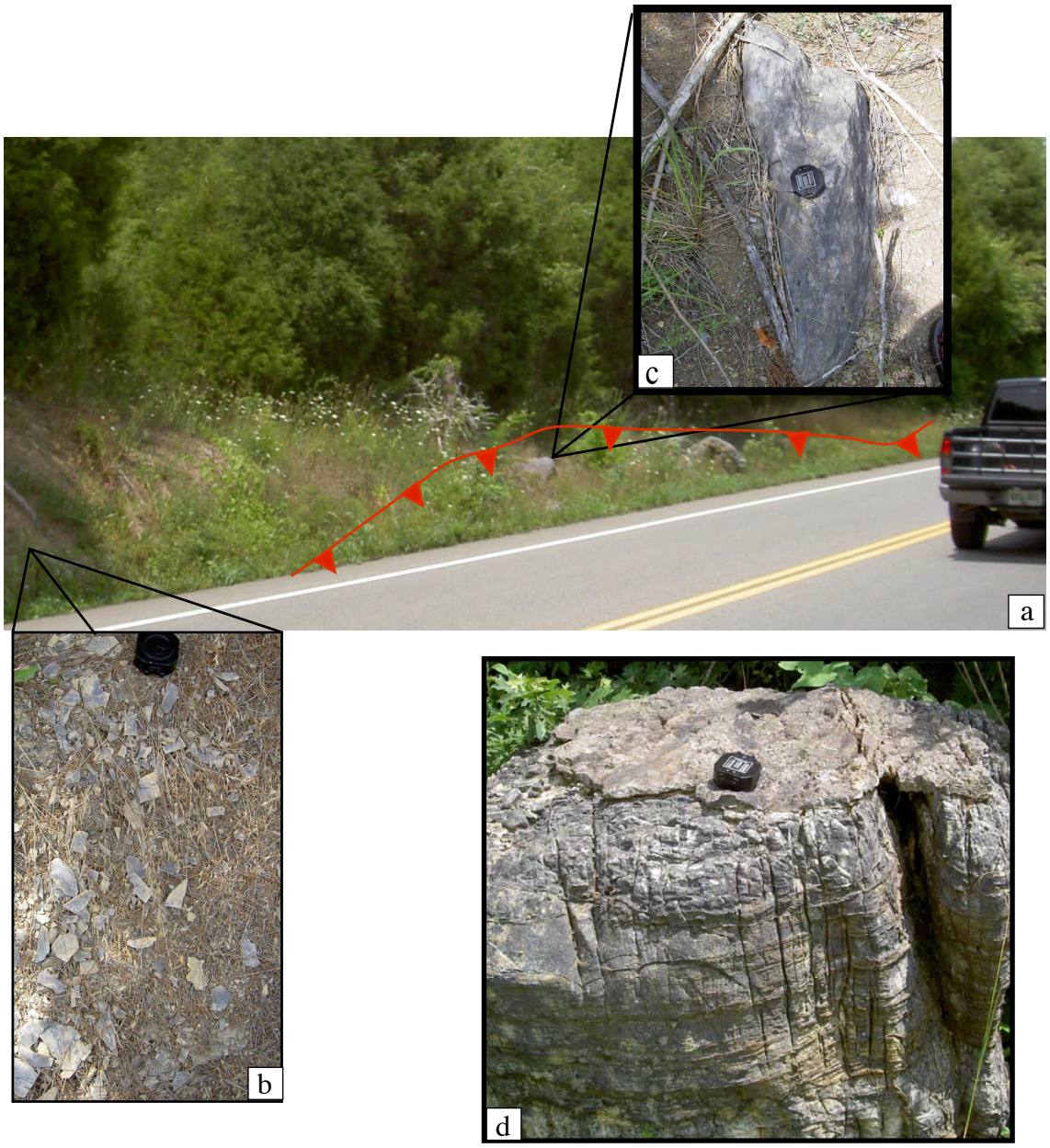

Figure 3-8. (a) Trace of Pulaski fault along Hwy 347-Spyder Lane (Baileyton quadrangle). The shale (b) along the Pulaski fault in the Babbs Knobs flap is cleaved and weathers as shown. Although it is identified as Jonesboro limestone, the limestone (c) is the only exposure along the Babbs Knobs flap trace that vaguely resembles Lenoir Limestone. Elsewhere (approx 1 km south) along the northwestern contact the ribboned Jonesboro Limestone (d) (base of the unit) is in contact with the Sevier Shale suggesting a stratigraphic discontinuity. Another deformation zone (Little Chucky fault) previously thought to be the Pulaski exists (Fig. 3-8) approximately 0.25 km northwest of this outcrop and may be traced across the Baileyton, Cedar Creek, Greeneville, Mosheim, and Parrotsville quadrangles (Lemiszki, 2003; Whitmer, 2005).

and Mosheim Limestones provide evidence for a stratigraphic truncation along the northwest boundary. This, coupled with the deformation zone noted at the Jonesboro-Sevier contact along the northwestern edge of the Babbs Knobbs flap, led me to this interpretation.

Mesoscale Structural Features

Bedding is the only primary planar structure preserved in the study area. The average strike (northeast-southwest) of bedding (N 052°) throughout the area is typical of the Valley and Ridge (Fig. 3-9) in this area. It should be noted that bed thickness, like stratigraphic thickness, varies at all scales throughout the study area and influences mesoscale structural features.

Ohlmacher (1991) made a detailed structural investigation of outcrops along a 1.3 km stretch of Interstate 181 in Kingsport, Tennessee. His research recognized progressive deformation sequences and geometric relationships among veins, faults, joints, folds, and pressure-solution surfaces formed during several stages of deformation of the upper Sevier Shale (limestone member). Ohlmacher (1991) formulated mathematical models to invert deformation to stress and then compared those to the outcrop. He found that the frictional resistance along faults, the angle made by the greatest compressive stress direction, and the fault plane controlled the local stress state. Contrasting styles of fault resistance were interpreted to result from periodic slip phases deformation based on the amount of fluid pressure.

Ohlmacher and Aydin (1995, 1997) focused on complex vein patterns, solution surfaces and faults at the I-181 outcrop in the Bays Mountain synclinorium. They noted contrasting structural patterns involving bed-parallel en echelon thrust fault arrays and indicated three cleavage forming events. They defined seven stages of deformation

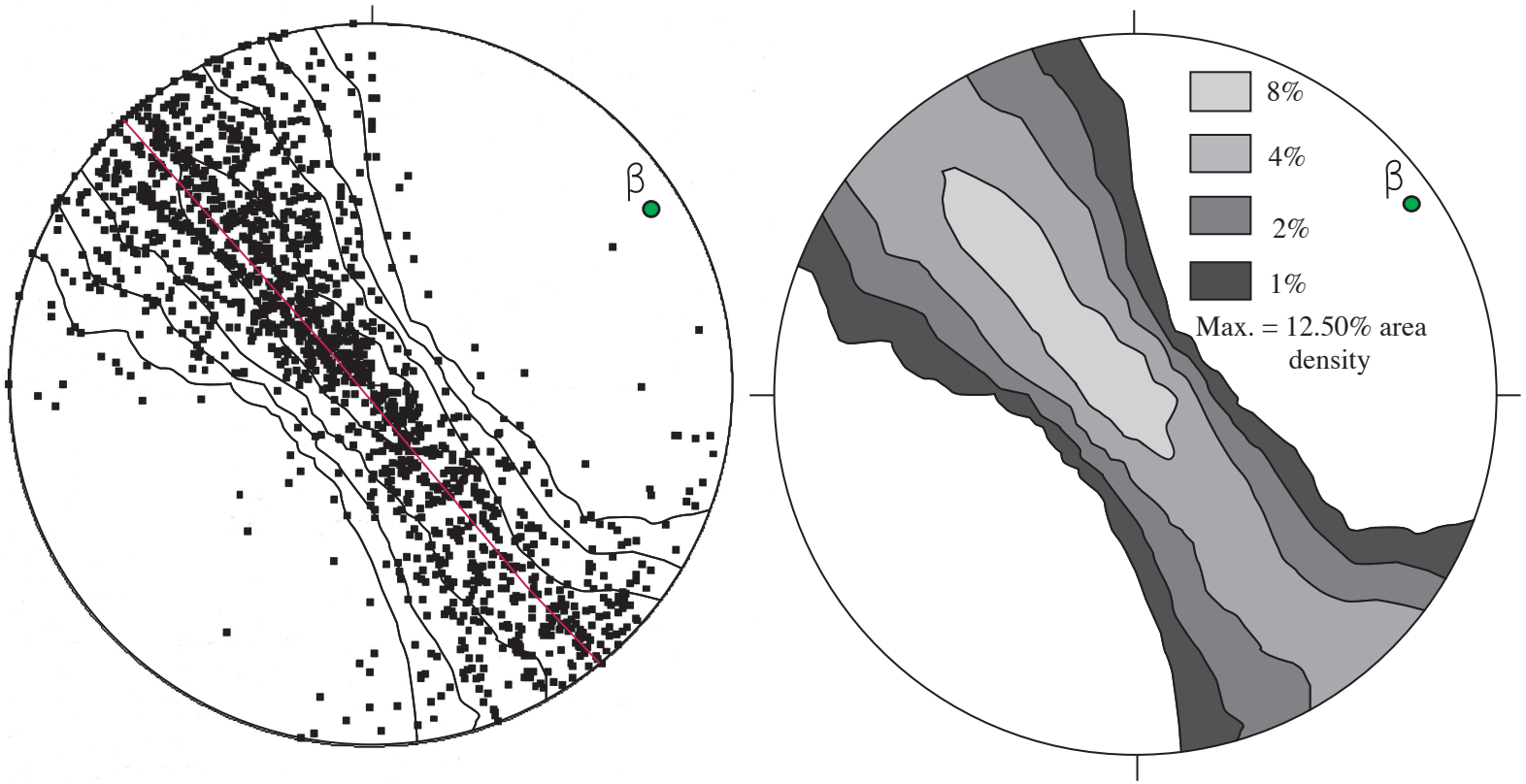

Figure 3-9. Lower-hemisphere, equal-area stereographic projections of 1,712 poles to bedding (this study) in the Bays Mountain synclinorium, northeast Tennessee. (a) Scatter plot of poles to bedding with cylindrical best fit great circle (red). Cylindrical folds plot along the great circle of the major structure (b) The same data contoured (1%, 2%, 4%, 8% per 1% density) using GeoOrient© v. 9.2.6 by Rod Holcombe, University of Queensland, AU (2005). The majority of bedding orientations indicate that they are overturned and verging to the northwest.β axis (similar to axial plane dip to the northeast) of the great circle (green) is 052, 3°.

and identified three nested fracture networks that were potential pathways for fluid migration.

Pressure solution, slaty, and fracture cleavage are dominant throughout the area (Swingle, 1962; Yust, 1976). Both types commonly occur in the same exposure and have different attitudes (Yust, 1976). Pressure solution cleavage associated with folds typically produces an axial-planar orientation in finer-grained lithologies. Fracture cleavage is common in sandy limestone units (Fig. 3-10). Cleavage planes in more competent units fan in the fold hinges (Fig. 3-11). Refracted cleavage was commonly observed in Bays Formation interbedded arenites and siltstones (Fig. 3-12), and sometimes between the siltstones and shales of the Sevier Shale. Fanned cleavage was observed throughout the study area indicating that the fold tightened further after cleavage development. Cleavage associated with folds in the lower Sevier Shale typically possess axial planar orientation with pencils (L_{1x0}) forming in the hinges. In few instances, nonaxial planar solution cleavage transects axial planar cleavage and may indicate episodic compression events (Fig. 3-3).

Cummings (1962), Yust (1976), and Ohlmacher and Aydin (1995) all recognized more than one cleavage throughout the synclinorium. Ohlmacher and Aydin (1995) defined seven stages of deformation (Fig. 3-13) and concluded that in some places the first and second cleavage developments in the Bays Mountain synclinorium are deformed. For this study two cleavages were noted at a few exposures in the region (Fig. 3-3, 3-10, 3-11, 3-13).

Pressure solution cleavage duplexes were noted on surfaces between stepping thrust faults. Aydin (1988) interpreted cleavage duplexes as a type of contractional stepover in the study area. Fault-normal veins are associated with parallel faults that have a low frictional resistance to slip. The veins are opening fractures perpendicular to the slickensides on the bounding faults (Olmacher and Aydin, 1995, 1997).

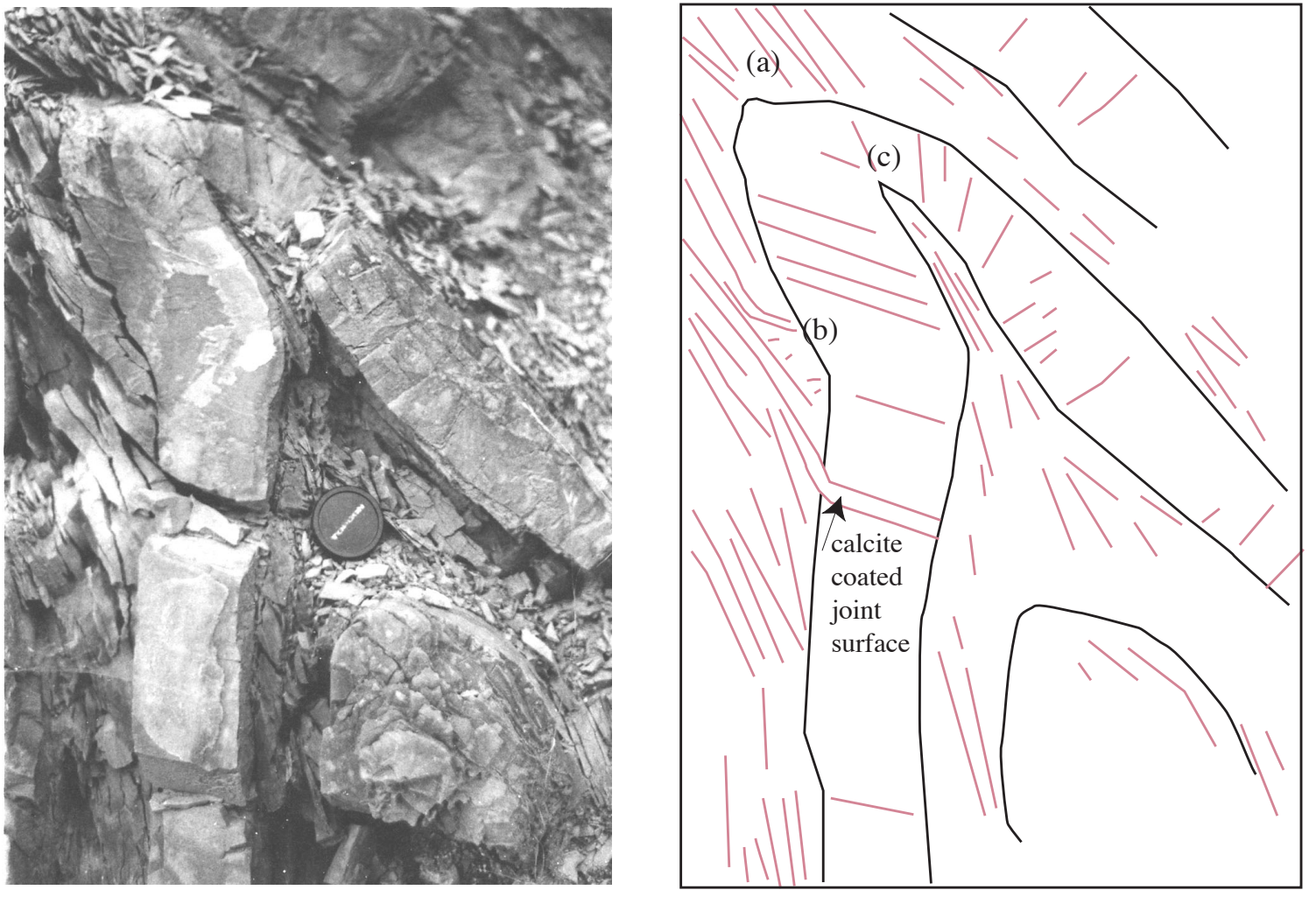

Figure 3-10. Tight fold and hinge collapse zone (Ramsay and Huber, 1987) from the compiled study area (Yust, 1976), illustrating axial planar cleavage (a) in the hinge that refracts (b) and is fanned (c) in the siltstone bed.

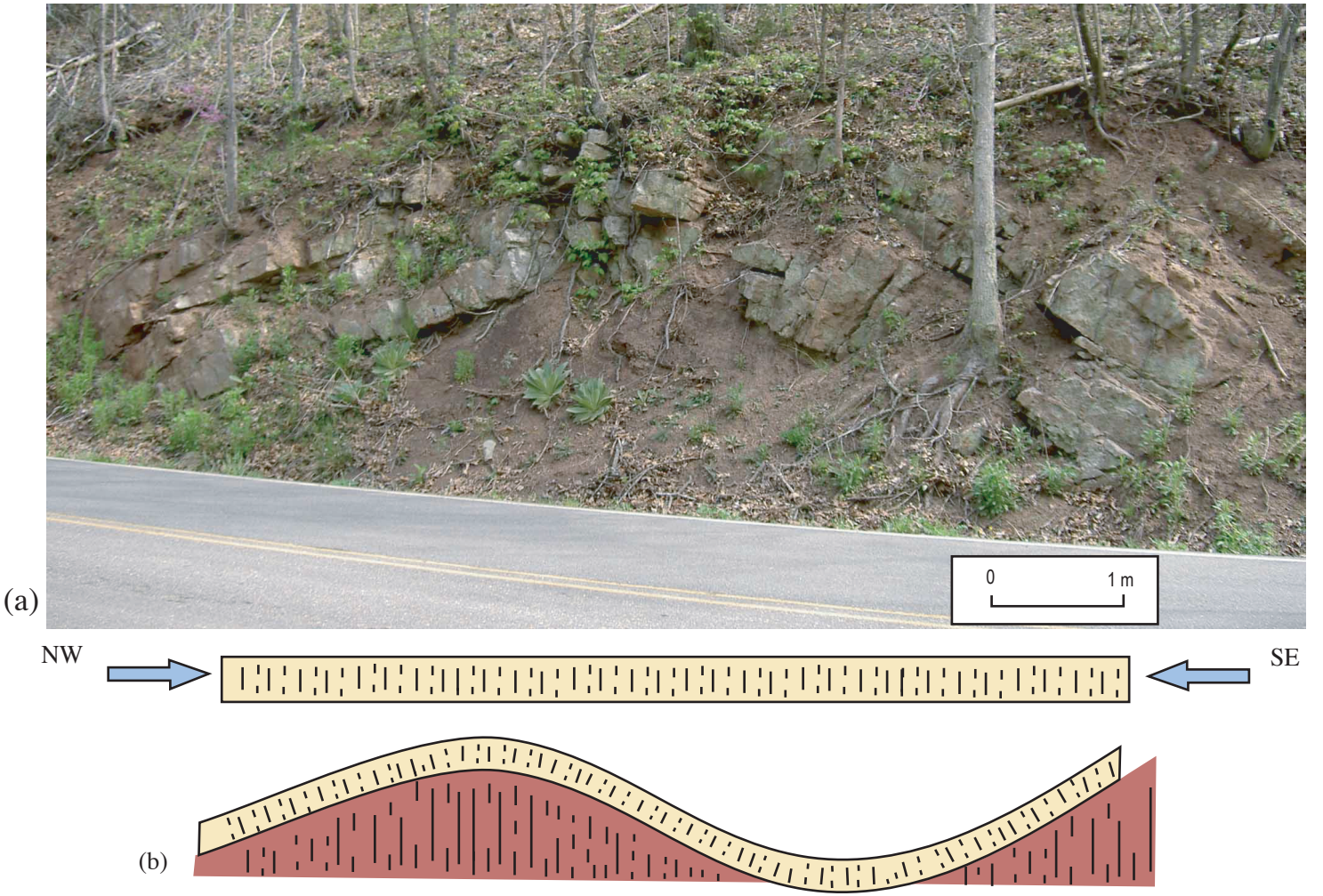

Figure 3-11. (a) Fanned cleavage in an open fold of the Bays Formation. (b) Sandstone bed (cream) displays fanned cleavage (layer-parallel shortening) while the red siltstone bed (red) displays near axial planar cleavage (Hatcher, 1990). Minor flexural slip occurs along contact.

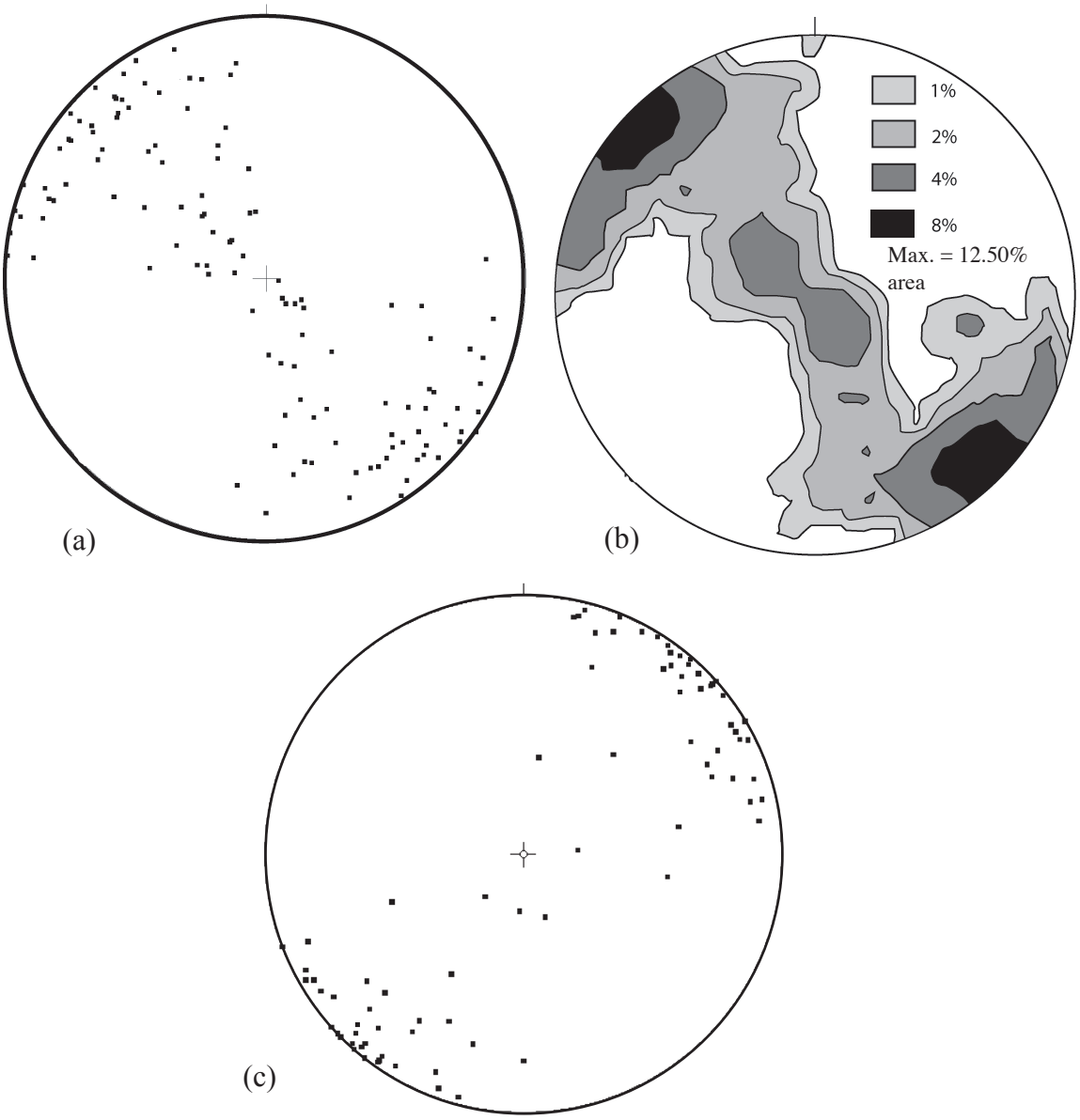

Figure 3-12. (a) Lower-hemisphere, equal-area stereographic projection of 121 poles to cleavage in the Bays Mountain synclinorium. (b) The same data contoured (1%, 2%, 4%, 8 per 1% area). (c) Lower hemisphere, equal-area projection of 118 cleavage-bedding intersections. The mean principal direction is 057°, 2°. Stereonet made using GeoOrient© v. 9.2.6 by Rod Holcombe, University of Queensland, AU (2005)

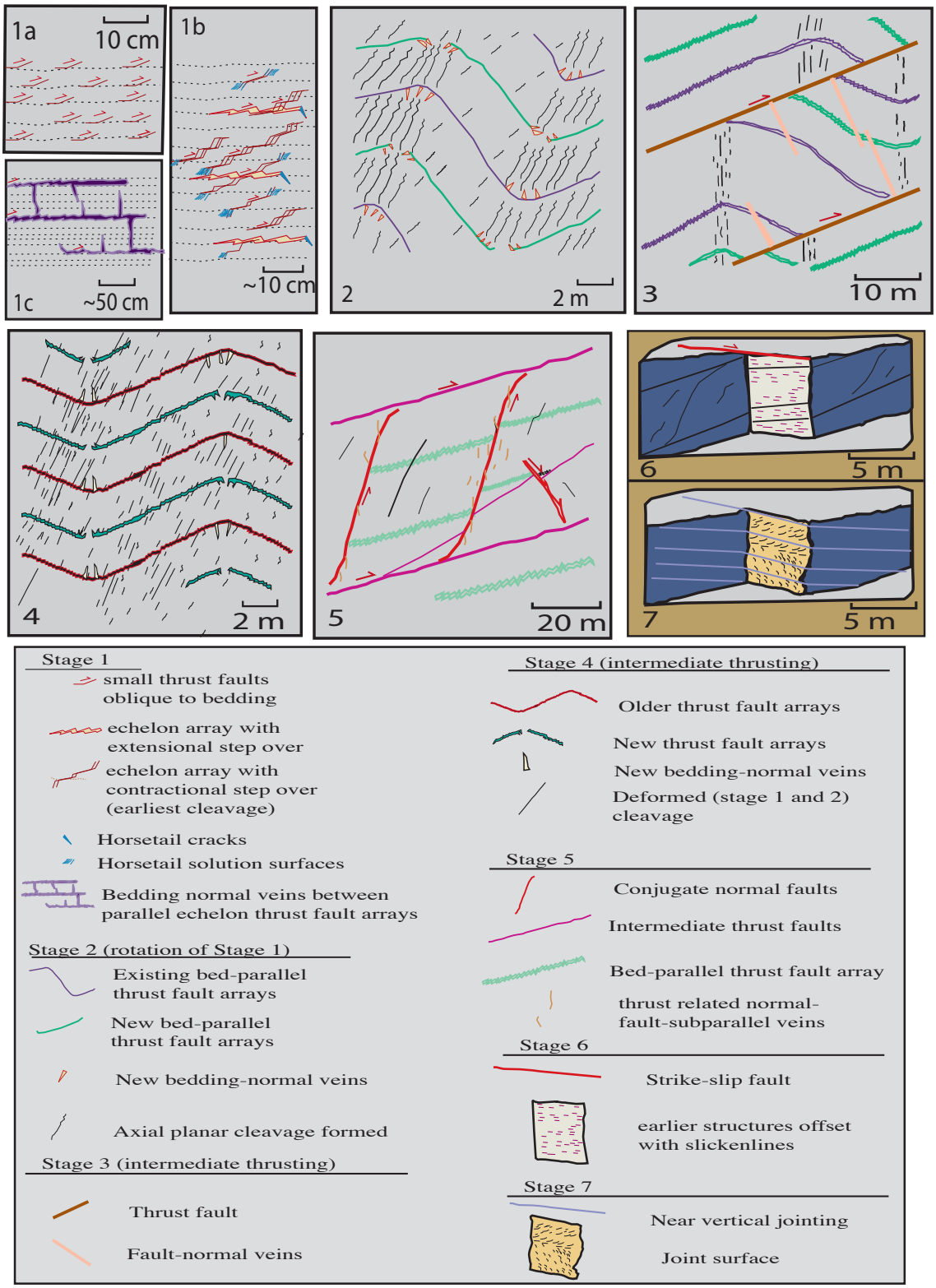

Figure 3-13. Seven stages of deformation at the Bays Mountain synclinorium (modified from Ohlmacher and Aydin, 1995) during the Alleghanian orogeny. Note the secondary cleavage development (black) and rotation of early stage 1 & 2 cleavage in stage 4.

Troensegaard (1965) mapped a small portion of the Springvale quadrangle (Hamblen and Cocke Counties, Tennessee) west of the study area. He concluded that cleavage: (1) developed by simple shear parallel to directions of mass elongation in the axial zones of the folds; (2) is not pervasive throughout the region but tends to be limited to areas of pronounced folding; (3) probably developed late in the folding since it is not displaced by slip along bedding; and (4) is related to folding.

It is unsure whether pure shear or simple shear is the dominant cleavage-forming mechanism in the study area. Based on the relationship between finite strain markers, the orientation of cleavage planes, and the relationships to fold axes or axial surfaces (Hatcher, 1990) it appears that simple shear is parallel to the direction of mass elongation in the axial zones of the folds (Troensegaard, 1965). However, pure shear with a rotational component at different stages could produce the same result. In the few outcrops where there are two cleavages noted, an early cleavage developed in the initial stages by simple shear parallel to directions of mass elongation in the axial zones of the folds and was later rotated and another cleavage developed under pure shear (Yust, 1976; Ohlmacher and Aydin, 1995, 1997). The initial weak cleavage development (Alvarez et al., 1978) varies compared to the latter and more prevalent strong cleavage. This is supported by transecting cleavages (Yust, 1976, p. 78; Ohlmacher and Aydin, 1995, 1997), abundant fanned cleavage oblique to axial planar cleavage and hooked pressure solution cleavages in thin sections observed by Ohlmacher and Aydin (1995, 1997), and this study (Fig. 3-14).

Yust's (1976) study included an analysis of mechanical style and kinematic interpretation of fabric elements within the Tellico-Sevier belt. Yust's (1976) thesis focused on two areas (in the lower Sevier Shale): the first (Yust, 1976, p. 5) located near Parrotsville in Cocke County recently mapped by Whitmer (2005), and the other

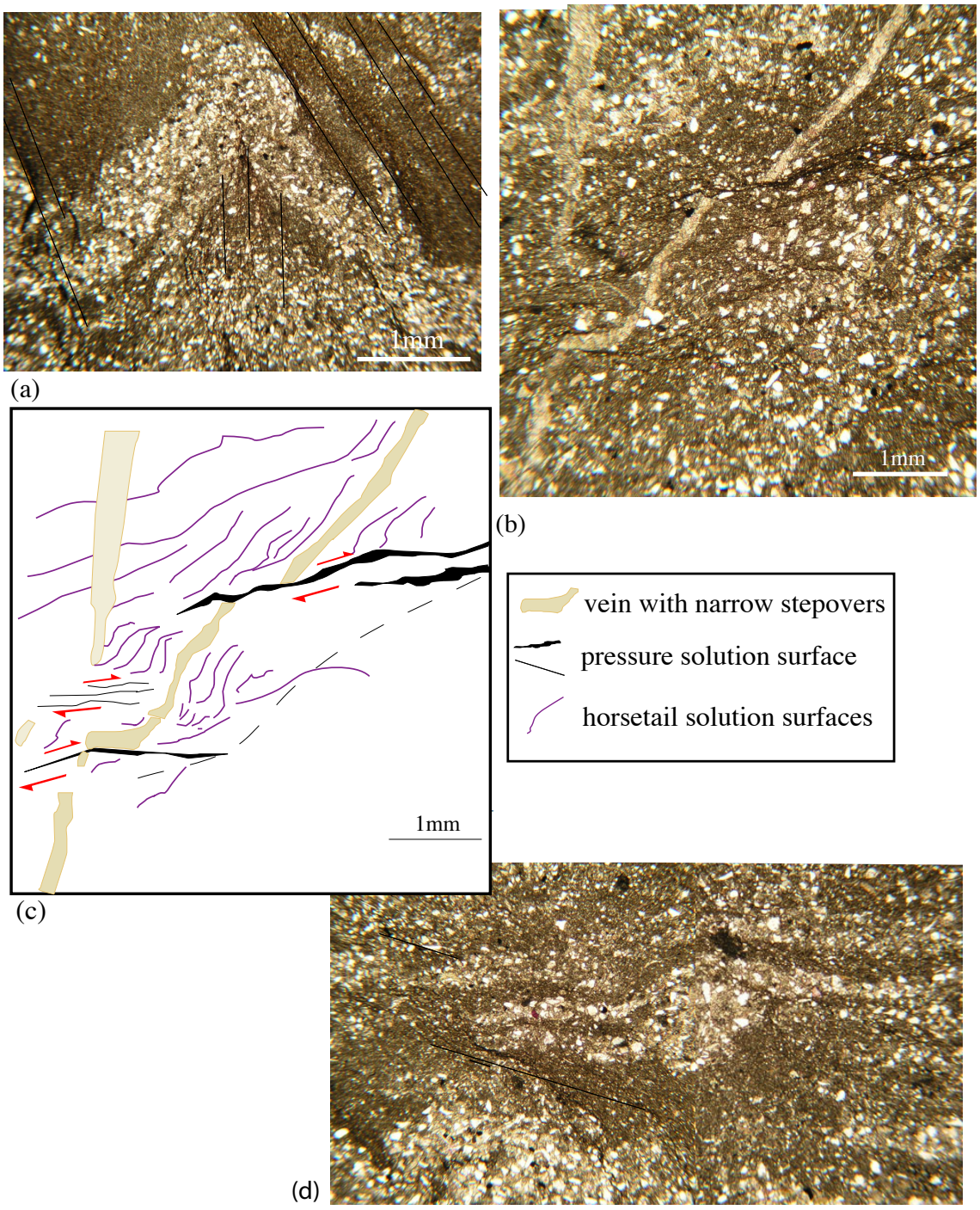

Figure 3-14. Photomicrographs of upper Sevier Shale. (a) Chevron fold with differing orientations of pressure solution surfaces. (b) Contractional stepover via horsetail cracks; thin lines at angles to the faults are horsetail pressure solution surfaces similar to what was seen by Ohlmacher and Aydin (1995). (c) Schematic sketch of (b) showing en echelon fault termination features, curved solution surfaces and shearing (d) Shear sense indicator (?) (top to the right).

near Surgoinsville located in the northern part of my study area (Fig. 1-3). The study also included a cross section through part of the present study area. From fabric data gathered at a few outcrops, Yust (1976) concluded that: 1) cleavage is essentially axial planar in both study areas; 2) observed structures are likely products of one phase of deformation (his recognition of transecting and non-axial planar cleavage conflict with these conclusions) (Yust, 1976, p. 78); and 3) compression was essentially perpendicular to regional strike.

Buckle folds are the most common folds seen during this investigation. The fold axes have a northeast-southwest strike, are commonly gently plunging (Fig. 3-15), and are usually not curved or convolute. Many of the folds within the Sevier Shale gently verge to the northwest. The vast majority of folds in the area are cylindrical but a few noncylindrical folds were noted in the lower Sevier Shale where they could be confidently traced along strike. The symmetry of buckle folds reflects the initial angular relationship between bedding and the direction of compression before the onset of folding.

Kink folds have planar limbs, sharp angular hinges, and consist of folds or couplets whose axial surfaces develop oblique to the axis of compression and along a plane of tangential stress (Ramsay and Huber, 1987; Hatcher, 1990). They may form either as isolated structures or conjugate sets (Fig. 3-16). Kink folds are likely to form where the average effective shear modulus of the entire layer sequence is greater than the cohesion between the layers (Johnson, 1977; Hatcher, 1990), under nonpenetrative strain. Folds of the incompetent units in the area were comparable to class 1C folds, whereas stronger units underwent flexural slip between beds and are considered class 1B folds (Ramsay and Huber, 1987) (Fig. 3-17).

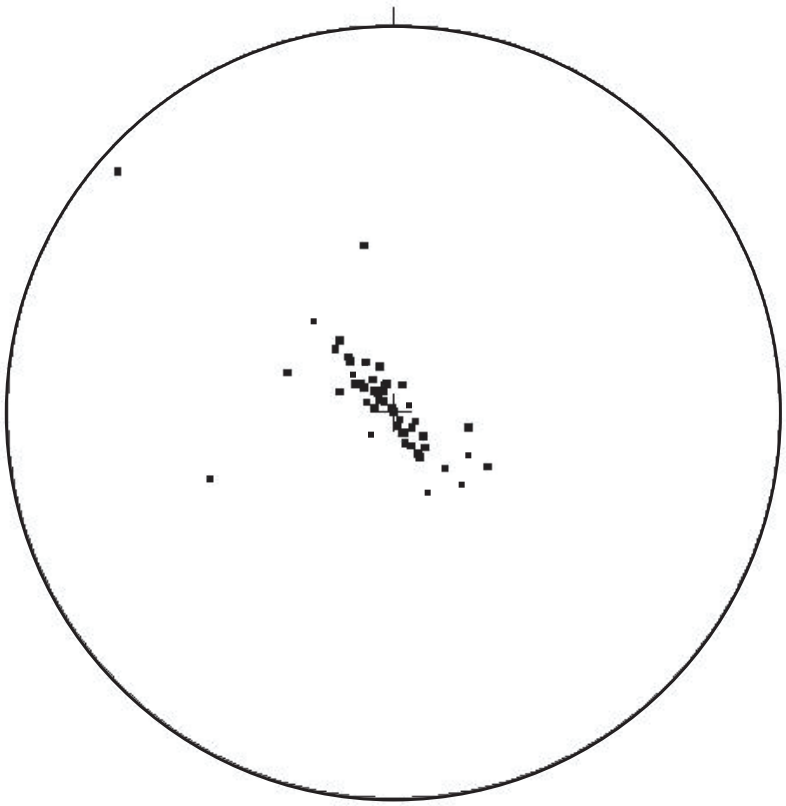

Figure 3-15. Lower-hemisphere, equal-area stereographic projection of 57 axial surfaces of mesoscale folds in the Bays Mountain synclinorium. Contoured at 1% are 1%, 2%, 4%, 8%, and 12% (red) area density. Stereonet made using GeoOrient© v.9.2.6 by Rod Holcombe, University of Queensland, AU (2005).

Figure 3-16. Conjugate (a) and broken conjugate kink folds (b) (upper left) in the upper member of the Sevier Shale along Tob Cooter (a) (Baileyton quadrangle) and Dru Haynes Roads (b) (McCloud quadrangle). The individual kink zones are generally developed by simple shear parallel to the layer surfaces with the shear displacements concentrated in the thin incompetent layers (Ramsay and Huber, 1987).

Figure 3-17: (a) Photo taken from I-181 roadcut in the upper Sevier Shale displaying non-concentric parallel and similar folds. (b) The variety of fold classes illustrate changes in strain across various beds. (c) Folds like the near parallel fold in layer P (Class 1C) underwent changes that bring them closer to the similar fold model, layer Q (Class 3) (Ramsay and Huber, 1987, p. 353-359). At the cut-off angle (R) the calcite filled saddle (shaded peach) becomes thinned to zero (Class 1B). Dip isogons in fold limb 1 plot closer to Class 2 (similar) than limb 2 (Hatcher, 1990). Where Isogon lines (green) cross fold lines they contain equal dips (purple). Rotated and folded calcite filled extension veins (light yellow) illustrate the different types of geometric modification of initially formed planar veins as a result of increased shear during folding (Ramsay and Huber, 1987). Partially calcite filled saddle reefs (pink) occur in the hinges and are developed by the precipitation of calcite from fluids saturated with pressure solution solutes during folding.

(a)

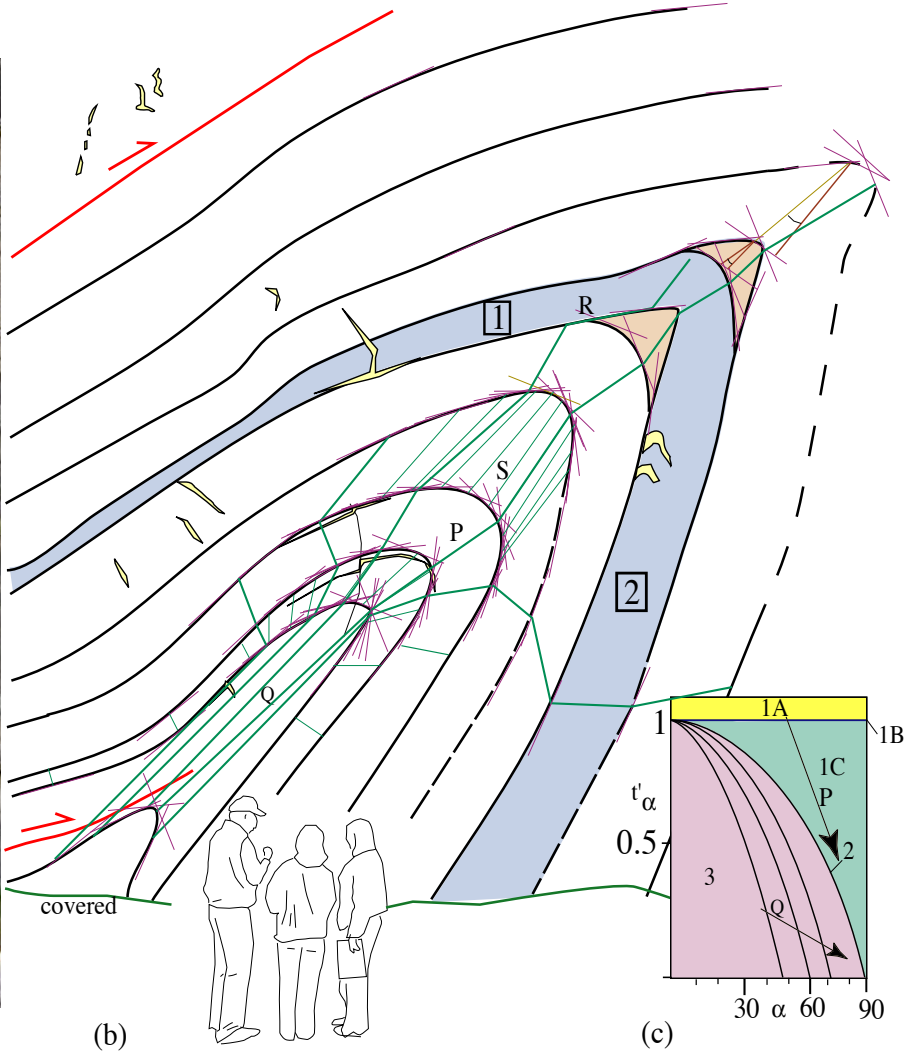

(b) (c)

Thrust, back-thrust, normal faults, strike-slip faults, and associated slickensides were observed at the mesoscale and mapscale. Most of the faults observed within the Sevier Shale were mesoscale break thrusts (formed by faulting the connecting limb of an anticline-syncline pair, overthrusting the hanging-wall anticline, and preserving a footwall syncline). Few faults are believed to be a result of fault propagation folds (Suppe, 1983; Hatcher, 1990), in which the fault propagates up a ramp and flat structure. As thrusting takes place, the fault tip migrates steadily upward. Beyond the fault tip, strain is accommodated by folding an overturned syncline. Above the fault tip in the hanging wall there is a complementary fault propagation fold: an overturned anticline whose axial plane dips more steeply than the thrust (Suppe, 1983).

Jointing is common in all units in the study area. Typically joints in the less competent units are more closely spaced than those of the stronger units and are unfilled. Calcite and quartz (rare) fill joints and are often further deformed (Fig. 3-14, 3-17). The mechanical aspects suggest brittle deformation implied by parallel form of folds throughout the area and abundant evidence of flexural slip in the Sevier Shale. Contrary to Cummings' (1962) conclusion that the area underwent plastic flow, copious fractures and other evidence for brittle deformation were found in the Sevier Shale and Bays Formation.

Through the competent units, most of the data reflect that the majority of the stress was directed from the southeast. This suggests a generally consistent direction of compression relative to the main body of rocks with varied stress trajectories occurring in the incompetent units. It remains unclear if the area experienced episodic deformation during the Alleghanian orogeny. As Yust (1976, p. 78), Reks and Gray (1983), Ohlmacher and Aydin (1995, 1997) indicated, the area may have experienced deformation with near homogeneous strain, and folds and cleavage forming at different stages of the same event.

Cross Sections

Three cross sections were constructed near perpendicular to regional strike at 1:24,000 (and reduced to 1:36,000) scale (Fig. 3-18) (Plate III). Cross-section locations were chosen to interpret representative and interesting structural problems in the area. Several workers including Keith (1905a), Rodgers (1953a), Cummings (1962), Byerly (1969), Yust (1976), Roeder et al. (1978), Woodward and Gray (1985), and Lemiszki (2003) produced cross sections in or near the study area. Many of the previously constructed cross sections lack accurate basement depths, stratigraphic, and structural details.

T.D.G. acquired a seismic reflection profile through part of the study area (line TC-2, shot points 1240 through 1870) located in the McCloud quadrangle (Milici et al., 1979). The seismic line was not migrated, uses common depth point method, has large sections that were shot parallel to strike, and most of the dipping reflectors include dips greater than 50° making most of the seismic reflection profile difficult to interpret. Most of the problems with the seismic interpretation arise from poor data quality and artifacts, but some salvageable information was gathered for my study.

Keith (1905b), Rodgers (1953a), Cummings (1962), Byerly (1969), Yust (1976) and Lemiszki (2003) produced cross sections with depths less than 609 m (2,000 ft) below sea level that didn't reach the master décollement. Roeder et al. (1978) and Woodward and Gray (1985) constructed cross sections through the area to basement, but their cross sections lack detail, contain inconsistent thicknesses of Sevier Shale, and have inaccurate basement depths (depths to basement are off by thousands of feet).

Geologic data gathered during the study were primarily used for construction of the cross sections. Some geophysical data such as seismic reflection profile (T.D.G.

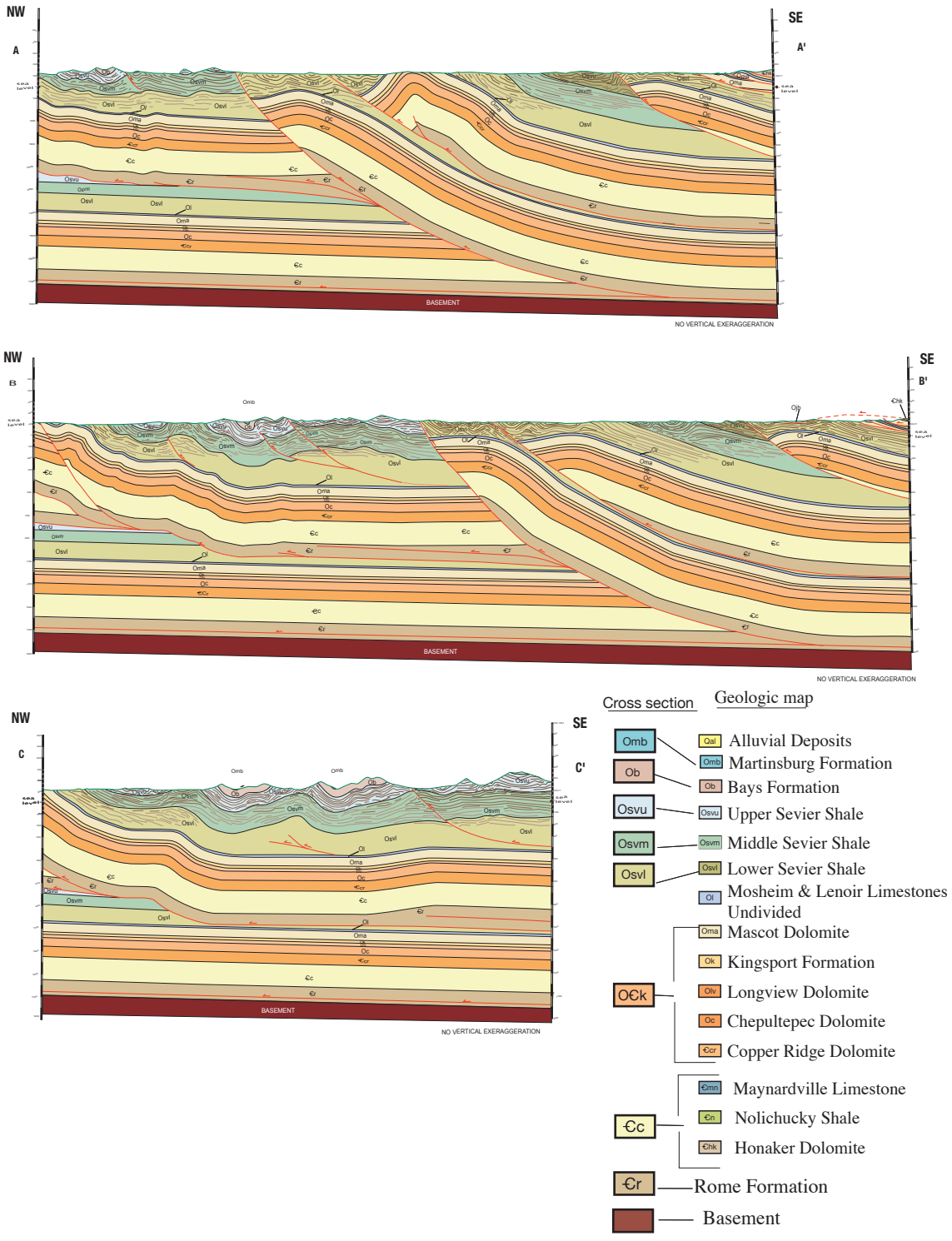

Figure 3-18. Geologic cross sections depicting the major structural features in the study area. See Plate II for detailed cross sections and locations. Form lines in Sevier Shale were drawn to represent structures observed.

T-2), and three geophysical well logs (Eastern American Energy Corp. permit # 7822, and 7864, Capital East Ventures permit # 9862, and Longyear Drilling Co. DDR Summary sheet) were also incorporated. Depth to basement (based on seismic reflection profiles, and comparisons made with Neil Whitmer's and other study) through the area ranges from 4.88 km (17,000 ft) to 5.8 km (19,000 ft) in the southern portion of the study area (Milici et al., 1979).

Cross sections were constructed using Adobe Illustrator™ 10 software. Surface data, structural measurements, and stratigraphic thickness estimates were transferred to the topographic profile gathered from topographic quadrangles. Subsurface information was interpreted using principles established by Woodward, Hatcher, Suppe, Boyer, and others. Mesoscale folding observed (indicated by form lines) in the Sevier Shale was not projected through the Knox Group. It is likely that smaller faults and folds exist in the incompetent units.

The Romeo fault is marked on the cross sections as an out of sequence thrust between the Cooter Hollow and Lick Creek faults. It extends through the study area (southwest to northeast) and likely connects to the fault at the southwestern extent of the I-181 roadcut (Brendt, 1996) in the Kingsport quadrangle. Based on seismic data this fault is believed to bring up the Knox Group (Fig. 3-18).

The restored sections were then evaluated based on criteria outlined by Woodward and Gray (1985) and Hatcher and Hooper (1990). Cross sections were restored one thrust sheet at a time from foreland toward the hinterland using line balancing techniques. The retrodeformed sections were adjusted to match the stratigraphic thickness of the Chickamauga Group from the northwesternmost to the

southeasternmost part of the cross section. Hanging wall and footwall cutoff angles were constructed so that they matched, and line lengths were preserved from the undeformed to deformed states.

A 3-D estimated thickness diagram (Fig. 3-19) was made from nine sections from the compiled study area using the most complete sections that contained structural and stratigraphic field data. Geophysical data were also considered using top of Knox Group picks across the study area. Stratigraphic columns were then placed on a horizontal plane in Adobe Illustrator with the Sevier-Bays contact lining up with the location on the geologic map and the Knox-Lenoir contact as the subsurface base. The sections were then matched along and perpendicular to strike. Where stratigraphic thickness estimates were not gathered (through unmapped quadrangles), lines were connected and inferred to complete the fence diagram. Since the cross sections were not completely restorable, the locations of the estimated thicknesses remained and were not palinspastically restored. However, the thicknesses exhibit the wedge shape of the Sevier basin. Sevier Shale thickness doubles from the northwest to southeast with the thickest part to the southwest near Neil Whitmer's (2005) study area. Shades of lighter colors in the section represent uncertainty in the stratigraphic column resulting from an incomplete section, or the joining of two inferred planes.

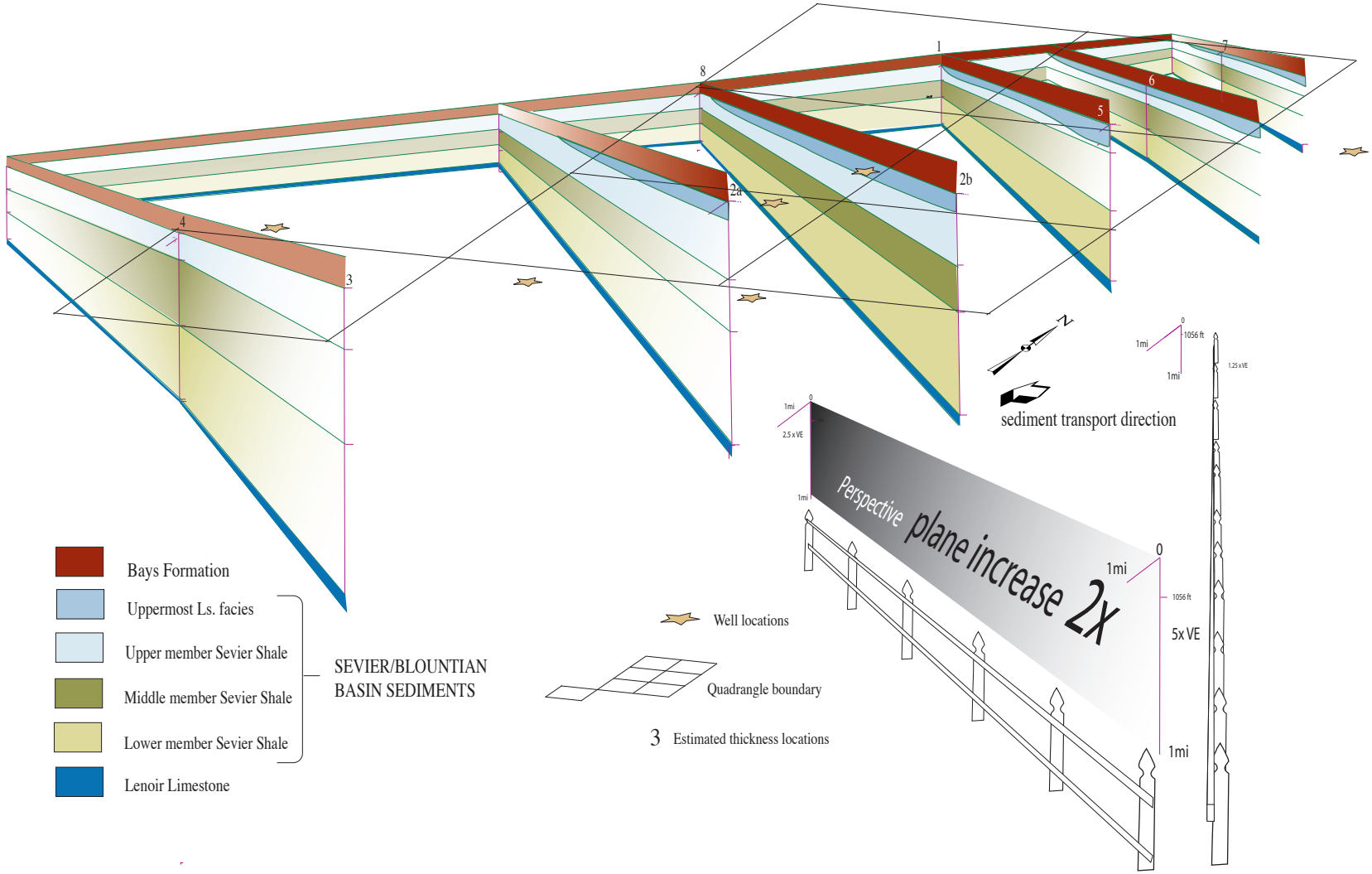

Figure 3-19. Simplified 3-D fence diagram depicting the thickness increase (~2x) to the southeast and generalized basin geometry in the vicinity of the study area. Perspective doubles from 2.5 x V.E. to 5 x V.E. (z axis). Darker colors indicate better delimited thickness estimates.

CHAPTER IV

SEVIER BASIN TECTONICS

Tectonic Background

In the early Ordovician the eastern Laurentia shelf (Proto-North America) was a passive margin of carbonates in the waters of the Iapetus ocean. During the Taconic orogeny, a volcanic island arc was obducted onto the thick continental crust as the western part of the Iapetus ocean closed (Ettensohn, 2004). As the volcanic island arc approached the region, tectonically induced subsidence forced the shallow-water carbonate platform downward (Shanmugam and Walker, 1978) (Fig. 4-1).

The earliest Taconic phase was concentrated along the southwestern parts of the Laurentian margin at the Virginia promontory, and perhaps at the Alabama promontory, during the late Middle to early Late Ordovician (late Llanvirn-mid Caradoc; late Whiterockian-late Mohawkian) time and may reflect collision of a microcontinent with one or both promontories (Vick et al., 1987; Ettensohn, 2004). This phase of Taconian orogeny is commonly called the Blountian tectophase, which produced a westwardly prograding Sevier-Blountian clastic wedge from what is now Tennessee into Alabama (Pope and Read, 1998) (Fig 4-2). The source terrane was likely composed of shelf-edge sedimentary rocks, arc volcanic rocks, deep-water sedimentary, and low-grade metamorphic rocks in an accretionary prism, and perhaps crystalline basement rocks of a microcontinent (Shanmugam, 1978; Mack, 1985).

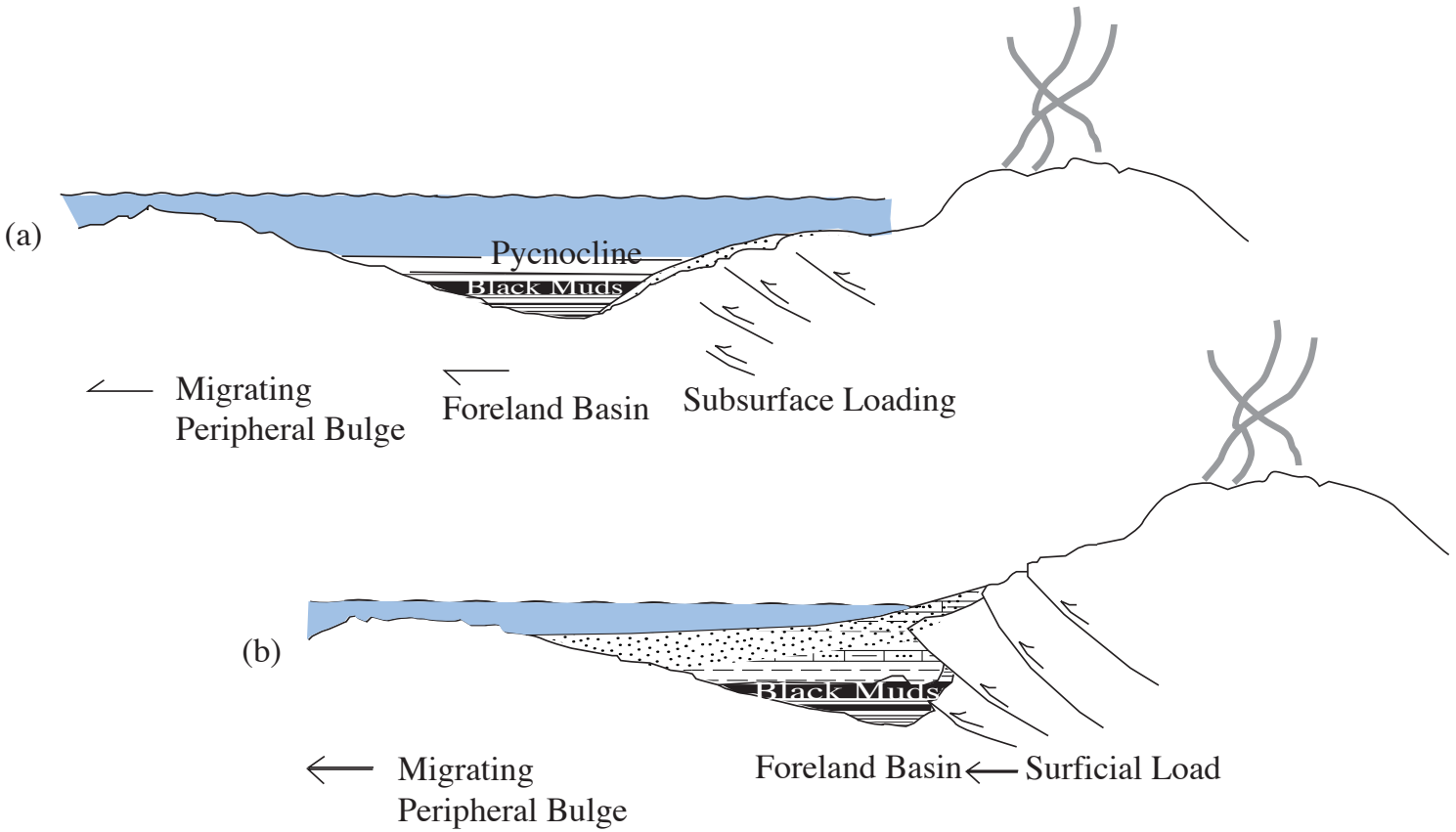

Figure 4-1. Schematic diagrams showing possible relationships between foreland-basin generation, infill, and deformational loading. Basin-bulge formation and migration during loading (a) with little siliciclastic influx (varied cross paleocurrent indicators, i.e., Chapman Ridge); "Loading-type" relaxation (b) in subsiding foreland basin filled with coarser siliciclastics derived from surficial load (east derived paleoindicators. Pycnocline - zone of thermohaline density gradation in deeper basins with declining O_2 content. Ettensohn's (2004) depiction of the Alleghanian orogeny (a, b) may be an analog for the Sevier-Blountian phase of the Taconic orogeny. Syntectonic faulting and other depositional evidence, however, are concealed under the Blue Ridge.

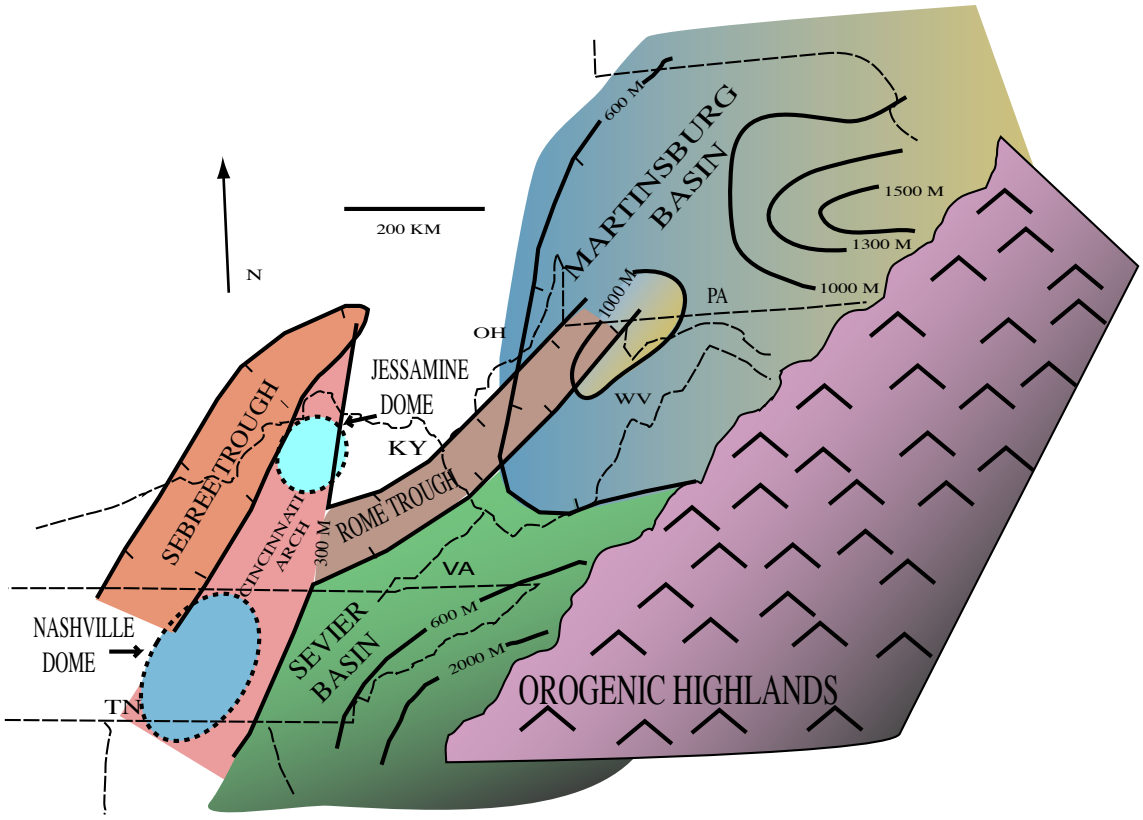

Figure 4-2: Isopach map showing major depocenters for upper Middle-Upper Ordovician rocks in the Appalachian basin. The Cincinnati arch, Jessamine and Nashville domes, and the Rome trough were all periodically active structures in the foreland basin (modified from Pope and Read, 1998).

Previous Models

The Sevier-Blountian basin has previously been thought of as a simple foreland basin (Rodgers, 1953b; Byerly, 1969; Shanmugam and Walker, 1978, 1980, 1983). Shanmugam and Walker (1978, 1980, 1983) were the first to recognize the bank-edge relationship and the significance of different facies (northwestward carbonates and southeastward siliciclastics) and concluded that the Sevier basin is a Taconic foredeep with sediments as thick as 3,000 m (10,000 ft) (Fig. 4-3). They found three components of subsidence: (1) subsidence initiated with coequal response to tectonic loading; (2) subsidence resulting from tectonic movement; and (3) sediment loading compaction-related subsidence (Shanmugam and Walker, 1980).

Shanmugam (1978) suggested that the basin revealed three main phases of subsidence: (1) an early tectonic and sediment loading phase with a subsidence rate of 3-4 cm/1,000 yrs; (2) a second tectonic phase with a subsidence rate of 60-65 cm/1,000 yrs; and (3) a final turbidite-sediment loading phase with a subsidence rate of 4-15 cm/1,000 yrs. He also recognized five stages of basin evolution: (1) stable-shelf development (Lenoir); (2) downwarping stage (Whitesburg); (3) a starved-basin stage (lower Sevier); (4) turbidite-fill stage (middle Sevier); and (5) contour-current stage (upper Sevier). Flexural responses of the crust were also outlined (Shanmugam and Walker, 1983) (Fig. 4-4).

More recent depositional models have been proposed to include the Sevier-Blountian basin as a back-bulge basin (Hatcher, 2004) (Fig. 4-5) or a complex basin (Whisner, 2005) (Fig. 4-6). Although the back-bulge model may account for sediment source incongruencies (Hatcher, 2004), it does not account for rheologic properties of the crust. Using MATLAB© software Whisner (2005) concluded that it is not rheologically possible to create a back-bulge deep enough for Sevier sediment

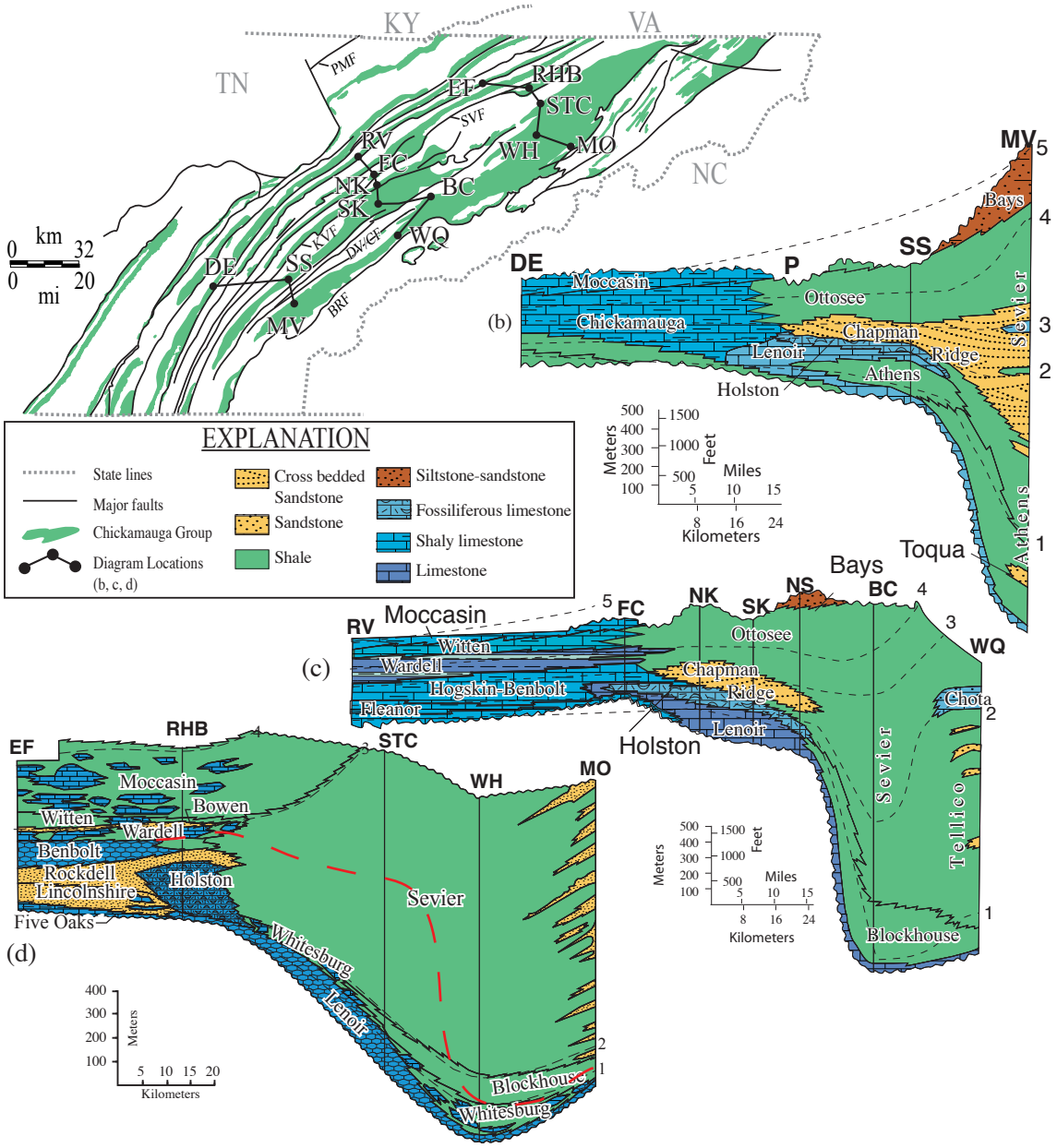

Figure 4-3. Schematic Middle Ordovician Tellico-Sevier basin diagrams and locations (a) from Walker et al. (1983). (b) Sections from Decatur (DE), Prospect (P), Sweetwater (SS), ending in Mount Vernon (MV). (c) Facies relationships from Raccoon Valley (RV), Fountain City (FC); north and south Knoxville (NK and SK); Neubert Springs (NS); Boyds Creek (BC) and Wildwood (WQ). Time lines 1 through 5 (dashed) show time equivalent horizons through both diagrams. Section from (d) EF (Evan's Ferry); RHB (Red House Branch); RV (Raccoon Valley); STC (St. Clair); WH (Whitesburg); and MO (Mosheim) differs from the thickness found in this study where the thickness at STC (dashed red) is half as thick as that depicted by Walker et al. (1983). Geological features are: BRF–Blue Ridge fault; DV/CF–Dumplin Valley/Chestuee faults; PMF–Pine Mountain fault; and SVF–Saltville fault. (Base map modified from Hatcher, 1990).

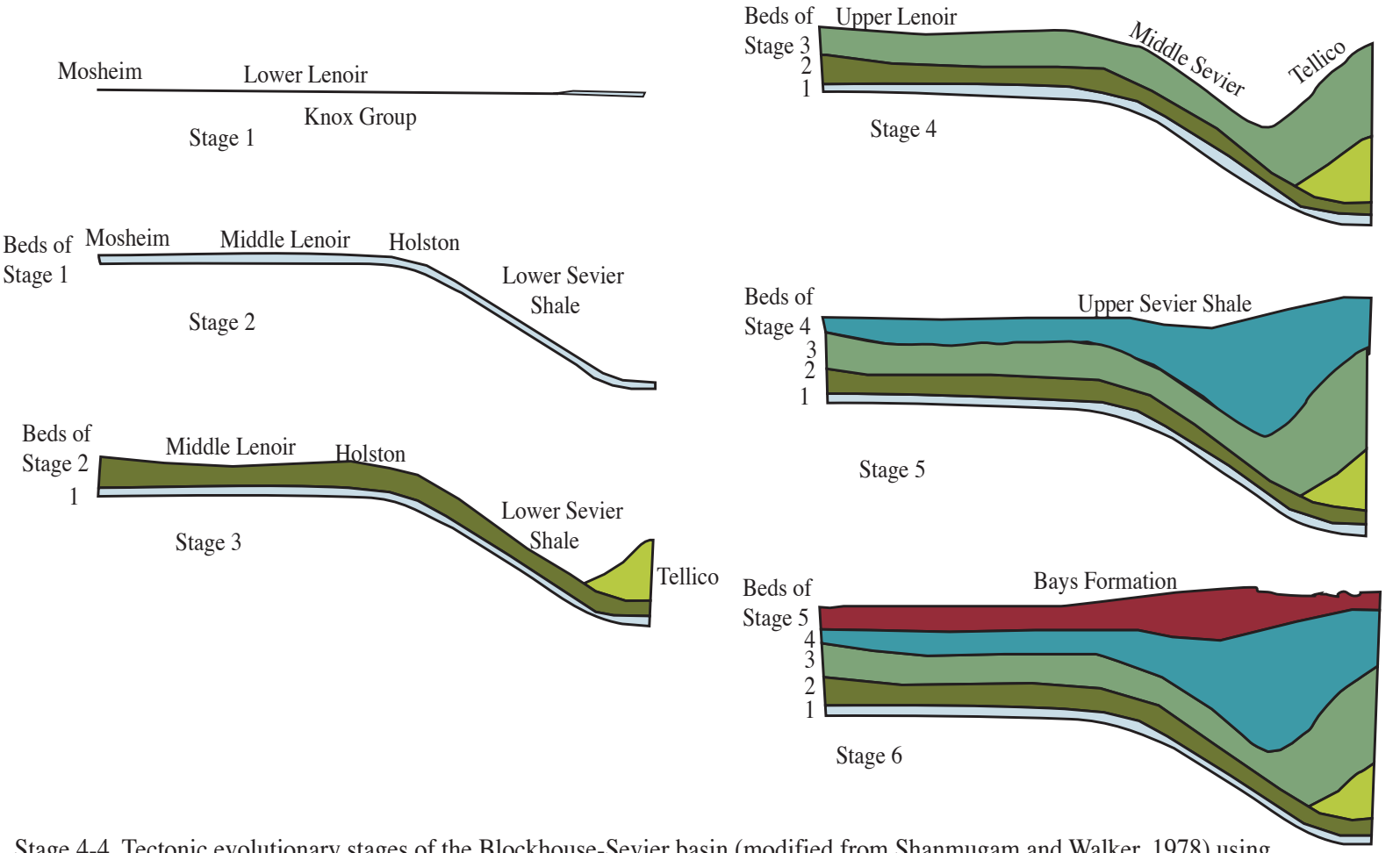

Stage 4-4. Tectonic evolutionary stages of the Blockhouse-Sevier basin (modified from Shanmugam and Walker, 1978) using a flexural bending model of basin subsidence (requires crustal load to the east). Stage 1 - carbonate shelf stage; Stage 2 - downwarping stage; Stage 3 - turbidite-fill stage; Stage 4 - contour-current stage; Stages 5 and 6 - shelf molasse stages.

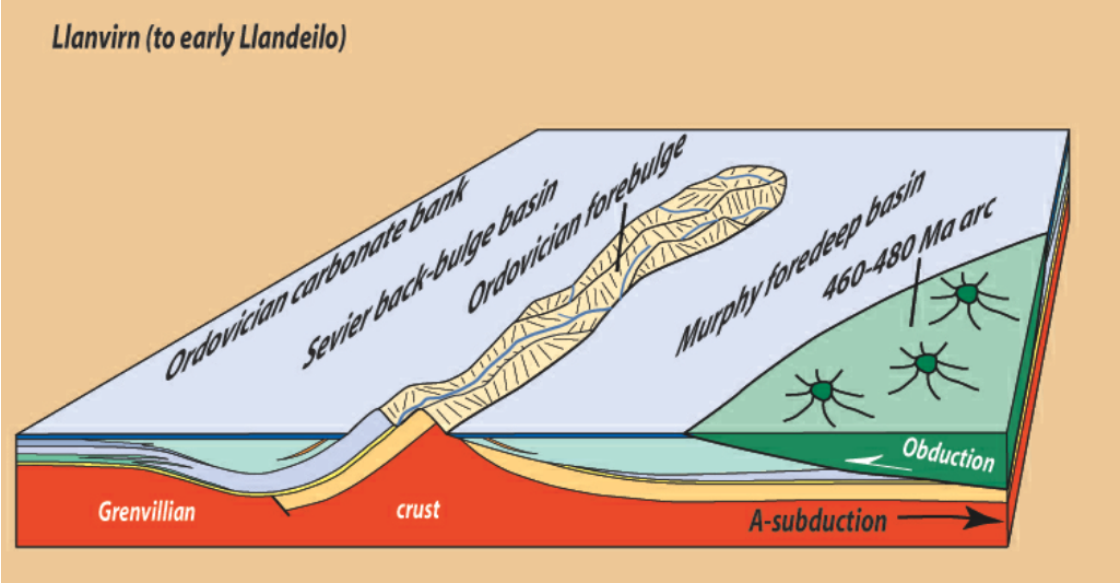

Figure 4-5. Sevier Basin as a back-bulge basin with the Murphy sediments as the foredeep (Hatcher, 2004).

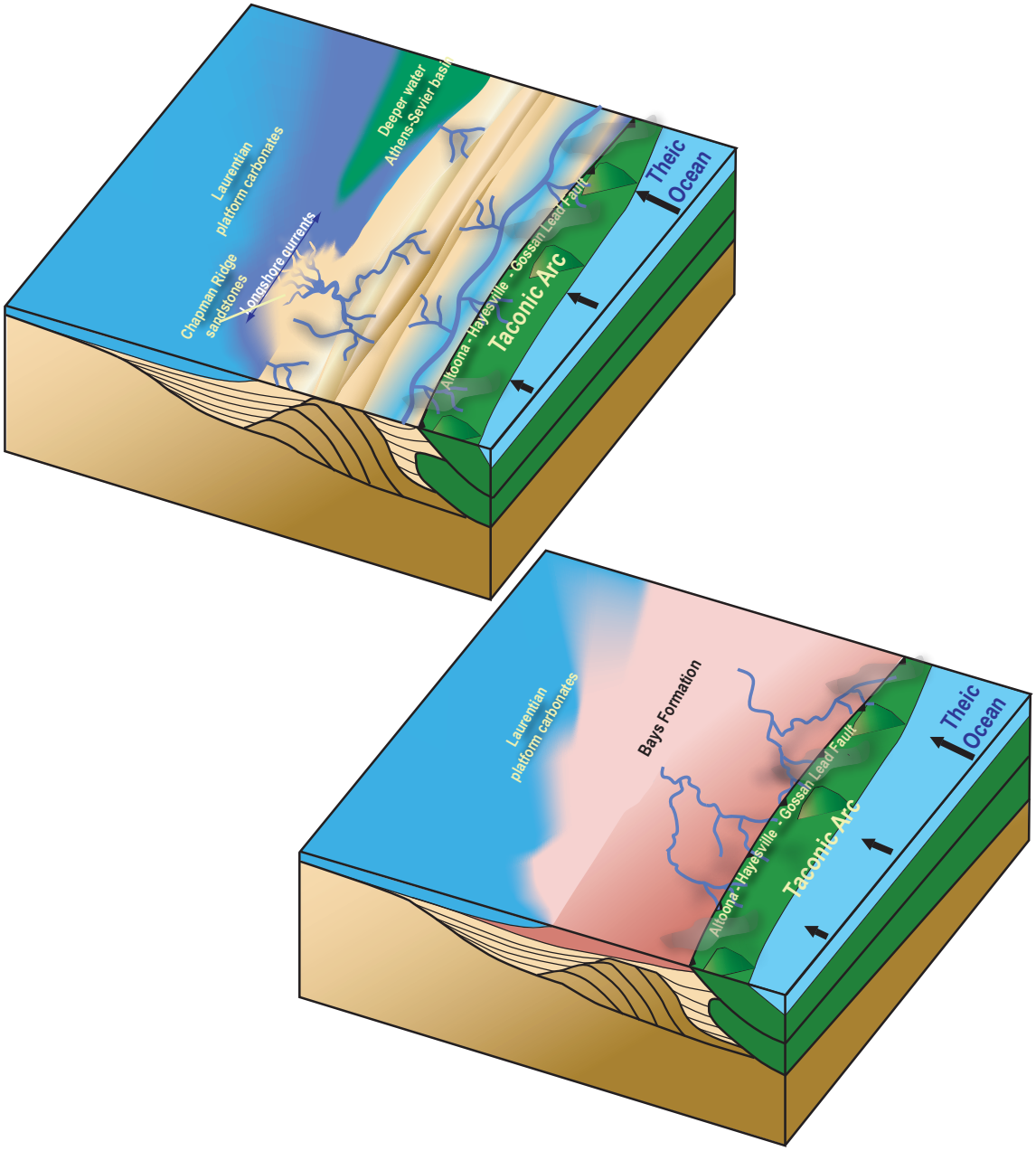

Figure 4-6. Block diagram using complex model of basin formation (Ricci-Lucchi, 1986; Whisner, 2005). Model depicts tectonic and depositional setting during the transition from the Sevier-Blountian (a) phase to the beginning of the "Taconic" phase (b) (Rodgers, 1971; Pope and Read, 1998).

depositional depths. He concluded that the Taconic peripheral bulge would have to be four times as great as any modern bulge to exhume a minimum of 1500 m (5000 ft) of rock and removing the overlying passive margin sequence to expose rifted margin sediments and underlying crystalline basement (Whisner, 2005).

Kellberg and Grant (1956), Cummings (1962), Shanmugam and Walker (1978), and this study indicate southeast derived material. If the sediment source was from the east, it is possible that some basement was uplifted because of the advancing arc (Bayona and Thomas, 2003) or that the approaching arc contained Grenville, Chilhowee, Rome, Conasauga, Knox, and Lenoir rocks that would then be obducted onto the margin and deposited into the basin (Bayona and Thomas, 2003).

Whisner (2005) favored a complex basin in which a foreland fold thrust belt exposed the entire stratigraphic section from Lenoir to Ocoee Supergroup rocks. These sediments were then deposited into the basin. In an alternative hypothesis Bayona and Thomas (2003) suggested that the migrating Taconic forebulge paused under the Birmingham inverted graben. Then reactivation of basement faults permitted higher relief and exposed the inverted graben, which was then eroded into the Sevier-Blountian basin.

Ettensohn (2004) devised a generalized model for foreland basin sedimentation. Sediments filling the hypothetical basin strikingly resemble the sediments of the Sevier-Blountian basin (Fig. 4-7). The succession may be summed up in four parts: a basal unconformity overlain by dark shale (lower Sevier Shale member), a flysch-like unit (middle and upper Sevier Shale), an upper marginal-marine or terrestrial unit with red beds (Bays Formation), and finally another unconformity followed by anoxic conditions (Martinsburg Formation) (Ettensohn, 2004). The relative abundance of algae decreases towards the upper part of the Lenoir.

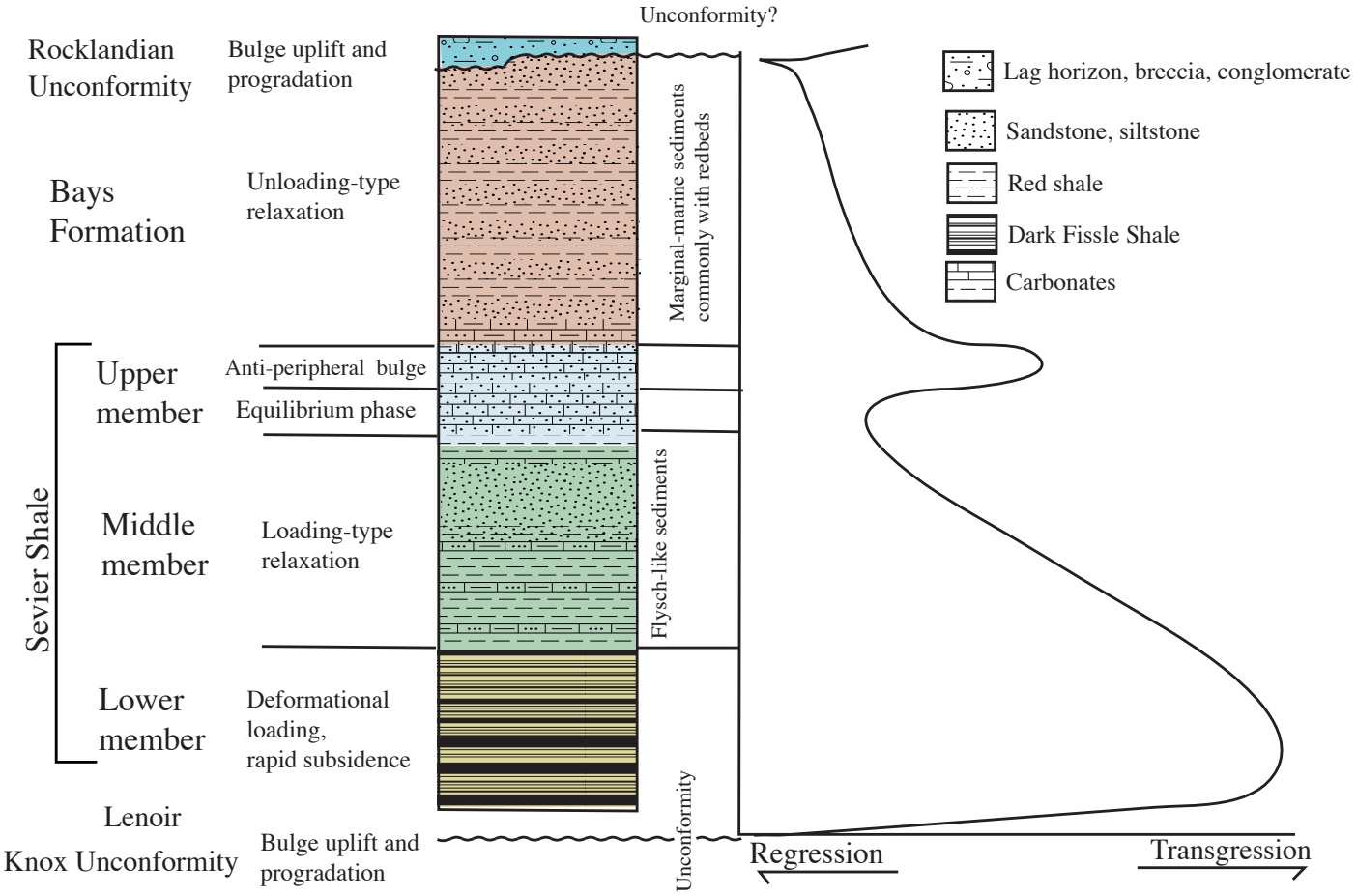

Figure 4-7. Comparison of Ettensohn's (2004) generalized sequence of flexural events, accompanying sequence of lithologies, and transgressive-regressive curve for early subduction-type orogenies on a continental margin as compared to Sevier-Blountian basin sediments. Sequences are unconformity-bound, but may be incomplete or eroded from the top. Upper marginal parts of the sequence are considered deltas (modified from Ettensohn, 2004).

This indicates a deepening of the basin (Benedict and Walker, 1978). The Lenoir Limestone would fit into Ettensohn's (2004) model as the deepening carbonate bank prior to the deposition of the Sevier Shale.

Current Model

The model proposed for this study depicts the transition of a remnant ocean basin (Fig. 4-8) to the Sevier-Blountian phase of the Taconic orogeny related to emplacement of the overthrusting tectonic load onto the Laurentian margin. In this model a prograding accretionary wedge, zone of subsidence, basin axes, and flexural foreland bulge migrated westward toward the foreland. Sediments evolve from marine (distal) to continental (proximal) and prograde over the shelf sequence of the former passive margin (Einsele, 2000). The Sevier-Blountian phase represents initiation of isostatic uplift (Bays Formation) of inner parts of the foreland basin.

The Sevier-Blountian phase represents rapid erosion of a highly elevated fold-thrust belt possibly comprised of Murphy belt and reworked basement sediments (western North Carolina) or similar lithologies. Deformation steps progressively into the foreland during collisional shortening (Dahlstrom, 1970; Allen et al., 1991; Busby and Ingersoll, 1995) and early basin-fill strata are therefore involved during deformation, and are cannabalized by uplift, erosion and subsequent recycling into the basin. Filling and basin uplift are diachronous, involving progressive collision, uplift and closure of remnant basins as the suture zips up along strike. Axial progradation into the basin emphasizes and amplifies a lateral shifting of depositional systems represented in differing facies expressed across the basin (Shanmugham and Walker, 1978, 1980, 1983). This requires that some deep-water facies that have presumably been overthrust as forming syndepositionally with nonmarine (molasse) facies. Evidence for the preliminary foreland fold thrust belt exists in the COCORP data (Cook

Figure 4-8. Model depicting the transition from a remnant oceanic basin (a, b) to the Sevier-Blountian phase of the Taconic orogeny (c, d) related to emplacement of the overthrusting tectonic load onto the Laurentian margin. With the prograding overthrust belt, the zone of subsidence, basin axes, and flexural foreland bulge migrate to the left (west) toward the foreland. Sediments tend to evolve from marine to continental and prograde over the shelf sequence of the former passive margin. The Sevier-Blountian phase represents rapid erosion of the highly elevated fold-thrust belt. Isostatic uplift is initiated in the of inner parts (Bays Formation) of the foreland basin. Presumably, this would be followed by an additional pulse with a rapid subsidence (unconformity) and finally creating the classic "Taconic" Martinsburg basin. (partially modified after Einsele, 2000).

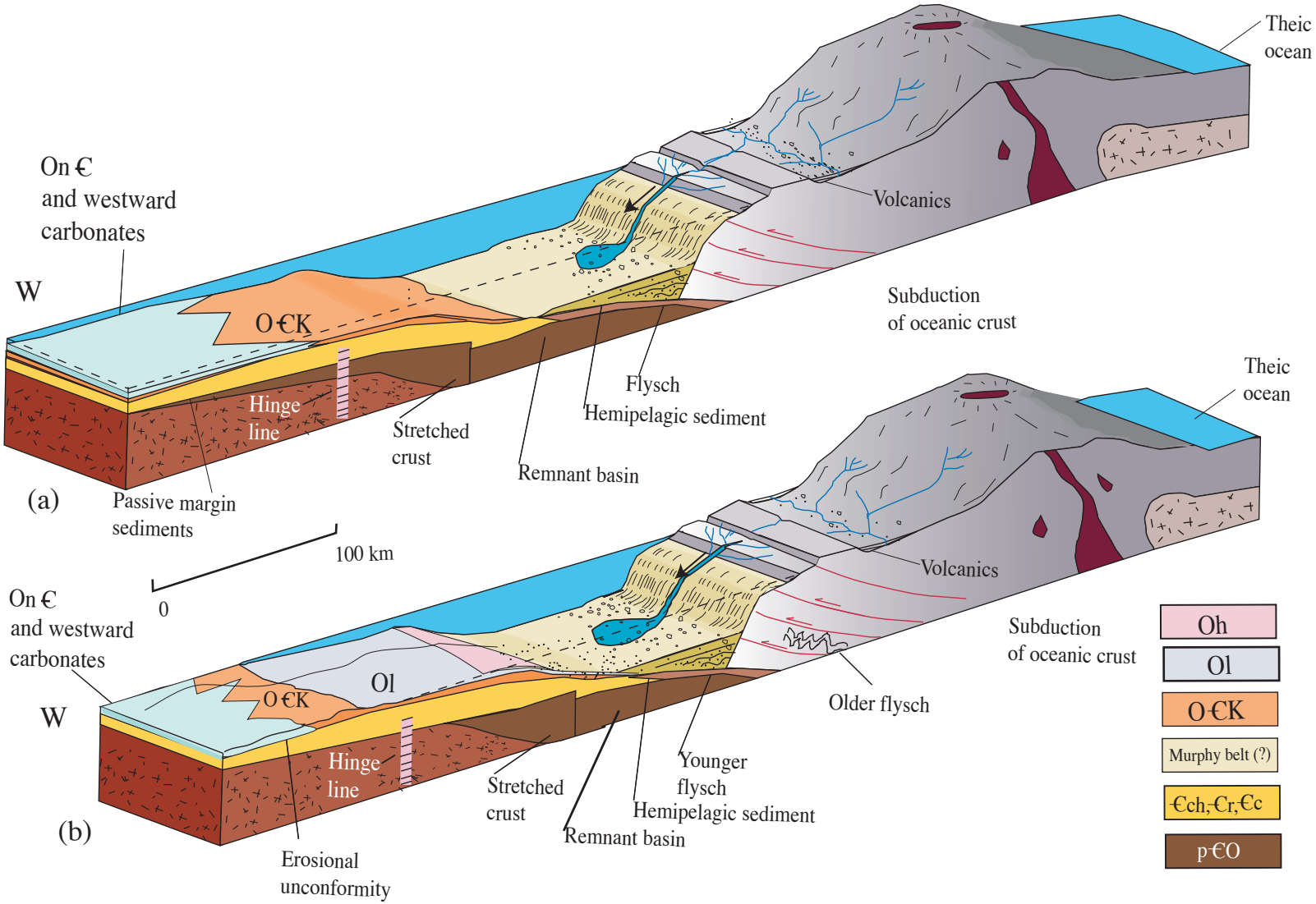
On €
and westward
carbonates
W
O€K
Hinge
line
Stretched
crust
Remnant basin
Flysch
Hemipelagic sediment
Volcanics
Subduction
of oceanic crust
Theic
ocean
(a)
Passive margin
sediments
100 km
0
On €
and westward
carbonates
W
Ol
O€K
Hinge
line
Stretched
crust
Remnant basin
Younger
flysch
Hemipelagic sediment
Older flysch
Volcanics
Subduction
of oceanic crust
Theic
ocean
(b)
Erosional
unconformity
Oh
Ol
O€K
Murphy belt (?)
€ch,€r,€c
p€O

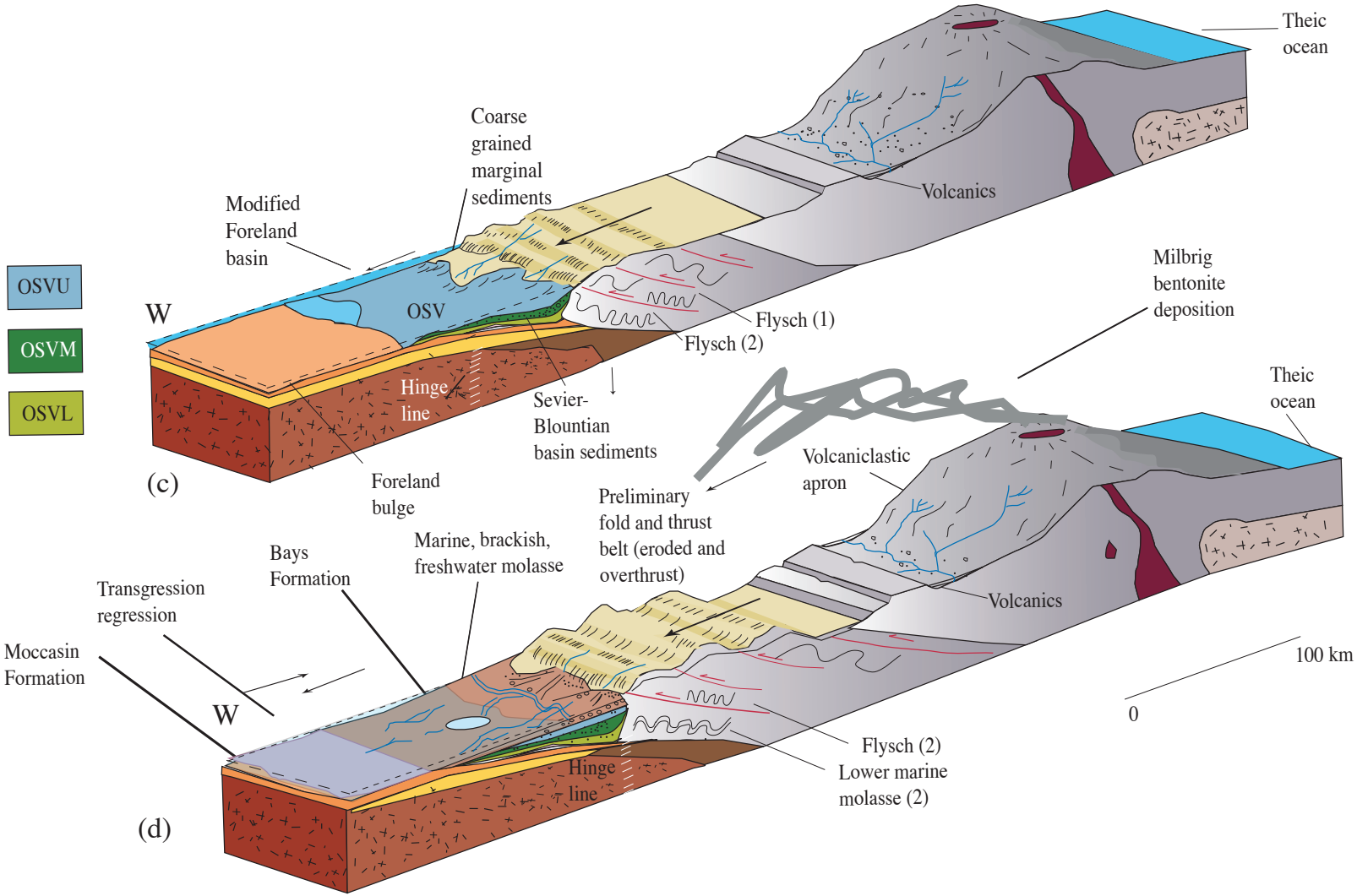
OSVU
OSVM
OSVL
W
Modified
Foreland
basin
Coarse
grained
marginal
sediments
OSV
Hinge
line
Foreland
bulge
Sevier-
Blountian
basin sediments
Flysch (1)
Flysch (2)
Volcanics
Theic
ocean
(c)
Milbrig
bentonite
deposition
Volcaniclastic
apron
Preliminary
fold and thrust
belt (eroded and
overthrust)
Theic
ocean
Transgression
regression
Bays
Formation
Marine, brackish,
freshwater molasse
Moccasin
Formation
W
Volcanics
100 km
0
Hinge
line
Flysch (2)
Lower marine
molasse (2)
(d)

et al., 1979) (GA-1) ~250 km east (near the Bravard fault zone) of the present exposed Sevier-Blountian foreland basin.

Paleozoic detrital zircons would have been restricted by a volcanic plateau and preliminary fold and thrrust belt. Delta-complex clastic wedges were produced from cycles of orogeny on the eastern margin of Laurentia during closure of the Iapetus ocean (Einsele, 2000). The "deltas" described in this study were also produced from the preliminary fold and thrust belt. The preliminary fold and thrust belt is no longer exposed and presumably the western portion has been eroded while eastern sections have been overthrust (Cook et al., 1979).

Based on biostratigraphic evidence (Twenhofel et al., 1952; Holland, 2003) Sevier- Blountian basin sediments were deposited more rapidly than previously thought (Drake et al, 1989). The timing of deposition for Sevier-Blountian sediments (including Bays Formation) would span approximately 7 m.y. (Twenhofel et al., 1952; Holland, 2003) versus the 20 m.y. previously thought (Drake et al., 1989). When also considering Wiener's (1979) conclusions regarding the rapid erosion, and accretion and mountain building related to the Taconic orogeny, the Sevier-Blountian Basin represents the rapid migration and cannibalization of a foreland basin.

CHAPTER V

CONCLUSIONS

1. The allochthonous Bays Mountain synclinorium contains stratigraphic divisions of the Sevier Shale: a lower member (thin bedded dark–gray calcareous shale with micritic limestone in the uppermost portion of the unit), a middle member (interbedded shale and sandstone), and an upper member (silty to sandy limestone).
2. Total thickness of the Sevier Shale increases from 1006 m (3,300 ft) in the northernmost part of the study area (where the entire unit is preserved) to an estimated 1830 to 1981 m (6,000 to 6,500 ft) in the southern part (5,000 ft preserved and 1,500 ft estimated removed).
3. Bays Formation and Sevier Shale siliciclastics become coarser grained and thicker to the southeast. Paleocurrent indicators and other sedimentary features support a southeast source by the indication of bimodal nearshore trend from southwest to northeast for sediments in the upper Sevier Shale. Sediments were derived perpendicular to the northeast-southwest trend from more coarse and thicker sediment side (southeast).
4. Graptolites from the lower Sevier Shale in the study area indicate that they are in the upper *Nemagraptus gracilis* zone. This is younger than the Athens Shale farther southwest (Finney et al., 1996).

5. Based on biostratigraphic data collected from this study and from the literature, the estimated age constraints for the Sevier Shale and Bays Formation are from 461 ± 2 m. y. to 453 ± 2 m. y. This agrees with the ages presented by Twenhofel et al. (1954) and Holland (2004) and is approximately 10 - 15 m. y. younger than that proposed by Drake and others (1989).
6. The middle Sevier Shale may be used for identifying tectonic sedimentary features within the basin, i.e., 1) graded beds that resemble Bouma cycle T_{cde} ultra-distal turbidite deposits; 2) proximal (more coarse) to distal (finer grained) relationships (Kellberg and Grant, 1956); and 3) turbidite sequences.
7. The Sevier Shale is similar to the typical orogenic package of sediments outlined by Ettensohn (2004).
8. Detailed geologic mapping has delineated previously unrecognized faults in part of the Bays Mountain synclinorium. These faults (Cooter Hollow, Romeo, and Little Chucky) have relatively small displacements. Evidence for the recognized faults in the Sevier Shale included: noted deformation zones (small faults, calcite chips, slickensides, abundant cleavage), stratigraphic discontinuities, and seismic reflection profiles.
9. The Lick Creek fault, a splay off the Saltville fault, serves as the main detachment for the Mosheim anticline, and has an estimated minimum displacement of 12 km.
10. The Sevier Shale exhibits disharmonic folding between the stronger structural lithic units of the Knox Group and Bays Formation.

11. The Town Knobs and Pulaski faults serve as major stratigraphic breaks from footwall to hanging wall rocks.
12. The stratigraphic discontinuity and deformation zone noted between the contact of the lower Jonesboro Limestone and Sevier Shale mark the Pulaski fault along the northwestern edge of the Babbs Knobs flap.
12. The area experienced heterogeneous strain with folds and cleavage forming at different stages of the same event, some of which overprint and are oblique to the initial deformation stages.
13. The model proposed for this study depicts a prograding accretionary wedge, zone of subsidence, basin axes, and flexural foreland bulge that migrated westward toward the foreland. The Sevier-Blountian phase represents rapid erosion of a highly elevated preliminary fold and thrust belt.
14. Based on biostratigraphic evidence (Twenhofel et al., 1952; Holland, 2003) Sevier- Blountian basin sediments were deposited more rapidly than previously thought (Drake et. al, 1989). The timing of deposition for Sevier-Blountian sediments (including Bays Formation) would span approximately 7 m.y. (Twenhofel et al., 1952; Holland, 2003) versus the 20 m.y. previously thought (Drake et al., 1989).

REFERENCES CITED

REFERENCES CITED

Anderson, C. B., 1995, Provenance of mudstones from two Ordovician foreland basins in the Appalachians, *in* Dorobek, S. L., and Ross, G. M., eds., Stratigraphic evolution of foreland basins: Society of Economic Paleontologists and Mineralogists Special Publication 52, p. 53-64.

Allen, P. A., Crampton, S. L., and Sinclair, H. D., 1991, The inception and early evolution of the North Alpine foreland baasin, Switzerland: Basin Research, v. 3, p. 143-163.

Alvarez, W., Engelder, T., and Geiser, P. A., 1978, Classification of solution cleavage in pelagic limestones: Geology, v. 6, p. 263-266.

Aydin, A., 1988, Discontinuities along thrust faults and the cleavage duplex, *in* Mitra, G., and Wojtal, S., eds., Geometries and Mechanisms of Thrusting, with Special Reference to the Appalachians: Geological Society of America Special Paper 222, p. 223-232.

Bartholomew, M. J., 1987, Structural evolution of the Pulaski thrust system, southwestern Virginia: Geological Society of America Bulletin, v. 99, p. 491-510.

Bayona, G., and Thomas, W. A., 2003, Distinguishing fault reactivation from flexural deformation in the distal stratigraphy of the Peripheral Blountian Foreland Basin, southern Appalachians, USA: Basin Research, v. 15, p. 503-526.

Benedict, G. L., III, and Walker, K. R., 1978, Paleobathymetric analysis in Paleozoic sequences and its geodynamic significance: American Journal of Science, v. 278, p. 579-607.

Bream, B. R., 2003, Tectonic implications of para- and orthogneiss geochronology and geochemistry from the southern Appalachian crystalline core [Ph.D. dissert.]: Knoxville, University of Tennessee, 296 p.

Brendt, W. B., 1993. Geologic map of the Kingsport quadrangle, Tennessee: Tennessee Division of Geology, scale 1:24,000.

Brokaw A. L., Dunlap, J. C., and Rodgers, J., 1966, Geology and mineral deposits of the Mosheim and Johnson anticlines, Greene County, Tennessee: U.S. Geological Survey Bulletin 1222-A, p. A1-A21.

Busby, C.J., and Ingersoll, R.V. (eds.), 1995, Tectonics of sedimentary basins: Blackwell Science, Cambridge, 579p.

Butts, C., 1933, Geologic map of the Appalachian Valley of Virginia with explanatory text: Virginia Geological Survey Bulletin 42, scale 1:62,500.

Byerly, D. W., 1966, Structural geology along a segment of the Pulaski fault, Greene County, Tennessee [Ph.D. dissert.]: Knoxville, University of Tennessee, 94 p.

Byerly, D. W., 1969, Geologic map of the Baileyton quadrangle, Tennessee: Tennessee Division of Geology, scale 1:24,000.

Byerly, D. W., 1996, Geologic map of the Greeneville quadrangle, Tennessee: Tennessee Division of Geology, scale 1:24,000.

Campbell, M. R., 1894, Estillville folio, U.S. Geological Survey Geologic Atlas, (no. 12), scale 1:125,000.

Campbell, M. R., 1925, The Valley coal fields of Virginia: Virginia Geological Survey Bulletin 25, 322 p.

Chapple, W. M., 1978, Mechanics of thin–skinned fold–and–thrust belts: Geological Society of America Bulletin, v. 89, p. 1189–1198.

Cook, F. A., Albaugh, D. S., Brown, L. D., Kaufman, S., Oliver, J. E., and Hatcher, R. D., Jr., 1979, Thin-skinned tectonics in the crystalline southern Appalachians: COCORP seismic-reflection profiling of the Blue Ridge and Piedmont: Geology, v. 7, p. 563-567.

Cooper, G. A., and Prouty, C. E., 1943, Stratigraphy of the lower Middle Ordovician Tazewell County, Virginia: Geological Society of America Bulletin, v. 54, p. 819-896.

Cummings, D., 1962, Geology of the Bays Mountain synclinorium, northeast Tennessee [Ph.D. dissert.]: East Lansing, Michigan State University, 152 p.

Cummings, D., 1965, Stratigraphy and heavy minerals of the Bays Formation, Bays Mountain synclinorium, northeast Tennessee: Geological Society of America Bulletin, v. 76, p. 591-600.

Dahlstrom, C. D. A., 1970, Structural geology in the eastern margin of the Canadian Rocky Mountains: Bulletin of Canadian Petroleum Geology, v. 18, p. 332-406.

Davis, D., Suppe, J., and Dahlen, F. A., 1983, Mechanics of fold-and-thrust belts and accretionary wedges: Journal of Geophysical Reasearch, v. 88, p. 1153-1172.

Dennison, J. M. and Woodward, H. P., 1963, Palinspastic maps of central Appalachians: Bulletin of American Association of Petroleum Geologists, v. 47, p. 666-680.

Drake, A. A., Jr., Sinha, A. K., Laird, J., and Guy, R. E., 1989, The Taconic orogen, *in* Hatcher, R. D., Jr., Thomas, W. A., and Viele, G. W., eds., The Appalachian-Ouachita orogen in the United States: Boulder, Colorado, Geological Society of America, The Geology of North America, v. F-2, p. 101-177.

Edwards, G., Henle, W. K., Osmond, J. K., and Adams, J. A. S., 1959, Further progress in absolute dating of the Middle Ordovician: Geological Society of America Bulletin, v. 70, p 1596-1599.

Einsele, G., 2000, Sedimentary basins: Evolution, facies, and sediment budget: Berlin, Springer-Verlag, 792 p.

Ettensohn, F. R., 2004, Modeling the nature and development of major Paleozoic clastic wedges in the Appalachian Basin, USA: Journal of Geodynamics, v. 37, p. 657–681.

Finney, S. C., Grubb, B. J., and Hatcher, R. D., Jr., 1996, Graphic correlation of Middle Ordovician graptolite shale, southern Appalachians: An approach for examining the subsidence and migration of a Taconic foreland basin: Geological Society of America Bulletin, v. 108, no. 3, p. 355-371.

Haney, D. C., 1966, Structural geology along a segment of the Saltville fault, Hawkins County, Tennessee [Ph. D. dissert.]: Knoxville, University of Tennessee, 127 p.

Hardeman, W. D., 1966, Geologic map of Tennessee: Tennessee Division of Geology, scale 1:250,000.

Harris, A. G., and Repetski, J. E., 1982, Conodonts revise the Lower-Middle Ordovician boundary and timing of miogeoclinal events in the east-central Appalachian basin: Geological Society of America Abstracts with Programs, v. 14, no. 5, p. 261.

Hatcher, R. D., Jr., 1989, Tectonic synthesis of the U.S. Appalachians, *in* Hatcher, R. D., Jr., Thomas, W. A., and Viele, G. W., eds., The Appalachian-Ouachita orogen in the United States: Boulder, Colorado, Geological Society of America, The Geology of North America, v. F-2, p. 511-535.

Hatcher, R. D., Jr., 1990, Structural geology principles, concepts, and problems: Englewood Cliffs, New Jersey, Prentice Hall, 525 p.

Hatcher, R. D., Jr., 2004, Sediments derived from mountain chains do not always land in foredeeps: Southern Appalachian Sevier-Blountian basin dynamics: Geological Society of America Abstracts with Programs, v. 36, no. 2, p. 92.

Hatcher, R. D., Jr., and Hooper, R. J., 1990, Laboratory manual for structural geology: Columbus, Ohio, Macmillan Publishing Company, 217 p.

Hayes, C. W., 1891, The overthrust faults of the southern Appalachians: Geological Society of America Bulletin, v. 2, 141-152 p.

Holland, S. 2003. Sequence Stratigraphy of the Middle and Upper Ordovician of the Eastern United States: online resource available University of Georgia Department of Geology Stratigraphy Lab, URL: http://www.uga.edu/~strata/ordoss/ordoseqstrat.pdf

House, W. M., and Gray, D. R., 1982, Cataclasites along the Saltville thrust, U.S.A. and their implications for thrust-sheet emplacement: Journal of Structural Geology, v. 4, p. 257-269.

Huff, W. D., Bergstrom, S. M., and Kolata, D. R., 1992, Gigantic Ordovician volcanic ash fall in North America and Europe: Biological, tectonomagmatic, and event-stratigraphy significance: Geology, v. 20, p. 875-878.

Johnson, A. M., 1977, Styles of folding: Mechanics and mechanisms of folding of natural elastic materials: Amsterdam, Elsevier, 406 p.

Keith, A., 1895, Description of the Knoxville folio (Tennessee-North Carolina): U.S. Geological Survey Geologic Atlas, Folio 16, 6 p.

Keith, A., 1896, Description of the Morristown folio (Tennessee-North Carolina): U.S. Geological Survey Geologic Atlas, Folio 27, 6 p.

Keith, A., 1905a, Description of the Greeneville folio (Tennessee-North Carolina): U.S. Geological Survey Geologic Atlas, Folio 118, 12 p.

Keith, A., 1905b, Description of the Morristown folio (Tennessee-North Carolina): U.S. Geological Survey Geologic Atlas, Folio 27, 13 p.

Kellberg, J. M, and Grant, L. F., 1956, Coarse conglomerates of the Middle Ordovician in the southern Appalachian valley: Geological Society of America Bulletin, v. 67, no. 6, p. 697-716.

Lemiszki, P. J., 2003, Geologic map of the Mosheim quadrangle, Tennessee: Tennessee Division of Geology, open file map scale 1:24,000.

Mack, G. H., 1985, Provenance of the Middle Ordovician Blount clastic wedge, Georgia and Tennessee: Geology, v. 13, p. 299-302.

Milici R., Harris, L. D., and Statler, A. T., 1979, An interpretation of seismic cross sections in the Valley and Ridge of eastern Tennessee: Tennessee Division of Geology, Oil and Gas Seismic Investigations Series 1, 2 sheets.

Mussman, W. J., and Read, J. F., 1986, Sedimentology and development of a passive- to convergent-margin unconformity: Middle Ordovician Knox unconformity, Virginia Appalachians: Geological Society of America Bulletin, v. 97, p. 282-295.

Neuman, R. B., 1955, Middle Ordovician rocks of the Tellico-Sevier belt, eastern Tennessee: Geological Survey Professional Paper 274-F, 178 p.

Ohlmacher, G. C., 1991, Mechanics of vein fault, and solution surface formation in Bays Mountain, Southern Appalachians [Ph. D., Dissert.]: West Lafayette, IN, Purdue University, 162 p.

Ohlmacher, G. C., and Aydin, A., 1995, Progressive deformation and fracture patterns during foreland thrusting in the southern Appalachians: American Journal of Science, v. 295, p. 943-987.

Ohlmacher, G. C., and Aydin, A., 1997, Mechanics of vein, fault and solution surface formation in the Appalachian Valley and Ridge, northeastern Tennessee, U.S.A.: implications for fault friction, state of stress and fluid pressure: Journal of Structural Geology, v. 19, 927-944.

Pope, M., and Read, J. F., 1998, Ordovician metre-scale cycles: implications for climate and eustatic fluctuations in the central Appalachians during a global greenhouse, non-glacial to glacial transition: Paleogeography, Palaeoclimatology, Palaeoecology v. 138, p. 27-42.

Prothero, D. R., and Schwab, F., 1999, Sedimentary Geology: An introduction to Sedimentary Rocks and Stratigraphy: W. H. Freeman and Company, New York, 575 p.

Ramsay, J. G., and Huber, M. I., 1987, The techniques of modern structural geology, v. 2: Folds and fractures: London, Academic Press, 392 p.

Read, J. F., and Tillman, C. G., 1977, Field trip guide to lower Middle Ordovician platform and basin facies rocks, southwestern Virginia, *in* Ruppel S.C., and Walker, K.R., eds., The ecostratigraphy of the Middle Ordovician of the southern Appalachians (Kentucky, Tennessee, and Virginia), U.S.A.: A field excursion: University of Tennessee Studies in Geology 71-1, p. 17-26.

Reks, I. J., and Gray, D. R., 1983, Strain patterns and shortening in a folded thrust sheet: An example from the southern Appalachians: Tectonophysics, v. 93, p. 99-128.

Rich, J. L., 1934, Mechanics of low-angle overthrust faulting as illustrated by Cumberland thrust block, Virginia, Kentucky, and Tennessee: American Association of Petroleum Geologists Bulletin, v. 18, no. 12, p. 1584-1596.

Ricci-Lucchi, F., 1986, The Oligocene to Recent foreland basins of the Northern Apennines, *in* Allen, P.A., and Homewood, P., eds, Foreland Basins: International Association of Sedimentologist Special Publication, 8, p. 105-139.

Rodgers, J., 1953a, Geologic map of East Tennessee with explanatory text: Tennessee Division of Geology, scale 1:125,000.

Rodgers, J., 1953b, Geologic map of East Tennessee with explanatory text: Tennessee Division of Geology Bulletin 58, Part II, 168 p.

Rodgers, J. L., 1971, The Taconic Orogeny: Geological Society of America Bulletin, v. 82, p. 1141-1178.

Roeder, D., Gilbert, O. E., Jr., and Witherspoon, W. D., 1978, Evolution and macroscopic structure of Valley and Ridge Province thrust belt, Tennessee and Virginia: Knoxville, University of Tennessee, Department of Geological Sciences, Studies in Geology no. 2, 25 p.

Rogers, H. D., 1838, Second annual report on the geological exploration of the state of Pennsylvania: Harrisburg, Lippincott, 91 p.

Safford, J. M., 1856, A geological reconnaissance of the state of Tennessee: Nashville, Mercer, 164 p.

Safford, J. M., 1869, Geology of Tennessee, State of Tennessee: Nashville, Mercer, 550 p.

Safford, J. M., and Killebrew, J. B., 1876, The elementary geology of Tennessee: Nashville, Mercer, 225 p.

Shanmugam, G., 1978, The stratigraphy, sedimentology and tectonics of the Middle Ordovician Sevier Shale basin in East Tennessee [Ph.D. Dissert.]: Knoxville, University of Tennessee, 222 p.

Shanmugam, G., and Lash, G. C., 1982, Analogous tectonic evolution of the Ordovician foredeeps, southern and central Appalachians: Geology, v. 11, p. 562-566.

Shanmugam, G., and Walker, K. R., 1978, Tectonic significance of distal turbidites in the Middle Ordovician Blockhouse and lower Sevier formations in East Tennessee: American Journal of Science, v. 278, p. 551-578.

Shanmugam, G., and Walker, K. R., 1980, Sedimentation, subsidence, and evolution of a foredeep basin in the Middle Ordovician, southern Appalachians: American Journal of Science, v. 280, p. 479-496.

Shanmugam, G., and Walker, K. R., 1983, Anatomy of the Middle Ordovician Sevier shale basin, eastern Tennessee: Sedimentary Geology, v. 34, p. 315-337.

Stevenson, J. J., 1885, Notes on the geological structure of Tazewell, Russell, Wise, Smyth, and Washington Counties of Virginia: Proceedings of the American Philosophical Society, vol. 22, p. 114-161.

Suppe, J., 1983, Geometry and kinematics of fault-bend folding: American Journal of Science, v. 283, p. 684-721.

Suter, D. R., and Tillman, C. G., 1973, The conodont genus *Multioistodus* from supratidal limestones in the Beekmantown Formation of the Appalachians of west-central Virginia: Geological Society of America Abstracts with Programs, v. 5, no. 5, p.441-442.

Swingle, G. D., 1962, Cleavage in the Valley and Ridge province of East Tennessee: Tennessee Academy of Sciences, v. 37, p. 66.

Thomas, W. A., Becker, T. P., Samson, S. D., and Hamilton, M. A., 2004, Detrital zircon evidence of a recycled orogenic foreland provenance for Alleghanian clastic-wedge sandstones: Journal of Geology, v. 112, p. 23-37.

Troensegaard, K. W., 1965, Development of cleavage in a portion of the Bays Mountain Synclinorium, Greene, Cocke, Hamblen, and Jefferson Counties, Tennessee [M.S. thesis]: Knoxville, University of Tennessee, 39 p.

Twenhofel, W. H., Bridge, Josiah, Cloud, P. E., Cooper, B. N., Cooper, G. A., Cummings, E. R., Cullison, J. S., Dunbar, C. O., Kay, Marshall, Liberty, B. A., McFarlan, A. C., Rodgers, John, Whittington, H. B., Wilson, A. E., and Wilson, C. W., 1954, Correlation of the Ordovician formations of North American, Geological Society of America Bulletin, v. 65, p. 247-298.

Ulrich, E. O., 1911, Revision of the Paleozoic systems: Geological Society of America Bulletin, v. 22, p. 281-681.

Ulrich, E. O., 1930, Ordovician trilobites of the family *Telephidae* and concerned stratigraphic relations: U. S. National Museum Proceedings v. 76, 21 p.

Vick, H. K., Channel, J. E. T., and Opdyke, N. D., 1987, Ordovician docking of the Carolina Slate Belt: Paleomagnetic data: Tectonics, v. 6, p. 573-583.

Walker, K. R., 1980, Rhythms in deep-sea, fine-grained turbidite and debris-flow sequences, Middle Ordovician, eastern Tennessee: Sedimentology, v. 27, p. 419-432.

Walker, K. R., ed., 1985, The geological history of the Thorn Hill Paleozoic section (Cambrian-Mississippian), eastern Tennessee: University of Tennessee, Department of Geological Sciences, Studies in Geology, no. 10, 128 p.

Walker, K. R., Shanmugam, G., and Ruppel, S. C., 1983, A model for carbonate terrigenous clastic sequences: Geological Society of America Bulletin, v. 94, p. 700-712.

Webb, R., Jr., 1959, Geology of the Middle Ordovician limestones in the Rich Valley area, Smyth County, Virginia [M.S. thesis]: Blacksburg, Virginia Polytechnic Institute, 96 p.

Whisner, S. C., 2005, The Middle Ordovician Tellico-Sevier syncline: a stratigraphic, structural and paleoseismic investigation [Ph.D. dissert.]: Knoxville, University of Tennessee, 171 p.

Wilson, G., 1952, Ptygmatic structures and their formation: Geology, v. 89, no. 1, p. 1-21.

Wiltschko, D. V., Madeweff, D. A., and Millson, H. E., 1985, Distribution and mechanisms of strain within rocks on the northwest ramp of the Pine Mount block, southern Appalachian foreland: Geological Society of America Bulletin, v. 96, p. 426-435.

Woodward, N. B., and Gray, D. R., 1985, Four southwestern Virginia-northeast Tennessee balanced cross sections, *in* Woodward, N. B., ed., Valley and Ridge thrust belt; Balanced structural sections, Pennsylvania to Alabama: Knoxville, University of Tennessee, Department of Geological Sciences Studies in Geology, v. 12, p. 40-43.

Yust, W. W., 1976, A mesoscopic fabric analysis of a portion of the Tellico-Sevier Belt of East Tennessee [M.S. Thesis]: Knoxville, University of Tennessee, 106 p.

Appendix:

Structural and lithology data for the McCloud, Baileyton, Burem, Greeneville, and Stony Point quadrangles

ABBREVIATIONS

Quadrangle Units

B - Baileyton OMB – Martinsburg Formation
BU - Burem OB - Bays Formation
G - Greeneville OSVU - Sevier Shale (upper)
M - McCloud OL - Lenoir Limestone
SP - Stony Point OM - Mosheim Member

Lithology

SA - Sandy (frequently comprised of quartz)
SI - Silt
CALC. - Calcareous
RED SS - Red sandstone (hematite)
CA. SILTST. - Calcareous siltstone
SH. - Shale
FOSSIL - Fossiliferous
QZ. - Quartz
GR-BL - Gray to black (frequently carboniferous [OSVL])
GREEN - Green (in this case referring to Martinsburg

Station	Quad	Lithology	BEDDING		Axial Surface		Cleavage		IL	Amp.	SLICKENSIDES		Joint		CROSS BED	
			Strike	Dip	DIP2	STRIKE	Strike	Dip2	Angle	(m)	Plunge3	Trend3	Strike 2	Dip3	Plunge4	Trend4
1	M	SI LS.	N52E	79SE												
2	M	SI LS.	N21E	34SE												
3	M	SI LS.	N10E	4SE												
4	M	SI LS.	N29E	10SE												
5	M	SI LS.	N68E	7SE												
6	M	THIN BED TAN SHALE	N63E	25SE												
7	M	DARK GREY SHALE	N52E	53SE												
8	M	SI/SA SHALE	N61E	14NW												
9	M	SA LS.	N59E	4NW												
10	M	SA LS.	N60E	2SE												
11	M	SA LS.	N38E	21SE												
12	M	CALC. SH.	N48E	77SE			N82E	72SE								
13	M	FISSILE SH.	N26E	41SE			N81E	21SE								
14	M	SA LS.	N41E	14SE												
15	M	SA LS.	N61E	68SE			N82W	69NE								
16	M	CALC. SH.	N57E	60SE												
17	M	PENCIL SH.	N41E	78SE			N39E	68NW					N48E	80NW		
18	M	SI LS.	N42E	72NW			N78E	61NW								
19	M	CA SILTST.	N78E	40NW												
20	M	SI LS.	N48E	41SE												
21	M	SI LS.	N39E	71SE			N35E	81SE								
22	M	CA SILTST.	N43E	64SE			N48E	80NW								
23	M	SI LS.	N23E	64SE												
24	M	QZ. SS	N55E	39NW			N68E	41SE								
25	M	GREEN SH.	N68E	43NW												
26	M	QZ. SS	N39E	30NW												
27	M	RED SS & QZ. SS	N54E	83SE			N76E	21SE			88SW	N39W	N20W	78SE		
28	M	SA LS.	N50E	30SE			N65E	46NW								
29	M	FISSILE SH.	N20E	53NW												
30	M	CALC. SH.	N51E	71NW												
31	M	CALC. SH.	N81E	43NW												
32	M	PENCIL SH.	N69E	32NW			N69E	71SE								
33	M	CALC. SH.	N36E	11NW												
34	M	CALC. SH.	N61E	25NW			N35E	82SE					N35W	78SW		
35	M	SA LS.	N51E	19NW												
36	M	SA LS.	N52E	14NW												
37	M	SA LS.	N42E	25NW												
38	M	SA LS.	N72W	27NE												
39	M	SA LS.	N42E	39NW	4SE	N40E			120	2						
40	M	SA LS.	N18E	23NW												

Station	Quad	Lithology	BEDDING		Axial Surface		Cleavage		IL	Amp.	SLICKENSIDES		Joint		CROSS BED	
			Strike	Dip	DIP2	STRIKE	Strike	Dip2	Angle	(m)	Plunge3	Trend3	Strike 2	Dip3	Plunge4	Trend4
41	M	SA LS.	N17E	9NW												
42	M	SA LS.	N18E	3NW												
43	M	SA LS.	N50E	8NW												
44	M	SA LS.	N54E	30NW												
45	M	SA LS.	N59E	79SE												
46	M	SA LS.	N56E	18NW												
47	M	SA LS.	N64E	19NW												
48	M	SA LS.	N52E	14NW												
49	M	CALC. SH.	N75E	10NW												
50	M	SA LS.	N0E	0SE												
51	M	SA LS.	N21E	4SE												
52	M	SA SH.	N22W	8NW												
53	M	SA LS.	N22E	2SE											3SE	N23E
54	M	SA LS. & CALC. SH	N0E	0SE												
55	M	OSV SA LS.	N41E	65SE			N41E	12NW							5SE	N52E
56	M	GREY THIN BED SH.	N10E	70SE			N38E	15NW								
57	M	GREY THIN BED SH.	N60E	34SE												
58	M	GREY THIN BED SH.	N58W	24SW												
59	M	GREY THIN BED SH.	N48E	23SE												
60	M	SA LS.	N57E	20SE												
61	M	SA LS.	N69E	22SE												
62	M	OSV SA LS.	N68E	36SE												
63	M	TAN FISSILE SH.	N59E	62SE												
64	M	SA LS.	N54E	84NW												
65	M	SA LS.	N84E	9SE												
66	M	THICK BED SH.	N37W	10NE												
67	M	SA LS.	N9E	19SE												
68	M	SA LS.	N42W	11SW												
69	M	UOSV SA LS.	N0E	0SE												
70	M	SA LS.	N0S	8W												
71	M	SA LS.	N31E	19SE											15SE	N48E
72	M	SA SH.	N60E	4SE												
73	M	UOSV SA LS.	N43E	6SE												
74	M	TAN SHALE	N38E	17SE												
75	M	TAN SHALE	N38E	63SE												
76	M	UOSV SA LS.	N21E	9NW			N34E	67NW								
77	M	UOSV SA LS.	N39E	12NW												
78	M	SA LS.	N79E	9SE												
79	M	UOSV SA LS.	N0E	0SE												
80	M	TAN SHALE	N0E	N0SE												

Station	Quad	Lithology	BEDDING		Axial Surface		Cleavage		IL	Amp.	SLICKENSIDES		Joint		CROSS BED	
			Strike	Dip	DIP2	STRIKE	Strike	Dip2	Angle	(m)	Plunge3	Trend3	Strike 2	Dip3	Plunge4	Trend4
81	M	UOSV SA LS.	N44E	15NW												
82	M	UOSV SA LS.	N29E	31NW												
83	M	THICK BED SH.	N46E	16NW												
84	M	UOSV SA LS.	N0E	0SE												
85	M	UOSV SA LS.	N66E	9NW												
86	M	UOSV FOSSIL LMS	N71E	26NW												
87	M	TAN SHALE	N56E	14NW												
88	M	UOSV SA LS.	N82E	9SE												
89	M	TAN SHALE	N38E	50SE												
90	M	TAN SHALE	N29W	4NE												
91	M	THICK BED SH.	N21W	16NE												
92	M	SA LS.	N21W	16NE												
93	M	UOSV SA LS.	N80E	3NW												
94	M	UOSV SA LS.	N0E	0SE												
95	M	SI/SA SHALE	N0E	0SE												
96	M	SA SH.	N5E	9SE			N75E	50SW								
97	M	UOSV SA LS.	N75W	11NE												
98	M	UOSV SA LS.	N0E	0SE												
99	M	THICK BED SH.	N0E	0SE												
100	M	SA SH.	N84W	9NE												
101	M	SA LS.	N51W	25NE											12SE	N52E
102	M	UOSV SA LS.	N20W	10SW												
103	M	UOSV SA LS.	N18E	14SE												
104	M	SA SH.	N5W	35SW												
105	M	DARK GREY SHALE	N35E	20SE												
106	M	TAN SHALE	N62E	57NW												
107	M	TAN SHALE	N31E	12SE												
108	M	TAN SHALE	N51E	90SE												
109	M	TAN SHALE	N29E	90SE												
110	M	TAN SHALE	N36E	16NW												
111	M	TAN SHALE	N38E	12SE			N76E	62NW								
112	M	TAN SHALE	N62E	62SE												
113	M	PENCIL SH.	N72E	55SE												
114	M	TAN SHALE	N70E	48SE			N12E	41NW								
115	M	TAN SHALE	N64E	62SE												
116	M	TAN SHALE	N51E	68SE												
117	M	UOSV SA LS.	N41E	72SE												
118	M	UOSV SA LS.	N48E	90SE												
119	M	UOSV SA LS.	N69E	42NW												
120	M	UOSV SA LS.	N77E	65NW												

Station	Quad	Lithology	BEDDING		Axial Surface		Cleavage		IL	Amp.	SLICKENSIDES		Joint		CROSS BED	
			Strike	Dip	DIP2	STRIKE	Strike	Dip2	Angle	(m)	Plunge3	Trend3	Strike 2	Dip3	Plunge4	Trend4
121	M	USOV FOSSIL LS.	N71E	55NW												
122	M	TAN SHALE	N51E	76SE												
123	M	SA SH.	N24E	45SE												
124	M	TAN SHALE	N54E	85SE												
125	M	TAN SHALE	N88E	28NW												
126	M	SA SH.	N50E	74NW												
127	M	SA SH.	N58W	14NE												
128	M	SA LS.	N71W	4NE												
129	M	UOSV SA LS.	N41E	4NE												
130	M	UOSV SA LS.	N69E	9SE												
131	M	UOSV SA LS.	N0E	0SE												
132	M	UOSV SA LS.	N0E	0SE												
133	M	UOSV SA LS.	N0E	0SE												
134	M	UOSV SA LS.	N67E	2NW												
135	M	UOSV SA LS.	N69E	15NW												
136	M	UOSV SA LS.	N71E	21NW												
137	M	SA SH.	N75E	5NW												
138	M	TAN FISSILE SH.	N80E	26NW												
139	M	TAN SHALE	N50E	35NW												
140	M	TAN SHALE	N32E	28NW												
141	M	SA LS.	N77W	35SW												
142	M	SA LS.	N63E	36SE												
143	M	TAN SHALE	N19E	76SE												
144	M	TAN SHALE	N21E	70SE	5NW	N24E			45	2						
145	M	PENCIL SH.	N48E	55SE			N69E	79NW								
146	M	TAN FISSILE SH.	N50E	86SE												
147	M	TAN SHALE	N49E	68SE												
148	M	UOSV SA LS.	N71E	66NE	5SE	N50E	N40E	88SE	15	15						
149	M	UOSV SA LS.	N67E	44NE												
150	M	UOSV SA LS.	N74E	18NW												
151	M	UOSV SA LS.	N70E	15NW												
152	M	UOSV SA LS.	N76E	66NW												
153	M	THICK BED SH.	N60E	62NW												
154	M	THICK BED SH.	N52E	60SE												
155	M	TAN FISSILE SH.	N60E	72NW												
156	M	TAN SHALE	N52E	34NW												
157	M	UOSV SA LS.	N58E	39NW											7N	N72E
158	M	UOSV SA LS.	N76E	29NW												
159	M	UOSV SA LS.	N82E	14SE												
160	M	UOSV SA LS.	N70E	16SE												
161	M	SA LS.	N68E	5SE												

Station	Quad	Lithology	BEDDING		Axial Surface		Cleavage		IL	Amp.	SLICKENSIDES		Joint		CROSS BED	
			Strike	Dip	DIP2	STRIKE	Strike	Dip2	Angle	(m)	Plunge3	Trend3	Strike 2	Dip3	Plunge4	Trend4
162	M	UOSV SA LS.	N90E	21SE												
163	M	UOSV SA LS.	N35W	6SW												
164	M	UOSV SA LS.	N0E	0SE												
165	M	SA SH.	N55W	10SW												
166	M	UOSV SA LS.	N34E	14SE												
167	M	TAN SHALE	N10E	10SE			N36E	90NW								
168	M	UOSV SA LS.	N75E	14NW												
169	M	TAN SHALE	N86E	15NW												
170	M	SA SH.	N59E	11NW												
171	M	UOSV SA LS.	N90E	4SE												
172	M	UOSV SA LS.	N20W	16SW												
173	M	TAN SHALE	N76E	90SE												
174	M	TAN SHALE	N46E	35NW												
175	M	TAN SHALE	N46E	73SE												
176	M	TAN SHALE	N86W	82NE												
177	M	TAN SHALE	N70E	90SE												
178	M	TAN SHALE	N56E	61NW												
179	M	TAN SHALE	N63E	90SE												
180	M	TAN SHALE	N70E	19NW												
181	M	UOSV SA LS.	N72E	28NW												
182	M	UOSV SA LS.	N89E	21NW												
183	M	UOSV SA LS.	N88E	24NW	N70E	25NW	N88E	24NW	30	10						
184	M	UOSV SA LS.	N45E	27NW												
185	M	UOSV SA LS.	N50E	45NW												
186	M	TAN SHALE	N48E	74NW												
187	M	TAN SHALE	N45E	58NW												
188	M	TAN SHALE	N72E	36NW												
189	M	THICK BED SH.	N64E	87SE												
190	M	UOSV SA LS.	N62E	24NW												
191	M	UOSV SA LS.	N50E	20NW			N67W	11NE								
192	M	UOSV SA LS.	N53E	15NW												
193	M	UOSV SA LS.	N67E	16NW												
194	M	TAN SHALE	N88E	30NW												
195	M	TAN SHALE	N30E	37SE												
196	M	TAN SHALE	N46E	24SE												
197	M	TAN SHALE	N41E	64SE												
198	M	UOSV SA LS.	N75E	53SE												
199	M	UOSV SA LS.	N44E	55SE												
200	M	TAN SHALE	N39E	70SE												
201	M	TAN SHALE	N66E	60NW												

Station	Quad	Lithology	BEDDING		Axial Surface		Cleavage		IL	Amp.	SLICKENSIDES		Joint		CROSS BED	
			Strike	Dip	DIP2	STRIKE	Strike	Dip2	Angle	(m)	Plunge3	Trend3	Strike 2	Dip3	Plunge4	Trend4
202	M	TAN SHALE	N60E	64SE												
203	M	TAN SHALE	N42E	70NW												
204	M	TAN SHALE	N52E	45SE												
205	M	TAN SHALE	N49E	31NW												
206	M	UOSV SA LS.	N66E	37NW												
207	M	UOSV SA LS.	N29E	24NW			N39E	78NW								
208	M	UOSV SA LS.	N15E	10NW												
209	M	UOSV SA LS.	N40E	12NW												
210	M	TAN SHALE	N0E	0SE												
211	M	UOSV SA LS.	N82E	5SE												
212	M	UOSV SA LS.	N68E	26SE												
213	M	UOSV SA LS.	N0E	0SE									N48E	76SE		
214	M	UOSV SA LS.	N58E	11NW												
215	M	TAN SHALE	N59E	43SE												
216	M	TAN SHALE	N51E	51NW												
217	M	TAN SHALE	N80E	61SE												
218	M	UOSV SA LS.	N55E	24SE												
219	M	SA LS.	N59E	30SE												
220	M	TAN SHALE	N0E	0SE												
221	M	THN BED SH.	N0E	0SE												
222	M	TAN SHALE	N44E	5SE												
223	M	UOSV SA LS.	N78E	5SE												
224	M	UOSV SA LS.	N10E	8NW												
225	M	SA SH.	N29W	9SW												
226	M	THICK BED SH.	N31E	14SE												
227	M	UOSV SA LS.	N37E	30SE												
228	M	UOSV SA LS.	N46E	45SE												
229	M	UOSV SA LS.	N40E	60SE												
230	M	UOSV SA LS.	N41E	30SE			N68E	84SE								
231	M	SA LS.	N47E	60SE												
232	M	UOSV SA LS.	N39E	84SE												
233	M	UOSV SA LS.	N60E	36SE												
234	M	UOSV SA LS.	N50E	55NW												
235	M	UOSV SA LS.	N59E	9NW												
236	M	TAN SHALE	N48E	4NW												
237	M	UOSV SA LS.	N55E	70SE												
238	M	UOSV SA LS.	N40E	69SE												
239	M	UOSV SA LS.	N50E	65SE												
240	M	UOSV SA LS.	N59E	75SE												
241	M	SA LS.	N45E	33SE												

Station	Quad	Lithology	BEDDING		Axial Surface		Cleavage		IL	Amp.	SLICKENSIDES		Joint		CROSS BED	
			Strike	Dip	DIP2	STRIKE	Strike	Dip2	Angle	(m)	Plunge3	Trend3	Strike 2	Dip3	Plunge4	Trend4
242	M	TAN SHALE	N68E	65SE												
243	M	UOSV SA LS.	N65E	89SE												
244	M	THICK BED SH.	N85E	32SE												
245	M	UOSV SA LS.	N81E	33SE												
246	M	SA LS.	N60E	15SE												
247	M	UOSV SA LS.	N65W	10NE												
248	M	TAN SHALE	N74E	65SE												
249	M	UOSV SA LS.	N40E	55SE												
250	M	TAN SHALE	N81E	79SE												
251	M	TAN SHALE	N46E	89NW												
252	M	TAN SHALE	N39E	69SE												
253	M	TAN SHALE	N45E	79NW												
254	M	UOSV SA LS.	N9E	40SE												
255	M	TAN SHALE	N80E	27SE			N15E	90SE								
256	M	UOSV SA LS.	N88E	85NW												
257	M	TAN FISSILE SH.	N55E	60NW												
258	M	UOSV SA LS.	N36E	37NW												
259	M	UOSV SA LS.	N35E	14SE			N52E	33SE								
260	M	TAN SHALE	N14E	31NW									N72E	59SE		
261	M	TAN SHALE	N58E	75SE												
262	M	TAN SHALE	N40E	72SE												
263	M	TAN SHALE	N44E	90SE												
264	M	TAN SHALE	N51E	80SE												
265	M	SA SH.	N48E	78SE			N48E	16SE								
266	M	TAN SHALE	N48E	64SE												
267	M	SA SH.	N66E	71SE												
268	M	TAN SHALE	N50E	90SE												
269	M	TAN SHALE	N50W	29NE												
270	M	TAN SHALE	N61E	79NW												
271	M	UOSV SA LS.	N41E	27SE												
272	M	UOSV SA LS.	N60E	56NW												
273	M	UOSV SA LS.	N22E	35SE												
274	M	UOSV SA LS.	N68E	59SE												
275	M	UOSV SA LS.	N76E	25SE												
276	M	SA LS.	N50E	87NW												
277	M	UOSV SA LS.	N50E	87NW												
278	M	SA LS.	N66E	36SE												
279	M	UOSV SA LS.	N40E	45SE												
280	M	UOSV SA LS.	N49E	49SE												
281	M	UOSV SA LS.	N62E	11SE												

Station	Quad	Lithology	BEDDING		Axial Surface		Cleavage		IL	Amp.	SLICKENSIDES		Joint		CROSS BED	
			Strike	Dip	DIP2	STRIKE	Strike	Dip2	Angle	(m)	Plunge3	Trend3	Strike 2	Dip3	Plunge4	Trend4
282	M	UOSV SA LS.	N9E	80NW	4SE	N10E	N48E	88SE	40	2						
283	M	UOSV SA LS.	N30E	39SE												
284	M	UOSV SA LS.	N59E	4NW												
285	M	UOSV SA LS.	N28E	30SE												
286	M	UOSV SA LS.	N41E	51SE												
287	M	UOSV SA LS.	N24E	18NW			N4E	18SE								
288	M	UOSV SA LS.	N29E	64SE												
289	M	UOSV SA LS.	N61E	61SE												
290	M	TAN FISSILE SH.	N52E	71NW												
291	M	SA SH.	N62E	30NW												
292	M	TAN SHALE	N57E	28NW												
293	M	SA LS.	N37E	79NW												
294	M	UOSV SA LS.	N69E	46NW												
295	M	UOSV SA LS.	N66E	55NW												
296	M	TAN SHALE	N69E	80NE												
297	M	UOSV SA LS.	N50E	60NW												
298	M	UOSV SA LS.	N24E	30SE			N35E	68SE								
299	M	UOSV SA LS.	N35E	60SE												
300	M	UOSV SA LS.	N47E	62NW												
301	M	UOSV SA LS.	N49E	88SE												
302	M	UOSV SA LS.	N43E	70SE												
303	M	UOSV SA LS.	N19E	21NW												
304	M	UOSV SA LS.	N69E	46SE												
305	M	UOSV SA LS.	N32E	30SE												
306	M	UOSV SA LS.	N5E	17NW												
307	M	UOSV SA LS.	N41E	81SE												
308	M	TAN SHALE	N35E	79SE												
309	M	UOSV SA LS.	N29E	67SE												
310	M	SA SH.	N35E	56NW												
311	M	UOSV SA LS.	N38E	84SE												
312	M	TAN SHALE	N15E	45SE												
313	M	SA SH.	N55E	84SE												
314	M	UOSV SA LS.	N36E	65NW												
315	M	TAN SHALE	N48E	68NW												
316	M	UOSV SA LS.	N62E	63SE												
317	M	CALC. MUDSTONE	N51E	69SE												
318	M	TAN SHALE	N34E	63SE												
319	M	UOSV SA LS.	N41E	90SE												
320	M	UOSV SA LS.	N40E	45NW									N10W	87NE		
321	M	UOSV SA LS.	N80E	71NW												

Station	Quad	Lithology	BEDDING		Axial Surface		Cleavage		IL	Amp.	SLICKENSIDES		Joint		CROSS BED	
			Strike	Dip	DIP2	STRIKE	Strike	Dip2	Angle	(m)	Plunge3	Trend3	Strike 2	Dip3	Plunge4	Trend4
322	M	UOSV SA LS.	N40E	50SE												
323	M	UOSV SA LS.	N50E	54SE												
324	M	UOSV SA LS.	N50E	83SE												
325	M	UOSV SA LS.	N46E	90SE												
326	M	TAN FISSILE SH.	N49E	86SE												
327	M	UOSV SA LS.	N41E	80NW												
328	M	UOSV SA LS.	N45E	58NW												
329	M	UOSV SA LS.	N49E	71SE												
330	M	UOSV SA LS.	N55E	72NW												
331	M	ARENITE	N39E	28NW												
332	M	RED SS	N55E	45NW												
333	M	ARENITE	N48E	56NW			N48E	50SE								
334	M	ARENITE	N49E	59NW												
335	M	ARENITE	N60E	56NW												
336	M	QZ. SS	N46E	54NW											54NW	N46E
337	M	QZ. SS	N39E	68NW												
338	M	QZ. SS	N49E	39NW												
339	M	UOSV SA LS.	N46E	30NW												
340	M	UOSV SA LS.	N65E	37NW												
341	M	UOSV SA LS.	N51E	80NW												
342	M	UOSV SA LS.	N50E	88NW												
343	M	TAN SHALE	N39E	80SE												
344	M	TAN SHALE	N30E	45SE												
345	M	TAN SHALE	N49E	88SE												
346	M	UOSV SA LS.	N45E	88SE												
347	M	TAN SHALE	N61E	25SE												
348	M	UOSV SA LS.	N40E	80NW												
349	M	UOSV SA LS.	N42E	78NW												
350	M	UOSV SA LS.	N51E	63NW												
351	M	QZ. SS	N47E	72NW												
352	M	RED SS	N29E	35NW			N44E	28SE					N39W	62NE		
353	M	QZ. SS	N39E	67NW												
354	M	QZ. SS	N40E	56NW												
355	M	QZ. SS	N51E	82SE												
356	M	QZ. SS	N50E	83SE												
357	M	QZ. SS	N49E	54SE												
358	M	QZ. SS	N57E	50SE												
359	M	QZ. SS	N51E	8SE												
360	M	QZ. SS	N50E	18SE												
361	M	QZ. SS	N45E	49NW												

Station	Quad	Lithology	BEDDING		Axial Surface		Cleavage		IL	Amp.	SLICKENSIDES		Joint		CROSS BED	
			Strike	Dip	DIP2	STRIKE	Strike	Dip2	Angle	(m)	Plunge3	Trend3	Strike 2	Dip3	Plunge4	Trend4
362	M	QZ. SS	N50E	59NW											4SE	N6E
363	M	QZ. SS	N82E	14SE												
364	M	QZ. SS	N30E	16SE												
365	M	QZ. SS	N50E	83NW												
366	M	UOSV SA LS.	N30E	60NW												
367	M	UOSV SA LS.	N69E	66SE												
368	M	UOSV SA LS.	N32E	13SE												
369	M	SA SH.	N59E	26SE												
370	M	TAN SHALE	N0E	16SE												
371	M	UOSV SA LS.	N60E	5SE												
372	M	UOSV SA LS.	N0E	0SE												
373	M	UOSV SA LS.	N45E	14SE												
374	M	FOSSILIFEROUS LMS	N86E	13SE												
375	M	SA LS.	N69E	16SE												
376	M	FOSSILIFEROUS LMS	N51E	24SE												
377	M	SA LS.	N62E	20SE												
378	M	SA LS.	N29E	15SE												
379	M	VEINED SA LS.	N50	60NW												
380	M	SA LS.	N50E	42NW												
381	M	SA LS.	N21W	8SW												
382	M	SA LS.	N10E	15SE												
383	M	TAN SHALE	N32E	31E												
384	M	SA LS.	N6E	16SE												
385	M	RED MUDSTONE	N26E	15SE												
386	M	RED MUDSTONE	N59E	12SE												
387	M	SA LS.	N50E	29SE											10NW	N30E
388	M	SA LS.	N38E	28SE												
389	M	SA LS.	N21E	86SE												
390	M	CALC. MDSTONE & LS.	N70E	38SE												
391	M	CALC. MUDSTONE	N46E	13SE												
392	M	SA LS.	N60E	14SE												
393	M	SA LS.	N67E	5SE												
394	M	SA LS.	N40E	31SE												
395	M	TAN SHALE	N31E	25SE												
396	M	TAN SHALE	N22E	29SE												
397	M	SA LS.	N40E	43SE												
398	M	SA LS.	N49E	23SE												
399	M	RED SS	N9E	6SE			N45E	72NW								
400	M	RED SS	N45E	15SE			N45E	72NW								
401	M	FOSSILIFEROUS LMS	N10E	15SE												

Station	Quad	Lithology	BEDDING		Axial Surface		Cleavage		IL	Amp.	SLICKENSIDES		Joint		CROSS BED	
			Strike	Dip	DIP2	STRIKE	Strike	Dip2	Angle	(m)	Plunge3	Trend3	Strike 2	Dip3	Plunge4	Trend4
402	M	SA LS.	N61E	8SE												
403	M	SA LS.	N52E	20SE												
404	M	SA LS.	N60E	17NW												
405	M	SA LS.	N35E	27NW												
406	M	SA LS.	N70E	78NW												
407	M	THICK BED LS.	N58E	48SE												
408	M	THICK BED LS.	N38E	23SE												
409	M	THIN BED LS.	N35E	30SE												
410	M	SA LS.	N46E	12SE			N46E	85NW								
411	M	TAN SHALE	N75E	10SE												
412	M	SA LS.	N40W	39SE												
413	M	SA LS.	N75E	18SE												
414	M	SA LS.	N22E	21SE												
415	M	TAN SHALE	N45E	56SE												
416	M	SA LS.	N20E	39SE												
417	M	THIN BED LS.	N29E	28SE												
418	M	TAN SHALE	N59E	49SE												
419	M	TAN SHALE	N40E	57SE												
420	M	TAN SHALE	N56E	37NW												
421	M	SA LS.	N79E	79SE												
422	M	RED SS	N58E	86NW												
423	M	ARENITE	N57E	88NW												
424	M	QZ. SS	N24E	12NW			N55E	84NW								
425	M	QZ. SS	N60E	36NW												
426	M	QZ. SS	N22E	14SE												
427	M	QZ. SS	N27E	26SE												
428	M	QZ. SS	N36E	32SE												
429	M	QZ. SS	N38E	22SE												
430	M	QZ. SS	N33E	29SE												
431	M	QZ. SS	N31E	4NW												
432	M	QZ. SS	N15E	9SE			N22E	81SE								
433	M	QZ. SS	N46E	34NW												
434	M	QZ. SS	N29E	46NW												
435	M	QZ. SS	N59E	4NW												
436	M	QZ. SS	N20E	3SE												
437	M	QZ. SS	N22E	10SE												
438	M	QZ. SS	N0E	0SE												
439	M	QZ. SS	N71E	6NW												
440	M	QZ. SS	N70E	37SE											5SE	N52E
441	M	QZ. SS	N19E	15SE												

Station	Quad	Lithology	BEDDING		Axial Surface		Cleavage		IL	Amp.	SLICKENSIDES		Joint		CROSS BED	
			Strike	Dip	DIP2	STRIKE	Strike	Dip2	Angle	(m)	Plunge3	Trend3	Strike 2	Dip3	Plunge4	Trend4
442	M	QZ. SS	N46E	59SE												
443	M	QZ. SS	N44E	23SE												
444	M	RED SS	N60E	47N												
445	M	RED SS	N49E	44NW												
446	M	QZ. SS	N55E	88NW												
447	M	QZ. SS	N54E	74NW												
448	M	QZ. SS	N49E	69NW												
449	M	QZ. SS	N40E	21NW												
450	M	QZ. SS	N46E	49NW												
451	M	QZ. SS	N49E	64NW												
452	M	SA LS.	N59E	76NW												
453	M	SA LS.	N54E	85NW												
454	M	SA LS.	N49E	82NW												
455	M	SA LS.	N40E	14SE												
456	M	SA LS.	N32E	35SE												
457	M	SA LS.	N46E	81SE												
458	M	SA LS.	N42E	90SE												
459	M	CALC. MDSTONE & LS.	N57E	90SE												
460	M	SA LS.	N50E	90SE												
461	M	SA LS.	N30E	26SE												
462	M	SA LS.	N40E	39SE												
463	M	SA LS.	N49E	90SE												
464	M	SA LS.	N30E	66NW												
465	M	SA LS.	N49E	76NW												
466	M	SA LS.	N65E	13SE	5SE	N63E										
467	M	SA LS.	N56E	45SE												
468	M	THIN BED LS.	N50E	44SE												
469	M	SA LS.	N45E	80SE												
470	M	SA LS.	N55E	35SE												
471	M	SA LS.	N50E	70SE												
472	M	SA LS.	N40E	85SE												
473	M	SA LS.	N42E	12SE												
474	M	SA LS.	N45E	39NW												
475	M	SA LS.	N56E	57NW												
476	M	SA LS.	N36W	10NE												
477	M	SA LS.	N28W	4NE												
478	M	SA LS.	N30E	66SE												
479	M	SA LS.	N15E	20SE												
480	M	SA LS.	N45E	79NW												
481	M	SA LS.	N35E	45SE												

Station	Quad	Lithology	BEDDING		Axial Surface		Cleavage		IL	Amp.	SLICKENSIDES		Joint		CROSS BED	
			Strike	Dip	DIP2	STRIKE	Strike	Dip2	Angle	(m)	Plunge3	Trend3	Strike 2	Dip3	Plunge4	Trend4
482	M	SA LS.	N20W	10SW												
483	M	SA LS.	N49E	51SE												
484	M	SA LS.	N46E	56SE												
485	M	THIN BED LS.	N22E	39SE	0SE	N20E										
486	M	FOSSILIFEROUS SH.	N60E	27SE	0SE	N29E										
487	M	QZ. SS	N62E	49SE												
488	M	QZ. SS	N56E	59SE												
489	M	ARENITE	N39E	53SE												
490	M	QZ. SS	N26E	61SE												
491	M	RED MUDSTONE	N22E	9SE												
492	M	QZ. SS	N78E	22NW												
493	M	SA LS.	N56E	74SE	8SW	N57E										
494	M	CALC MUDSTONE	N80E	15NW												
495	M	QZ. SS	N87E	15NW												
496	M	QZ. SS	N72E	56NW												
497	M	QZ. SS	N85E	41NW												
498	M	QZ. SS	N65E	55NW												
499	M	QZ. SS	N42E	79NW												
500	M	QZ. SS	N42E	90SE												
501	M	QZ. SS	N65W	10NE												
502	M	SA. LS.	N35W	7NE												
503	M	SA LS.	N20W	6NE												
504	M	SA LS.	N80W	30NE												
505	M	SA LS.	N45W	16NE												
506	M	FOSSILIFEROUS LMS	N75E	46NW												
507	M	THIN BED LS.	N40E	51NW												
508	M	SA SH.	N75E	75NW												
509	M	THIN BED LS.	N62E	80NW												
510	M	SA LS.	N56E	78NW												
511	M	THIN BED LS.	N45E	56SE												
512	M	SA LS.	N40E	49SE												
513	M	SA LS.	N50E	36SE												
514	M	SA LS.	N30E	47SE												
515	M	THIN BED LS.	N50E	78SE												
516	M	THIN BED LS.	N55E	67NW												
517	M	SA SH.	N41E	45SE												
518	M	THIN BED LS.	N59E	47SE												
519	M	THICK BED SH.	N50E	42SE												
520	M	THIN BED LS.	N45E	90SE												
521	M	SA LS.	N55E	81SE												

Station	Quad	Lithology	BEDDING		Axial Surface		Cleavage		IL	Amp.	SLICKENSIDES		Joint		CROSS BED	
			Strike	Dip	DIP2	STRIKE	Strike	Dip2	Angle	(m)	Plunge3	Trend3	Strike 2	Dip3	Plunge4	Trend4
522	M	SA LS.	N50E	84SE												
523	M	MICRITIC LS.	N62E	72SE												
524	M	THIN BED SH.	N60E	79SE			N31E	13NW								
525	M	SA LS.	N40E	83N												
526	M	QZ. SS	N65E	84SE												
527	M	SA LS.	N55E	78SE												
528	M	THIN BED SH.	N60E	20NW												
529	M	SA LS.	N75E	41NW												
530	M	SA LS.	N42E	26SE												
531	M	RED MUDSTONE	N60E	19SE												
532	M	RED MUDSTONE	N51E	20SE												
533	M	QZ. SS	N47E	22SE			N20E	78NW			N20W	78NE				
534	M	QZ. SS	N20E	6SE												
535	M	QZ. SS	N40E	10SE												
536	M	QZ. SS	0NE	0SE												
537	M	QZ. SS	N50E	26NW												
538	M	QZ. SS	N38E	31NW												
539	M	QZ. SS	N89W	16NE												
540	M	QZ. SS	N25E	28SE												
541	M	RED MUDSTONE	N5E	8SE												
542	M	SA LS.	N50E	26SE												
543	M	SA LS.	N75E	35NW												
544	M	QZ. SS	N50E	81SE												
545	M	QZ. SS	N45E	82SE												
546	M	QZ. SS	N50E	13SE												
547	M	QZ. SS	N42E	85SE												
548	M	QZ. SS	N60E	67SE												
549	M	QZ. SS	N40E	46SE												
550	M	QZ. SS	N57E	30SE												
551	M	QZ. SS	N53E	45SE												
552	M	QZ. SS	N49E	12SE												
553	M	QZ. SS	N47E	49SE												
554	M	QZ. SS	N50E	80SE									N38E	70SE		
555	M	SA LS.	N62E	67SE			N60E	71SE								
556	M	CALC SH.	N48E	75SE												
557	M	CALC SH.	N56E	44SE												
558	M	SA SH. W/ FELDSPAR	N49E	57SE												
559	M	CALC SH.	N39E	59SE												
560	M	CALC SH.	N30E	44SE												
561	M	CALC SH.	N41E	82SE												

Station	Quad	Lithology	BEDDING		Axial Surface		Cleavage		IL	Amp.	SLICKENSIDES		Joint		CROSS BED	
			Strike	Dip	DIP2	STRIKE	Strike	Dip2	Angle	(m)	Plunge3	Trend3	Strike 2	Dip3	Plunge4	Trend4
562	M	SA LS.	N40E	27NW												
563	M	SS W/FELDSPAR	N51E	71SE												
564	M	SS W/FELDSPAR	N52E	48SE												
565	M	SS W/FELDSPAR	N50E	41NW												
566	M	QZ. SS	N60E	50NW												
567	M	QZ. SS	N42E	40SE												
568	M	QZ. SS	N57E	56NW												
569	M	QZ. SS	N52E	74NW												
570	M	QZ. SS	N51E	11NW												
571	M	QZ. SS	N65E	34SE												
572	M	QZ. SS	N54E	50SE												
573	M	SA SH.	N51E	74SE												
574	M	QZ. SS	N55E	34SE												
575	M	QZ. SS	N43E	28NW												
576	M	RED SS	N48E	30NE												
577	M	RED MUDSTONE	N50E	43NW												
578	M	RED SS	N47E	41NW												
579	M	RED SS	N46E	85NW												
580	M	SA SH.	N41E	57SE												
581	M	SA LS.	N65E	8SE												
582	M	SA LS.	N64E	28SE												
583	M	SA LS.	N52E	61SE												
584	M	SA LS.	N30E	11SE												
585	M	SA SH.	N60E	30SE												
586	M	SA SH.	N50E	44SE												
587	M	SA LS.	N44E	26SE												
588	M	SA LS.	N62E	19NW												
589	M	RED SS	N70E	26NW												
590	M	QZ. SS	N43E	9SE												
591	M	QZ. SS	N66E	27SE											25SW	N49W
592	M	QZ. SS	N25E	16SE												
593	M	QZ. SS	N40E	15SE												
594	M	QZ. SS	N60E	8NW			N48E	74SE								
595	M	QZ. SS	N56E	42NW			N72E	69SE			N61W	69SE				
596	M	QZ. SS	N43E	36NW												
597	M	QZ. SS	N45E	41NW												
598	M	QZ. SS	N68E	50NW												
599	M	QZ. SS	N53E	39NW												
600	M	QZ. SS	N66E	8NW												
601	M	QZ. SS	N39E	6NW												

Station	Quad	Lithology	BEDDING		Axial Surface		Cleavage		IL	Amp.	SLICKENSIDES		Joint		CROSS BED	
			Strike	Dip	DIP2	STRIKE	Strike	Dip2	Angle	(m)	Plunge3	Trend3	Strike 2	Dip3	Plunge4	Trend4
602	M	SA LS.	N61E	15NW												
603	M	FOSSILIFEROUS LMS	N51E	4NW												
604	M	SA LS.	N0E	0SE												
605	M	SA LS.	N61E	52NW												
606	M	SA LS.	N64W	11NE												
607	M	SA LS.	N50E	60NW												
608	M	SA LS.	N54E	31NW												
609	M	SA LS.	N52E	10NW												
610	M	SA LS.	N4W	10NE												
611	M	SA LS.	N45E	51SE												
612	M	SA LS.	N40E	32SE												
613	M	SILTY LS.	N43E	35SE												
614	M	SA LS.	N42E	53SE												
615	M	SA SH.	N59E	46SE												
616	M	THIN BED SH.	N47E	65SE												
617	M	SA LS.	N80E	83SE												
618	M	SA LS.	NN49W	90SE												
619	M	SA LS.	N59E	20SE												
620	M	SA LS.	N72E	16SE												
621	M	SA LS.	N64E	38SE			N10E	4NW								
622	M	SA LS.	0NE	NSE												
623	M	SA LS.	N5E	3NW												
624	M	SA LS.	N40E	14NW												
625	M	SA LS.	N41E	15NW												
626	M	SA LS.	N54E	12SE												
627	M	SA LS.	N31E	31SE												
628	M	SA LS.	N59E	90SE												
629	M	SA LS.	N45E	56SE												
630	M	FISSILE SH.	N68E	21NW												
631	M	FISSILE SH.	N21E	73SE												
632	M	THIN BED SH.	N39E	57SE												
633	M	FISSILE SH.	N45E	74SE												
634	M	SA LS.	N50E	66SE												
635	M	SA LS.	N46E	62SE												
636	M	SILTY LS.	N56E	85SE												
637	M	THIN BED SH.	N49E	79SE												
638	M	SA LS.	N44E	46SE												
639	M	SA LS.	N41E	72SE												
640	M	SA LS.	N32E	50SE												
641	M	THIN BED LS.	N39E	74SE												

Station	Quad	Lithology	BEDDING		Axial Surface		Cleavage		IL	Amp.	SLICKENSIDES		Joint		CROSS BED	
			Strike	Dip	DIP2	STRIKE	Strike	Dip2	Angle	(m)	Plunge3	Trend3	Strike 2	Dip3	Plunge4	Trend4
642	M	SA LS.					N26E	81NW								
643	M	SA LS.	N54E	23SE												
644	M	SA LS.	N49E	3SE												
645	M	SA LS.	N49E	14SE												
646	M	SA LS.	N55E	9SE												
647	M	THIN BED LS.	N30E	8SE												
648	M	SA LS.	N11E	9SE												
649	M	SA LS.	N51E	16NW			N20E	76SE								
650	M	SA LS.	N26E	10NW												
651	M	SILTY LS.	N51E	51NW												
652	M	FISSILE SH.	N24E	66SE												
653	M	THIN BED SH.	N29E	63SE												
654	M	THIN BED SH.	N31E	72SE												
655	M	GR-BL SH.	N34E	60SE												
656	M	FISSILE SH.	N62E	60NW												
657	M	SA LS.	N48E	49SE												
658	M	THIN BED LS.	N36E	6NW												
659	M	SA LS.	N46E	10SE			N19E	72NW								
660	M	SILTY LS.	N28E	12SE												
661	M	SA LS.	N54E	13SE												
662	M	SA LS.	N69E	56SE												
663	M	SA LS.	N62E	55SE												
664	M	SA LS.	N51E	50SE	4NE	N40E			60	1						
665	M	SA LS.	N61E	15NW	9NE	N40E	N47E	73SW	95	3						
666	M	SA LS.			12NE	N20E			130							
667	M	RED MUDSTONE	N33E	61SE												
668	M	FOSSILIFEROUS LMS	N12E	10NW												
669	M	THIN BED LS.	N56E	48SE												
670	M	SA LS.	N20E	39NW			N5E	37SE								
671	M	SA SH.	N43E	47NW												
672	M	SA LS.	N56E	50NW												
673	M	CALC. MUDSTONE	N76E	69SE			N15E	78SE								
674	M	CALC. MUDSTONE	N60E	30NW												
675	M	SA LS.	N45E	20SE												
676	M	SA LS.	N0E	0SE												
677	M	SA SH.	N42W	17NE												
678	M	SA LS.	N80W	13SE												
679	M	SA LS.	N70E	42SE												
680	M	SA SH.	N50E	26SE												
681	M	SA SH.	N48E	65SE												

Station	Quad	Lithology	BEDDING		Axial Surface		Cleavage		IL	Amp.	SLICKENSIDES		Joint		CROSS BED	
			Strike	Dip	DIP2	STRIKE	Strike	Dip2	Angle	(m)	Plunge3	Trend3	Strike 2	Dip3	Plunge4	Trend4
682	M	SA LS.	N41E	44SE												
683	M	SA LS.	N45E	30SE												
684	M	SA LS.	N48E	16SE												
685	M	RED MUDSTONE	N40E	10SE			N38E	85NW								
686	M	QZ. SS	N0E	0SE												
687	M	QZ. SS	N0E	0SE												
688	M	SA LS.	N48E	26NW												
689	M	FISSILE SH.	N56E	30NW												
690	M	SA SH.	N50E	40NW												
691	M	SH & CALC. CHIPS	N50E	31NW												
692	M	FISSILE SH.	N55E	28NW												
693	M	QZ. SS	N54E	28NW												
694	M	QZ. SS	N0E	0NW												
695	M	QZ. SS	N60E	30SE												
696	M	RED SS	N56E	6SE												
697	M	QZ. SS	N30E	39SE												
698	M	SH & CALC. CHIPS	N46E	55SE												
699	M	SA LS.	N37E	40SE												
700	M	SA LS.	N45E	20NW												
701	M	CALC. SH.	N52E	8NW												
702	M	CALC SH.	N42E	20SE												
703	M	SA SH.	N49E	18SE												
704	M	SA SH.	N70E	14SE												
705	M	SA LS.	N50E	3SE												
706	M	SA LS.	N61E	19SE												
707	M	SA LS.	N70E	39NW												
708	M	SA LS.	N55E	46NW												
709	M	SA LS.	N68E	18NW												
710	M	SA SH.	N56E	41SE												
711	M	CALC. MUDSTONE	N61E	82SE												
712	M	SA SH.	N50E	71SE												
713	M	FISSILE SH.	N60E	86NW												
714	M	CALC SH.	N39E	72NW												
715	M	CALC SH.	N18E	55SE												
716	M	CALC SH.	N63E	44SE												
717	M	CALC. MUDSTONE	N51E	88SE												
718	M	CALC. MUDSTONE	N48E	88NW												
719	M	CALC. MUDSTONE	N39E	79SE												
720	M	CALC. SH.	N30E	90SE												
721	M	CALC SH.	N38E	85SE												

Station	Quad	Lithology	BEDDING		Axial Surface		Cleavage		IL	Amp.	SLICKENSIDES		Joint		CROSS BED	
			Strike	Dip	DIP2	STRIKE	Strike	Dip2	Angle	(m)	Plunge3	Trend3	Strike 2	Dip3	Plunge4	Trend4
722	M	GR-BL SH.	N27E	40NW												
723	M	GR-BL SH.	N50E	79NW												
724	M	FISSILE SH.	N50E	33SE												
725	M	FISSILE SH.	N49E	86SE												
726	M	CALC. MUDSTONE	N49E	51SE												
727	M	FISSILE SH.	N59E	69SE												
728	M	CALC SH.	N5E	41SE												
729	M	CALC SH.	N34E	24SE												
730	M	CALC SH.	N67E	46SE												
731	M	CALC SH.	N70E	22SE												
732	M	SA SH.	N41E	37SE												
733	M	SA LS.	N49E	22SE			N82E	65NW								
734	M	SA LS.	N30E	6SE			N44E	10SE								
735	M	SA LS.	N0E	0SE												
736	M	CALC SH.	N49E	14SE												
737	M	SA SH.	N3E	59SE												
738	M	SA SH.	N26E	86SE												
739	M	CALC SH.	N26E	86SE												
740	M	CALC SH.	N26E	70SE												
741	M	CALC SH.	N46E	39SE												
742	M	CALC SH.	N19E	68SE												
743	M	CALC SH.	N56E	59SE												
744	M	FISSILE SH.	N30E	74SE												
745	M	FISSILE SH.	N28E	87SE			N10E	10SE								
746	M	FISSILE SH.	N36E	82SE												
747	M	CALC SH.	N40E	68NW												
748	M	CALC SH.	N39E	80NW												
749	M	SA SH.	N46E	76SE												
750	M	SA SH.	N39E	40SE												
751	M	CALC SH.	N11E	34SE												
752	M	SA SH.	N44E	80NW												
753	M	CALC SH.	N85W	19SE												
754	M	THIN BED LS.	N59E	31SE												
755	M	SA LS.	N50E	51SE	N31E	21NE	N30E	45SE	10	6						
756	M	SA LS.	N20W	25SW												
757	M	FISSILE SH.	N60E	79SE												
758	M	THIN BED LS.	N82W	20NE												
759	M	SA SH.	N60E	75NW	12SE	N61E			105	2						
760	M	CALC SH.	N40E	26SE												
761	M	FISSILE SH.	N46E	56SE												

Station	Quad	Lithology	BEDDING		Axial Surface		Cleavage		IL	Amp.	SLICKENSIDES		Joint		CROSS BED	
			Strike	Dip	DIP2	STRIKE	Strike	Dip2	Angle	(m)	Plunge3	Trend3	Strike 2	Dip3	Plunge4	Trend4
762	M	QZ. SS	N40E	66SE												
763	M	QZ. SS	N54E	65SE												
764	M	QZ. SS	N42E	80SE												
765	M	QZ. SS	N53E	48NW												
766	M	CALC SH.	N42E	43SE												
767	M	SA LS.	N51E	70SE												
768	M	SA LS.	N39E	25SE												
769	M	SA LS.	N71E	24SE												
770	M	GREEN SH.	N20E	49SE												
771	M	SA LS.	N79W	89NE												
772	M	SA LS.	N70E	36SE												
773	M	FOSSILIFEROUS LMS	N41E	79SE												
774	M	SA LS.	N70E	64NW	5NE	N68E			87	1						
775	M	CALC SH.	N40E	42SE												
776	M	GREEN SH.	N39E	60SE												
777	M	SA LS.	N41E	54SE												
778	M	QZ. SS	N30E	48SE												
779	M	QZ. SS	N51E	68NE												
780	M	QZ. SS	N50E	21SE												
781	M	GREEN SH.	N51E	34SE												
782	M	GREEN SH.	N49E	44SE												
783	M	GREEN SH.	N50E	76NW	84SE	N41E										
784	M	GREEN SH.	N50E	32SE												
785	M	GREEN SH.	N61E	73NW												
786	M	SA LS.	N51E	64SE												
787	M	SA LS.	N72E	53SE												
788	BU	SA LS.	N20E	29SE												
789	M	SA LS.	N45E	40NW												
790	M	SA LS.	N80E	19NW												
791	M	CALC SH.	N33E	52SE												
792	M	CALC SH.	N45E	79SE												
793	M	CALC SH.	N29E	34SE												
794	M	SH. & LS.	N51E	58SE												
795	M	SA LS.	N40E	24NW												
796	M	SA LS.	N50E	19SE	15SE	N51E			130	4						
797	M	SA LS.	N52E	53NW												
798	M	THIN BED LS.	N50E	46NW												
799	M	SA LS.	N31E	63NW												
800	M	SA LS.	N50E	20NW												
801	M	SA LS.	N42E	49N												

Station	Quad	Lithology	BEDDING		Axial Surface		Cleavage		IL	Amp.	SLICKENSIDES		Joint		CROSS BED	
			Strike	Dip	DIP2	STRIKE	Strike	Dip2	Angle	(m)	Plunge3	Trend3	Strike 2	Dip3	Plunge4	Trend4
802	M	SA LS.	N53E	72NW												
803	M	SA LS.	N45E	83NW												
804	M	SA LS.	N49E	69NW												
805	M	SA LS.	N55E	63SE												
806	M	SA LS.	N75E	89SE												
807	M	CALC SH.	N39E	79NW												
808	M	GR-BL SH.	N69E	87NW	6SE	N48E			40	2						
809	M	CALC SH.	N49E	76SE												
810	M	CALC SH.	N51E	59SE												
811	M	CALC SH.	N66E	46SE												
812	M	CALC SH.	N47E	7SE												
813	M	CALC SH.	N66E	41SE												
814	M	CALC SH.	N73E	65SE	3NE	N73E			120	2						
815	M	CALC SH.	N31E	30SE												
816	M	CALC SH.	N88E	20NW												
817	M	SA SH.	N48E	3NW												
818	M	SA SH.	N79E	9NW												
819	M	CALC SH.	N13E	21SE												
820	M	CALC SH.	N17E	42SE												
821	M	THIN BED LS.	N85E	6NW												
822	M	SA LS.	N44E	87NW												
823	M	SA LS.	N50E	38SE	10NW	N60E	N58E	88NW	60	3						
824	M	GREEN SH.	N60E	71NW												
825	M	GREEN SH.	N69E	79SE												
826	M	FISSILE SH.	N41E	82NW												
827	M	CALC SH.	N0E	0SE												
828	M	SA LS.	N20E	10NW												
829	M	SA LS.	N70W	12SW												
830	M	SA LS.	N89W	14SW												
831	M	SA LS.	N80E	10SE												
832	M	SA SH.	N72E	12SE												
833	M	SA SH.	N88W	14SW												
834	M	CALC SH.	N46E	83NW												
835	M	SA LS.	N63E	65SE												
836	M	CALC SH.	N6W	11NE												
837	M	CALC SH.	N52E	64SE												
838	M	CALC SH.	N13E	41SE												
839	M	SA LS.	N31E	26SE												
840	M	SA LS.	N58E	52SE												
841	M	SA LS.	N17E	39SE												

Station	Quad	Lithology	BEDDING		Axial Surface		Cleavage		IL	Amp.	SLICKENSIDES		Joint		CROSS BED	
			Strike	Dip	DIP2	STRIKE	Strike	Dip2	Angle	(m)	Plunge3	Trend3	Strike 2	Dip3	Plunge4	Trend4
842	M	CALC SH.	N32E	70SE												
843	M	CALC SH.	N51E	64SE												
844	M	CALC SH.	N40E	29SE												
845	M	SA SH.	N81E	25SE												
846	M	SA LS.	N52E	38SE												
847	M	CALC SH.	N51E	63SE												
848	M	QZ. SS	N50W	44NE												
849	M	QZ. SS	N53E	21SE												
850	M	QZ. SS	N44E	33NW												
851	M	CALC SH.	N53E	85SE												
852	M	CALC SH.	N61E	70SE												
853	M	GR-BL SH.	N35E	79NW												
854	M	GR-BL SH.	N11E	72SE												
855	M	GR-BL SH.	N20E	22SE												
856	M	GR-BL SH.	N41E	69SE												
857	M	GR-BL SH.	N50E	76SE			N82E	44NW								
858	M	GR-BL SH.	N40E	68SE												
859	M	GR-BL SH.	N40E	79NW												
860	M	GR-BL SH.	N30E	74NW												
861	M	GR-BL SH.	N35E	90SE												
862	M	CALC SH.	N38E	82SE												
863	M	CALC SH.	N33E	75SE												
864	M	CALC SH.	N8E	84NW												
865	M	CALC SH.	N10E	73SE												
866	M	CALC SH.	N18E	82NW												
867	M	CALC SH.	N49E	50SE												
868	M	CALC SH.	N12E	55SE												
869	M	CALC SH.	N28E	50SE												
870	M	CALC SH. & BL LS.	N11E	17SE												
871	M	CALC SH. & BL LS.	N25E	69SE												
872	M	FISSILE SH.	N41E	56SE												
873	M	FISSILE SH.	N51E	84SE												
874	M	CALC SH.	N41E	49NW												
875	M	CALC SH.	N20E	85NW												
876	M	CALC SH.	N51E	76NW												
877	M	CALC SH.	N86E	75SE												
878	M	CALC SH.	N50E	68NW												
879	M	CALC SH.	N46E	72SE												
880	M	FISSILE SH.	N9E	75NW												
881	M	CALC SH.	N45E	66NW												

Station	Quad	Lithology	BEDDING		Axial Surface		Cleavage		IL	Amp.	SLICKENSIDES		Joint		CROSS BED	
			Strike	Dip	DIP2	STRIKE	Strike	Dip2	Angle	(m)	Plunge3	Trend3	Strike 2	Dip3	Plunge4	Trend4
882	M	CALC SH.	N49E	72SE												
883	M	CALC SH.	N81W	76NE												
884	M	CALC SH.	N41E	26SE	3NE	39NE	N45E	16SE	40	1						
885	M	CALC SH.	N25E	54SE												
886	M	CALC SH.	N49E	78NW												
887	M	SH & CALC. CHIPS	N44E	35NW												
888	M	SH & CALC. CHIPS	N90E	25NW			N72E	29NW								
889	M	THICK BED SH.	N74E	47NW												
890	M	THICK BED SH.	N61E	50SE												
891	M	CALC SH.	N81W	87NW												
892	M	CALC SH.	N60E	25NW												
893	M	CALC SH.	N48E	49SE												
894	M	CALC SH.	N55E	73NW												
895	M	SI LS.	N65E	61NW	10SE	N73E			55	10						
896	M	SI LS.	N60E	52NW												
897	M	SA LS.	N76E	55NW												
898	M	SA LS.	N64E	9NW												
899	M	SA LS.	N61E	12NW												
900	M	SA LS.	N63E	4NW												
901	M	SA LS.	N0E	0SE			N59E	87SE								
902	M	SI LS.	N0E	0SE												
903	M	SA LS.	N40E	7NW												
904	M	SA LS.	N0E	0SE												
905	M	CALC SH.	N53E	27SE												
906	M	SA LS.	N40E	19SE												
907	M	SA LS.	N43E	6SE	0SE	N0E	N20E	30SE		20						
908	M	THICK BED SH.	N69E	89N	6SE	N48E	N50E	71NW	79	1						
909	M	THICK BED SH.	N49E	76SE												
910	M	THICK BED SH.	N51E	59SE												
911	M	THICK BED SH.	N66E	46SE												
912	M	THICK BED SH.	N47E	7SE												
913	M	THICK BED SH.	N66E	41SE												
914	M	SA LS. & SH.	N75E	65SE	3NE	N73E			90	3						
915	M	SA LS. & SH.	N31E	30SE												
916	M	SA LS. & SH.	N88E	20NW												
917	M	SA SH.	N48E	3NW												
918	M	SA LS.	N79E	9NW												
919	M	SA LS.	N13E	21SE												
920	M	CALC. MUDSTONE	N17E	42SE												
921	M	THICK BED SH.	N85E	6NW												

Station	Quad	Lithology	BEDDING		Axial Surface		Cleavage		IL	Amp.	SLICKENSIDES		Joint		CROSS BED	
			Strike	Dip	DIP2	STRIKE	Strike	Dip2	Angle	(m)	Plunge3	Trend3	Strike 2	Dip3	Plunge4	Trend4
922	M	THICK BED SH.	N44E	87NW	5NW	N64E			60	2						
923	M	SA LS.	N50E	38SE												
924	M	CALC SH.	N60E	71NW												
925	M	CALC SH.	N69E	70SE												
926	M	CALC SH.	N76E	64SE												
927	M	SH & CALC. CHIPS	N71E	72NW												
928	M	SH & CALC. CHIPS	N68E	59SE												
929	M	SI LS.	N46E	52NW												
930	M	SH & CALC. CHIPS	N61E	39NW												
931	M	CALC SH.	N30W	19SE												
932	M	SH & CALC. CHIPS	N76E	51NW												
933	M	CALC SH.	N62E	43SE			N47E	56SE								
934	M	SI LS.	N41E	49SE												
935	M	SA SH.	N35E	72SE												
936	M	SI LS.	N21E	5NW												
937	M	SI LS.	N15E	10NW												
938	M	SI LS.	N75E	79SE												
939	M	FOSSIL LMS	N51E	36SE	42N	N20W										
940	M	SA LS.	N20E	31W												
941	M	SA LS.	N52E	62NW												
942	M	SA LS.	N49E	61SE												
943	M	SA LS.	N49E	61SE												
944	M	SA LS.	N45E	90SE											26SE	N38E
945	M	SA LS.	N77E	20NW												
946	M	CALC SH.	N30E	70SE												
947	M	THIN BED LS.			5SE	N50E										
948	M	CALC SH.	N31E	67SE												
949	M	SI LS.	N40E	90SE												
950	M	SA LS.	N60E	48NW											45NW	N72E
951	M	SA LS. & SH.	N18E	22SE												
952	M	SA LS. & SH.	N81E	72SE												
953	M	SA LS. & SH.	N60E	80SE												
954	M	WHITE LS. OM	N59E	36SE												
955	M	NODULAR LS. OL	N69E	59NW												
956	M	WHITE LS. OM	N15E	20SE							N79E	79NW				
957	M	WHITE LS. OM	N60E	41NW												
958	M	WHITE LS. OM	N55E	25SE												
959	M	NODULAR LS. OL	N61E	86SE												
960	M	NODULAR LS. OL	N0E	0SE												
961	M	CALC SH.	N52E	60SE												

Station	Quad	Lithology	BEDDING		Axial Surface		Cleavage		IL	Amp.	SLICKENSIDES		Joint		CROSS BED	
			Strike	Dip	DIP2	STRIKE	Strike	Dip2	Angle	(m)	Plunge3	Trend3	Strike 2	Dip3	Plunge4	Trend4
962	M	CALC SH.	N49E	40SE												
963	M	CALC SH.	N56E	50SE												
964	M	CALC SH.	N52E	20SE												
965	M	CALC SH.	N56E	70SE												
966	M	CALC SH.	N48E	70NW												
967	M	CALC SH.	N45E	85SE												
968	M	CALC SH.	N42E	29NW												
969	M	CALC SH.	N53E	50SE												
970	M	CALC SH.	N5E	30SE												
971	M	GREEN SH.	N40E	25SE												
972	M	QZ. SS	N40E	70SE												
973	M	QZ. SS	N42E	82NW												
974	M	QZ. SS	N53D	85SE												
975	M	CALC SH.	N51E	50SE												
976	M	CALC SH.	N52E	50NW												
977	M	CALC SH.	N54E	70SE												
978	M	CALC SH.	N54E	65NW												
979	M	CALC SH.	N52E	10NW												
980	M	CALC SH.	N51E	10NW												
981	M	SI LS.	N10E	15SE												
982	M	GR-BL SH.	N25E	71SE												
983	M	SA LS.	N81E	45SE												
984	M	CALC. MUDSTONE	N32E	12NW												
985	M	CALC. MUDSTONE	N30E	10NW												
986	M	SI LS.	N50E	56SE			N10E	51NW								
987	M	CALC SH.	N31E	43SE												
988	M	CALC SH.	N44E	32SE												
989	M	CALC SH.	N65E	24SE												
990	M	SA LS.	N20E	24SE												
991	M	SA LS.	N59E	39SE												
992	M	SA LS.	N74E	45SE												
993	M	QZ. SS & RED MUDSTONE	N50E	49SE	5SE	N50E			150	10						
994	M	GREEN LS.	N79E	83NW												
995	M	GREEN FOSSIL LS.	N29E	24SE												
996	M	GREEN SH.	N311E	47SE												
997	M	CALC SH.	N46E	30SE												
998	M	QZ. SS	N41E	80NW												
999	M	GREEN FOSSIL LS.			2NE	N54E										
1000	M	CALC SH.	N21E	20NW												
1001	M	CALC SH.	N50E	25SE												

Station	Quad	Lithology	BEDDING		Axial Surface		Cleavage		IL	Amp.	SLICKENSIDES		Joint		CROSS BED	
			Strike	Dip	DIP2	STRIKE	Strike	Dip2	Angle	(m)	Plunge3	Trend3	Strike 2	Dip3	Plunge4	Trend4
1002	M	CALC SH.	N60E	51SE												
1003	M	CALC SH.	N48E	39SE			N48E	31NW								
1004	M	THIN BED LS.	N66E	66NW												
1005	M	THIN BED LS.	N48E	6NW												
1006	M	THIN BED LS.	N60E	21NW												
1007	M	THIN BED LS.	N25E	11NE												
1008	M	THIN BED LS.	N38E	9NW												
1009	B	SA LS. & SH.	N54E	64SE												
1010	B	SA LS.	N54E	79NW												
1011	B	CALC. SILTSTONE	N68E	73NW												
1012	B	SA LS. & SH.	N36E	77SE			N50E	80SE								
1013	B	FISSILE SH.	N79E	75SE												
1014	B	FISSILE SH.	N39E	57SE												
1015	B	CALC SH.	N74E	60SE												
1016	B	SA LS. & SH.	N40E	65SE												
1017	B	SA LS. & SH.	N41E	52SE												
1018	B	SA LS.	N30E	54SE												
1019	B	SA LS.	N20E	54SE												
1020	B	SA LS. & SH.	N60E	27SE	1SE	N65E			90	1						
1021	B	FISSILE SH.	N36E	56SE												
1022	M	FISSILE SH.	N80E	62NW			N70E	45SE								
1023	B	CALC SH.	N80E	22NW												
1024	B	CALC. SILTSTONE	N90E	27NW												
1025	M	CALC. SILTSTONE	N86E	70SE												
1026	B	CALC SH.	N60E	25NW												
1027	B	GR-BL SH.	N60E	16SE												
1028	B	GR-BL SH.	N0E	0NW												
1029	B	CALC SH.	N52E	28NW												
1030	B	CALC SH.	N38E	16SE												
1031	B	CALC SH.	N70E	75NW												
1032	B	CALC SH.	N29E	40NW												
1033	B	CALC SH.	N56E	15SE												
1034	B	CALC SH.	N66E	79SE												
1035	B	CALC SH.	N66E	21NE												
1036	B	CALC SH.	N90E	68SE												
1037	B	SA LS. & SH.	N70E	78SE												
1038	B	SA LS. & SH.	N67E	49N												
1039	B	CALC SH.	N85E	78NW												
1040	B	CALC SH.	N35E	12NW												
1041	B	CALC SH.			4SE	N40E										

Station	Quad	Lithology	BEDDING		Axial Surface		Cleavage		IL	Amp.	SLICKENSIDES		Joint		CROSS BED	
			Strike	Dip	DIP2	STRIKE	Strike	Dip2	Angle	(m)	Plunge3	Trend3	Strike 2	Dip3	Plunge4	Trend4
1042	B	SA LS.	N36E	29SE												
1043	B	SA LS.	N5E	30SE												
1044	B	CALC SH.	N80E	3SE												
1045	B	SA LS.	N30E	70SE												
1046	B	CALC SH.	N10W	81NW												
1047	B	SA LS.	N53E	46SE									N50E	60NW		
1048	B	SA LS.	N47E	64SE												
1049	B	SI LS.	N30E	27SE												
1050	B	CALC SH.	N60E	72NW												
1051	B	CALC SH.	N20E	79SE												
1052	B	CALC SH.	N60E	71SE												
1053	B	CALC SH.	N70E	82NW												
1054	B	SA LS.	N45E	70SE												
1055	B	SA LS. & SH.	N50E	81SE												
1056	B	SA LS. & SH.	N41E	39SE												
1057	B	SA LS. & SH.	N40E	26SE												
1058	B	SI LS.	N47E	66NW												
1059	B	SA LS. & SH.	N69E	13SE												
1060	B	SA LS. & SH.	N81E	40SE												
1061	B	SA LS.	N32E	57SE												
1062	B	SA LS. & SH.	N50E	74SE												
1063	B	FISSILE SH.	N40E	39SE												
1064	B	CALC SH.	N40E	81SE			N65E	61SE								
1065	B	CALC SH.	N41E	80NW												
1066	B	FISSILE SH.	N44E	53NW												
1067	B	FISSILE SH.	N31E	90SE												
1068	B	FISSILE SH.	N68E	62NW												
1069	B	CALC SH.	N76E	45NW												
1070	B	CALC SH.	N90E	80SE												
1071	B	THICK BED SH.	N81E	44SE												
1072	B	CALC. SILTSTONE	N30E	28SE			N58E	77SE								
1073	B	SA LS. & SH.	N90E	5SE												
1074	B	SA LS. & SH.	N15E	6NW												
1075	B	CALC SH.	N50E	51SE												
1076	B	THICK BED SH.	N82E	84NW												
1077	B	CALC SH.	N49E	74NW												
1078	B	CALC SH.	N30E	41SE												
1079	B	CALC SH.	N80E	70NW												
1080	B	CALC SH.	N70E	11SE												
1081	B	CALC SH.	N15E	13SE												

Station	Quad	Lithology	BEDDING		Axial Surface		Cleavage		IL	Amp.	SLICKENSIDES		Joint		CROSS BED	
			Strike	Dip	DIP2	STRIKE	Strike	Dip2	Angle	(m)	Plunge3	Trend3	Strike 2	Dip3	Plunge4	Trend4
1082	B	CALC SH.	N41E	53NW												
1083	B	SH. & CALC. CHIPS	N49E	82NW												
1084	B	CALC SH.	N41E	50SE												
1085	B	CALC SH.	N60E	72SE												
1086	B	SA LS.	N50E	86SE												
1087	B	SA LS. & SH.	N50E	60SE												
1088	B	SA LS. & SH.	N6E	29SE												
1089	B	SA LS. & SH.	N58E	67NW												
1090	B	CALC SH.	N48E	85NW												
1091	B	SA LS. & SH.	N52E	54NW												
1092	B	CALC SH.	N49E	49SE												
1093	M	CALC SH.	N41E	88NW												
1094	B	CALC SH.	N21E	68SE												
1095	B	CALC SH.	N0E	74E												
1096	B	CALC SH.	N64E	76SE												
1097	B	SI SH.	N39E	67SE												
1098	B	CALC SH.	N14E	90SE												
1099	B	CALC SH.	N70E	90SE												
1100	B	CALC SH.	N30E	39SE												
1101	B	CALC SH.	N21E	90SE												
1102	B	CALC SH.	N82E	19SE												
1103	B	CALC SH.	N31E	81SE			N21E	90SE								
1104	B	CALC SH.	N34E	84SE												
1105	B	CALC SH.	N16E	85NW												
1106	B	CALC SH.	N33E	85SE												
1107	B	CALC SH.	N30E	23SE												
1108	B	CALC SH.	N55E	54SE												
1109	B	CALC SH.	N47E	49NW												
1110	B	CALC SH.	N5E	19SE												
1111	B	SA SH.	N30E	27SE												
1112	B	THICK BED SH.	N41E	43SE	6SW	N72W	N59E	73NW	90	2						
1113	B	SA LS.	N60E	66NW												
1114	B	SA LS.	N68E	58NW												
1115	B	SA LS.	N65E	41NW												
1116	B	SA LS.	N69E	44NW												
1117	B	SA LS.	N80E	42SE												
1118	B	SA LS.	N70E	50NW												
1119	B	SA LS.	N70E	66NW												
1120	B	SA LS.	N63E	59NE												
1121	B	SA LS.	N61W	14NE												

Station	Quad	Lithology	BEDDING		Axial Surface		Cleavage		IL	Amp.	SLICKENSIDES		Joint		CROSS BED	
			Strike	Dip	DIP2	STRIKE	Strike	Dip2	Angle	(m)	Plunge3	Trend3	Strike 2	Dip3	Plunge4	Trend4
1122	B	SA LS.	N82E	29SE												
1123	B	SA LS.	N5E	14SE												
1124	B	SA LS.	N5E	29SE			N10E	78NW								
1125	B	SA LS.	N21E	24SE												
1126	B	SA LS.	N22W	9NE												
1127	B	SA LS.	N36E	39SE												
1128	B	SA LS.	N50E	31SE												
1129	M	SA LS.	N49E	24SE												
1130	B	SA LS.	N72E	27NW												
1131	B	SA LS.	N71E	15NW			N5E	90SE								
1132	B	SA LS.	N70E	20NW												
1133	B	SA LS.	N70W	21NW												
1134	B	SA LS.	N85E	11NW												
1135	B	SA LS.	N48E	79SE												
1136	B	CALC SH.	N64E	90SE												
1137	B	SA LS.	N42E	90SE												
1138	B	SA LS. & SH.	N50E	68SE												
1139	B	SA LS.	N70E	52SE												
1140	B	SA LS.	N10E	41SE												
1141	B	SA LS.	N49E	79NW												
1142	B	CALC SH.	N5E	52SE												
1143	B	CALC SH.	N20E	62SE												
1144	B	SA LS.	N40E	32SE			N34E	65NW								
1145	B	SA LS.	N40E	70SE	8NE	N62E										
1146	B	SA LS.	N70E	72NW												
1147	B	THIN BED LS.	N68E	66SE												
1148	B	THICK BED SH.	N51E	32SE												
1149	B	THICK BED SH.	N64E	82SE												
1150	B	SA SH.	N44E	73SE												
1151	B	SA SH.	N89E	63NW												
1152	B	FISSILE SH.	N62E	20NW			N51E	77SE								
1153	B	CALC SH.	N70E	32NW			N81E	35SE								
1154	B	SA LS.	N58E	49NW												
1155	B	SA LS.	N68E	15NW												
1156	B	SA LS.	N67E	37SE												
1157	B	SA LS.	N57E	84SE												
1158	B	SA LS.	N69E	90SE											22SE	N55E
1159	B	SA LS.	N70E	57NW												
1160	B	SA LS.	N51E	73NW												
1161	B	SA LS.	N54E	81SE												

Station	Quad	Lithology	BEDDING		Axial Surface		Cleavage		IL	Amp.	SLICKENSIDES		Joint		CROSS BED	
			Strike	Dip	DIP2	STRIKE	Strike	Dip2	Angle	(m)	Plunge3	Trend3	Strike 2	Dip3	Plunge4	Trend4
1162	B	SA LS.			11NE	N60E										
1163	B	SA LS.	N70E	56NW	0NE	N64E			40	1						
1164	M	SA LS.	N52E	38NW												
1165	B	SA LS.	N56E	37NW												
1166	M	CALC SH.	N74E	44NW			N80E	68SE								
1167	B	SI SH.	N80E	9SE												
1168	B	SI SH.	N66E	36NW												
1169	B	SA SH.	N4W	21NE												
1170	B	SA SH.	N54E	48NW												
1171	B	SA SH.	N82W	46SE												
1172	B	CALC SH.	N30E	68NW												
1173	B	SA LS.	N72E	74NW												
1174	B	SA LS.	N79E	70NW												
1175	B	SA LS.	N60E	39NW												
1176	B	SA LS.	N76E	25NW												
1177	B	SA LS.	N74W	14NE	8NE	N41E	N90E	79NW	65	5						
1178	M	SA LS.	N28E	85NW	23N	N30E	N87E	54NW	70	2						
1179	SP	SA LS.	N87E	90SE												
1180	SP	SA LS.	N54E	74SE												
1181	SP	SA LS.	N52E	88NW												
1182	SP	OB/OMB CONTACT	N5E	38SE			N50E	80NW			22SE	N51W				
1183	M	GREEN FOSSIL SH. & LS.	N9E	37SE												
1184	SP	GREEN FOSSIL SH. & LS.	N25E	51SE												
1185	SP	QZ. SS	N39E	7SE			N40E	83SE			83SE	N40W			9SE	N72E
1186	M	RED MUDSTONE/QZ SS	N62E	51NW												
1187	SP	QZ. SS	N75E	68SE												
1188	M	SA LS. & SH.	N54E	66SE												
1189	SP	SA LS.	N68E	40SE												
1190	M	SA LS.	N40E	21NE												
1191	M	SA LS.	N69E	86NW											76NW	N78E
1192	M	RED MUDSTONE/QZ SS	N0E	90SE												
1193	M	SI SH.	N60E	47SE												
1194	M	SI SH.	N57E	52SE												
1195	BU	SA LS.	N49E	81NW												
1196	BU	SA LS.	N49E	80SE												
1197	BU	SA LS.	N4W	76SE			N50E	8NW								
1198	BU	SA LS. & SH.	N2W	81NE												
1199	BU	SA LS.	N68E	70NW												
1200	BU	SA LS.	N15E	35NW												
1201	BU	SA LS. & SH.	N70E	8SE												

Station	Quad	Lithology	BEDDING		Axial Surface		Cleavage		IL	Amp.	SLICKENSIDES		Joint		CROSS BED	
			Strike	Dip	DIP2	STRIKE	Strike	Dip2	Angle	(m)	Plunge3	Trend3	Strike 2	Dip3	Plunge4	Trend4
1202	BU	SA LS.	N49E	42SE												
1203	BU	SA LS.	N20E	82NW												
1204	M	SA LS.	N0E	64W											4NE	N74E
1205	BU	SA LS.	N20E	71W												
1206	BU	SA LS.	N90E	78N												
1207	SP	SA LS. & SH.	N80E	12NW												
1208	SP	SA LS.	N59E	48SE												
1209	SP	FISSILE SH.	N63E	69SE												
1210	SP	SI LS.	N18E	18SE												
1211	SP	THICK BED SH.	N6E	64SE												
1212	SP	SI LS.	N54E	42SE												
1213	SP	SA LS.	N44E	59SE												
1214	SP	SI LS.	N60E	60SE												
1215	SP	SI LS.	N56E	57SE												
1216	SP	SA LS.	N49E	78SE												
1217	SP	SA LS.	N60E	54SE												
1218	SP	CALC SH.	N30W	66NW												
1219	SP	GREEN FOSSIL SH. & LS.	N68E	48NW												
1220	SP	GREEN FOSSIL SH. & LS.	N55E	54NW												
1221	SP	GREEN SH.	N90E	50NW												
1222	SP	GREEN FOSSIL SH. & LS.	N80E	20NW												
1223	B	CALC SH.	N11E	86NW												
1224	B	GR - BL SH.	N31E	88SE												
1225	B	SA LS. & SH.	N39E	62SE												
1226	B	GR - BL SH.	N56E	13NW			N10E	90SE								
1227	B	SA LS. & SH.	N53E	52NW			N12E	19SE	110	1						
1228	B	CALC SH.	N46E	70SE												
1229	B	CALC SH.	N59E	89SE												
1230	B	SA LS. & SH.	N49E	19NW												
1231	B	SI LS.	N61E	72NW												
1232	B	SI LS.	N45E	30NW	16N	N12E	N5E	79SE	20	2						
1233	B	SA LS. & SH.	N46E	21NW												
1234	B	SI LS.	N79E	31SE												
1235	B	SA LS.	N40E	22W												
1236	B	SA LS.			10N	N49E			150	10						
1237	B	SA LS.	N50E	61SE												
1238	B	SA LS.	N11E	40SE												
1239	B	SA LS.	N61E	65NW												
1240	B	SA LS.	N40E	30NW												
1241	B	SI LS.	N60E	52NW												

Station	Quad	Lithology	BEDDING		Axial Surface		Cleavage		IL	Amp.	SLICKENSIDES		Joint		CROSS BED	
			Strike	Dip	DIP2	STRIKE	Strike	Dip2	Angle	(m)	Plunge3	Trend3	Strike 2	Dip3	Plunge4	Trend4
1242	B	SA LS.	N20E	70SE												
1243	B	SA LS.	N56E	48SE												
1244	B	SA LS.	N28E	51SE												
1245	B	SI LS.	N58E	19SE												
1246	B	SA LS. & SH.	N75E	7SE												
1247	B	CALC SH.	N81E	72SE												
1248	B	SA LS.	N36E	80NW												
1249	B	CALC SH.	N29E	90SE												
1250	B	SA LS.	N33E	50SE												
1251	B	SA LS.	N50E	90SE												
1252	B	CALC SH.	N72E	45SE												
1253	B	SI LS.	N41E	39SE												
1254	B	CALC SH.	N65E	48SE												
1255	B	CALC SH.	N64E	30NW												
1256	B	SA LS.	N58E	31NW												
1257	B	SA LS.	N72E	90SE												
1258	B	FISSILE SH.	N25E	8SE	6SE	N70E	N20E	78SE	100	0.5						
1259	B	SA LS. & SH.	N51E	74NW												
1260	B	SA LS. & SH.	N47E	79NW												
1261	B	SA LS. & SH.	N54E	71NW												
1262	B	SA LS.	N72E	59SE											2NW	N53E
1263	B	SA LS. & SH.	N63E	62SE												
1264	B	SA LS. & SH.	N50E	41NW												
1265	B	SA LS. & SH.	N90E	62S												
1266	B	SA LS. & SH.	N65E	43NW												
1267	B	CALC SH.	N90E	68N												
1268	B	CALC SH.	N65E	58N												
1269	B	SI LS.	N74E	90SE												
1270	B	SI LS.	N72E	72NW												
1271	B	SA LS.	N60E	51SE												
1272	B	SA LS. & SH.	N80E	50NW												
1273	B	RED MUDSTONE/QZ SS	N59E	24NW			N5W	74SW								
1274	B	RED MUDSTONE/QZ SS	N54E	30SE												
1275	B	RED MUDSTONE/QZ SS	N57E	32SE												
1276	B	SA LS. & SH.	N51E	56SE												
1277	B	SA LS. & SH.	N20E	20SE	6SE	N20E			135	20						
1278	B	SA LS. & SH.	N31E	34NW			N50E	79SE								
1279	B	SA LS.	N45E	46SE												
1280	B	SA LS.	N46E	38NW												
1281	B	SA LS.	N50E	79SE												

Station	Quad	Lithology	BEDDING		Axial Surface		Cleavage		IL	Amp.	SLICKENSIDES		Joint		CROSS BED	
			Strike	Dip	DIP2	STRIKE	Strike	Dip2	Angle	(m)	Plunge3	Trend3	Strike 2	Dip3	Plunge4	Trend4
1282	B	CALC SH.	N59E	59SE												
1283	B	SA LS.	N48E	38SE												
1284	B	SI LS.	N49E	4NW												
1285	B	SA LS.	N52E	7NW												
1286	M	SA LS.	N46E	16SE												
1287	M	SA LS.	N42E	19SE												
1288	M	SA LS.	N63E	31SE												
1289	M	SA LS.	N58E	27NW												
1290	B	SI LS.	N61E	86SE												
1291	B	SA LS.	N50E	60SE												
1292	B	SA LS.	N60E	85SE												
1293	B	QZ. SS	N32E	59NW												
1294	B	SA LS. & SH.	N61E	38NW												
1295	B	SA LS.	N46E	65SE												
1296	B	SA LS. & SH.	N39E	59NW												
1297	B	SA LS. & SH.	N33E	70SE												
1298	B	SA LS. & SH.	N41E	90SE												
1299	B	SA LS.	N52E	90SE												
1300	B	SA LS. & SH.	N21E	72NW												
1301	SP	CALC SH.	N51E	54NW												
1302	SP	CALC SH.	N23E	33SE												
1303	SP	SI LS.	N38E	75SE												
1304	SP	SA SH.	N61E	50SE												
1305	SP	SA LS.	N31E	48NW												
1306	SP	SI LS.	N70E	79SE												
1307	SP	SI LS.	N50E	74NW												
1308	SP	QZ. SS	N60E	17NW												
1309	SP	SA LS.	N41E	73SE												
1310	M	SA LS.	N45E	22NW											5NW	N28E
1311	SP	SA LS.	N50E	90SE												
1312	SP	SA LS.	N69E	75NW												
1313	SP	SA LS. & SH.	N4W	53SE												
1314	SP	SA LS.	N50E	70SE												
1315	SP	SA LS.	N46E	60SE												
1316	SP	SA LS.	N51E	56SE												
1317	SP	SA LS.	N50E	71SE												
1318	M	SA LS.	N71E	65SE	14SE	N49E			70	10						
1319	SP	SA LS.	N62E	64SE												
1320	SP	SA LS.	N40E	75NW												
1321	SP	SI LS.	N69E	68SE												

Station	Quad	Lithology	BEDDING		Axial Surface		Cleavage		IL	Amp.	SLICKENSIDES		Joint		CROSS BED	
			Strike	Dip	DIP2	STRIKE	Strike	Dip2	Angle	(m)	Plunge3	Trend3	Strike 2	Dip3	Plunge4	Trend4
1322	SP	SI LS.	N80E	67SE												
1323	SP	SI LS.	N70E	61SE												
1324	SP	SI LS.	N61E	72NW												
1325	SP	SA LS.	N70E	90SE												
1326	SP	SA LS.	N64E	90SE												
1327	SP	SA LS.	N50E	80NW												
1328	M	QZ. SS	N59E	39NW												
1329	M	SA LS. & SH.	N36E	20SE												
1330	M	THICK BED SH.	N46E	26SE												
1331	M	SA LS. & SH.	N40E	10SE												
1332	M	SA LS.	N60E	84NW												
1333	M	SA LS.	N56E	82SE												
1334	M	SA LS. & SH.	N50E	9NW												
1335	M	SA LS.	N73E	72SE												
1336	M	RED MUDSTONE/QZ SS	N51E	81SE												
1337	M	SA LS.	N40E	10NW												
1338	M	SA LS. & SH.	N70E	17SE												
1339	M	SA LS. & SH.	N42E	76NW												
1340	BU	SA LS. & SH.	N19E	71SE												
1341	BU	SA LS. & SH.	N5E	60SE												
1342	BU	CALC SH.	N35E	62SE												
1343	BU	CALC SH.	N60E	80NW												
1344	BU	SA LS. & SH.	N53E	78SE												
1345	BU	CALC SH.	N33E	67SE												
1346	BU	SA LS.	N41E	60SE												
1347	BU	SA LS.	N63E	53NW												
1348	BU	SA LS.	N48E	49SE												
1349	BU	SA LS.	N80E	70NW												
1350	BU	THICK BED SH.	N48E	49SE	7NW	N70E										
1351	BU	CALC SH.	N53E	78SE												
1352	BU	SA LS.	N45E	90SE												
1353	BU	SA LS.	N60E	88SE												
1354	BU	SA SH.	N82E	84NW												
1355	BU	SA SH.	N88W	66NW												
1356	BU	SA LS.	N82E	20NW												
1357	BU	CALC SH.	N61E	81NW												
1358	BU	SA LS.	N52E	70NW												
1359	BU	SA LS.	N54E	61NW											11NW	N50E
1360	BU	SA LS.	N50E	76NW												
1361	BU	SA LS.	N59E	53NW												

Station	Quad	Lithology	BEDDING		Axial Surface		Cleavage		IL	Amp.	SLICKENSIDES		Joint		CROSS BED	
			Strike	Dip	DIP2	STRIKE	Strike	Dip2	Angle	(m)	Plunge3	Trend3	Strike 2	Dip3	Plunge4	Trend4
1362	BU	CALC SILTSTONE	N68E	30NW			N14E	87SE								
1363	BU	SA LS.	N60E	51NW												
1364	BU	SA LS.	N60E	49NW												
1365	BU	SA LS.	N29E	18NW												
1366	BU	RED MUDSTONE/QZ SS	N46E	14NW			N51E	73SE								
1367	BU	RED MUDSTONE/QZ SS	N50E	6NW												
1368	BU	QZ. SS	N46E	30NW												
1369	BU	RED MUDSTONE/QZ SS	N60E	40NW												
1370	BU	QZ. SS	N71E	82SE												
1371	BU	QZ. SS	N50E	26SE												
1372	BU	GREEN SH	N40E	45SE												
1373	BU	GRN FOS. SH. & LS.	N64E	44SE												
1374	BU	GRN FOS. SH. & LS.	N70E	75NW												
1375	BU	GRN FOS. SH. & LS.	N48E	85NW												
1376	M	SA LS.	N41E	90SE												
1377	SP	GRN FOS. SH. & LS.	N32E	84SE												
1378	BU	GRN FOS. SH. & LS.	N41E	50NW												
1379	SP	QZ. SS	N46E	39SE												
1380	SP	RED MUDSTONE/QZ SS	N50E	69NW												
1381	SP	QZ. SS	N59E	38NW			N39E	50SE								
1382	B	SA SH.	N24E	76SE												
1383	B	SA LS. & SH.	N39E	37SE												
1384	B	SA LS. & SH.	N42E	35SE												
1385	B	SA LS. & SH.	N46E	36NW												
1386	B	CALC SH.	N31E	13SE												
1387	B	CALC SH.	N30E	21NW												
1388	B	CALC SH.	N51E	16NW												
1389	B	CALC SH.	N41E	46SE			N40E	76SE								
1390	B	SA LS. & SH.	N80E	71NW	6SE	N77E			85	2						
1391	B	SA LS. & SH.	N79E	79SE												
1392	B	SA LS. & SH.			36SE	N80E										
1393	B	CALC SH.	N54E	74NW												
1394	B	FISSILE SH.	N27E	43SE												
1395	B	SA LS.	N73E	34NW												
1396	B	SA LS.	N74E	81SE												
1397	B	CALC SH.	N41E	32NW												
1398	B	GR - BL SH.	N70E	58SE												
1399	B	GR - BL SH.	N40E	51SE												
1400	B	GR - BL SH.	N41E	62SE												
1401	B	GR - BL SH.	N57E	60SE												

Station	Quad	Lithology	BEDDING		Axial Surface		Cleavage		IL	Amp.	SLICKENSIDES		Joint		CROSS BED	
			Strike	Dip	DIP2	STRIKE	Strike	Dip2	Angle	(m)	Plunge3	Trend3	Strike 2	Dip3	Plunge4	Trend4
1402	B	SA LS.	N40E	32SE												
1403	B	SA LS.	N48E	28NW												
1404	B	CALC SH.	nN57E	62NW												
1405	B	SA LS.	N69E	22NW												
1406	B	SA LS. & SH.	N50E	90SE												
1407	B	SA LS.	N71E	42NW												
1408	B	GR - BL SH.	N69E	39NW			N50E	56SE								
1409	B	SA LS. & SH.	N21E	53SE												
1410	B	CHRT. LS.	N50E	72SE	3SE	N50E			35	2						
1411	B	SA LS.	N50E	83SE												
1412	B	SA LS.	N85E	35SE												
1413	B	SA LS.	N60E	64SE												
1414	B	SA LS.	N61E	77SE												
1415	B	SA LS. & SH.	N33E	42SE												
1416	B	SA LS. & SH.	N31E	62SE												
1417	B	SA LS.	N61E	51SE												
1418	B	SA LS.	N36E	84NW												
1419	B	SA LS.	N56E	61NW												
1420	B	SA LS.	N51E	82NW												
1421	B	SA LS.	N30E	34SE												
1422	B	SA LS.	N63E	70NW												
1423	B	SA LS.	N26E	73SE												
1424	B	CALC SH.	N71E	76SE												
1425	B	CALC SH.	N5W	39SE												
1426	B	CALC SH.	N21E	54SE												
1427	B	CALC SH.	N80E	60SE												
1428	B	FISSILE SH.	N84E	39SE												
1429	B	FISSILE SH.	N90E	60SE												
1430	B	CALC SH.	N51E	64SE												
1431	B	SA LS.	N80E	61SE												
1432	B	SA LS.	N70E	72NW												
1433	B	CALC SH.	N71E	75SE			N40E	35SE								
1434	B	CALC SH.	N61E	66SE												
1435	B	SA LS.	N69E	60SE												
1436	B	SA LS. & SH.	N64E	51NW												
1437	B	GR - BL SH.	N41W	24SE												
1438	B	CALC SH.	N33E	74SE												
1439	B	CALC SH.	N59E	69NW												
1440	M	GR - BL SH.	N61E	74SE												
1441	M	CALC SH.	N31E	72NW												

Station	Quad	Lithology	BEDDING		Axial Surface		Cleavage		IL	Amp.	SLICKENSIDES		Joint		CROSS BED	
			Strike	Dip	DIP2	STRIKE	Strike	Dip2	Angle	(m)	Plunge3	Trend3	Strike 2	Dip3	Plunge4	Trend4
1442	M	CALC SH.	N65E	61NW												
1443	M	SH & CALC. CHIPS	N87E	64SE												
1444	M	FISSILE SH.	N69E	54NW												
1445	M	SA LS.	N70E	90SE												
1446	M	SA LS. & SH.	N51E	81NW												
1447	M	SA LS. & SH.	N55E	85SE			N55E	85SE								
1448	M	SA LS. & SH.	N46E	69NW			N25E	74SE								
1449	M	SA LS. & SH.	N52E	84NW												
1450	M	FISSILE SH.	N15E	40SE			N74E	40NW								
1451	M	FISSILE SH.	N51E	61NW												
1452	M	SA LS.	N46E	75NW												
1453	M	SA LS.	N70E	69NW												
1454	M	SA LS.	N40E	81NW												
1455	M	SA LS.	N70E	66NW												
1456	M	SA LS.	N12E	79SE												
1457	M	SA LS.	N40E	31SE			N80E	27NW								
1458	M	CALC SILTSTONE	N24E	39SE												
1459	B	CALC SH.	N40E	42E												
1460	B	CALC SH.	N39E	19SE												
1461	B	CALC SH.	N50E	55NW	5NW	N41E	N32E	83SE	45	0.5						
1462	B	CALC SH.	N48E	50SE												
1463	B	CALC SH.	N32E	71NW												
1464	B	CALC SH.	N50E	60SE												
1465	M	CALC SH.	N58E	60SE	24SE	N20E	N20E	57NW	25	1						
1466	M	CALC SH.	N41E	42SE												
1467	B	CALC SH.	N39E	70SE												
1468	B	CALC SH.	N39E	70SE			N40E	87NW								
1469	B	SA LS.	N90E	10S			N11E	22SE								
1470	B	CALC SH.	N5W	25SW												
1471	B	SA LS.	N50E	41SE												
1472	B	SA LS.	N51E	30NW												
1473	B	SA LS.	N41E	71SE												
1474	B	SA LS.	N39E	64SE												
1475	B	SA LS.	N41E	87NW												
1476	B	SA LS.	N51E	50SE												
1477	B	SA LS.	N60E	65NW												
1478	B	SA LS.	N50E	90NW												
1479	B	SA LS.	N69E	85NW												
1480	B	SA LS. & SH.	N60E	42SE												
1481	BU	NODULAR LS OL	N5E	31SE												

Station	Quad	Lithology	BEDDING		Axial Surface		Cleavage		IL	Amp.	SLICKENSIDES		Joint		CROSS BED	
			Strike	Dip	DIP2	STRIKE	Strike	Dip2	Angle	(m)	Plunge3	Trend3	Strike 2	Dip3	Plunge4	Trend4
1482	BU	GR - BL SH.	N66E	86SE												
1483	BU	SA LS. & SH.	N65E	85SE												
1484	BU	SA LS.	N30E	49SE												
1485	BU	SA LS. & SH.	N30E	49SE												
1486	BU	SA LS. & SH.	N36E	71SE												
1487	M	SA LS.	N30E	61SE												
1488	BU	SA LS.	N58E	49SE												
1489	BU	CALC SH.	N69E	39SE												
1490	BU	SA LS.	N41E	51SE												
1491	BU	WHITE LS DOL.	N60E	53SE												
1492	BU	NODULAR LS OL	N60E	40SE												
1493	BU	CALC SH.	N58E	52SE												
1494	BU	SA SH.	N46E	74SE												
1495	BU	SA LS. & SH.	N90E	74SE												
1496	BU	SA LS. & SH.	N50E	3SE												
1497	BU	SA LS.	N40E	29SE												
1498	BU	SA LS.	N31E	36SE												
1499	BU	SA LS.	N45E	44SE												
1500	BU	SA LS.	N79E	38SE												
1501	BU	THICK BED SH.	N0E	0SE												
1502	BU	THICK BED SH.	N35E	19SE												
1503	BU	THICK BED SH.	N2E	56SE												
1504	BU	CALC SILTSTONE	N61E	70SE			N57E	21NW								
1505	BU	SA LS.	N0E	0SE												
1506	BU	SA SH.	N39E	25SE												
1507	B	QZ. SS	N68E	11SE											6NW	N42E
1508	B	QZ. SS	N63E	69SE												
1509	B	SA LS.	N0E	0SE												
1510	B	QZ. SS	N78W	41NE												
1511	M	SA LS.	N0E	0SE												
1512	SP	QZ. SS	N41E	51SE												
1513	SP	THICK BED SH.	N42E	37SE												
1514	SP	QZ. SS	N65E	66SE												
1515	SP	CALC SH.	N67E	41SE												
1516	SP	CALC SH.	N65E	51SE												
1517	SP	SA SH.	N60W	68NE												
1518	SP	SA LS.	N60E	14SE												
1519	SP	SA LS.	N61E	48NW												
1520	SP	SA SH.	N58E	24SE												
1521	SP	SA LS. & SH.	N71E	65SE												

Station	Quad	Lithology	BEDDING		Axial Surface		Cleavage		IL	Amp.	SLICKENSIDES		Joint		CROSS BED	
			Strike	Dip	DIP2	STRIKE	Strike	Dip2	Angle	(m)	Plunge3	Trend3	Strike 2	Dip3	Plunge4	Trend4
1522	SP	SA LS. & SH.	N64E	24SE												
1523	SP	SA LS. & SH.	N57E	84SE												
1524	SP	SA LS. & SH.	N67E	71SE												
1525	SP	SA LS.	N62E	68SE												
1526	SP	SA LS. & SH.	N67E	79SE												
1527	M	SA LS. & SH.	N51E	36SE												
1528	SP	CALC SH.	N72E	29SE												
1529	SP	CALC SH.	N61E	70NW												
1530	SP	CALC MUDSTONE	N41E	57SE												
1531	SP	SI LS.	N79E	78NW												
1532	SP	SI LS.	N79E	68SE												
1533	SP	SA LS. & SH.	N81E	46SE												
1534	SP	SI LS.	N65E	43SE												
1535	SP	SA LS. & SH.	N61E	66SE												
1536	SP	SA LS.	N40E	13SE												
1537	SP	SA LS.	N43E	87NW												
1538	SP	SA LS.	N50E	30SE												
1539	SP	SI LS.	N33E	82NW												
1540	SP	SA LS.	N48E	51SE												
1541	SP	FOSSILIFEROUS LS.	N45E	76NW												
1542	SP	FOSSILIFEROUS LS.	N47E	90SE												
1543	SP	SA LS.	N45E	51SE												
1544	SP	SA LS. & SH.	N53E	49SE												
1545	SP	SA LS.	N64E	54NW												
1546	SP	SA LS.	N51E	41SE												
1547	SP	SA SH.	N50E	90SE												
1548	SP	THICK BED SH.	N60E	48SE												
1549	SP	SI LS.	N69E	85NW												
1550	SP	SA LS.	N42E	8SE	8NE	N39E			150	2						
1551	SP	SI LS.	N59E	49NE												
1552	SP	SA LS.	N49E	76SE												
1553	SP	SI LS.	N49E	41SE												
1554	SP	SA LS.	N59E	60SE												
1555	SP	SA LS.	N65E	55SE												
1556	SP	SI LS.	N50E	24SE												
1557	SP	SA LS.	N64E	64NW												
1558	SP	SA LS.	N59E	65SE												
1559	M	DARK LS.	N48E	62SE												
1560	B	GR-BL SH	N25E	79NW			N46E	28SE					N73W	69NE		
1561	B	GR-BL SH	N35E	71NW												

Station	Quad	Lithology	BEDDING		Axial Surface		Cleavage		IL	Amp.	SLICKENSIDES		Joint		CROSS BED	
			Strike	Dip	DIP2	STRIKE	Strike	Dip2	Angle	(m)	Plunge3	Trend3	Strike 2	Dip3	Plunge4	Trend4
1562	B	DOLOMITE	N9E	74NW												
1563	B	THICK BED SH.	N14E	80SE												
1564	B	FISSILE SH.	N31E	77SE												
1565	B	FISSILE SH.	N31E	77SE												
1566	B	FISSILE SH.	N41E	49SE												
1567	M	WHITE LS DOL.	N45E	53SE												
1568	M	SI LS.	N21E	64SE												
1569	M	SI LS.	N23E	51SE												
1570	BU	WHITE LS DOL.	N21E	41SE												
1571	BU	SA LS. & SH.	N51E	51SE												
1572	BU	FOSSILIFEROUS LS.	N48E	20SE												
1573	BU	FOSSILIFEROUS LS.	N69E	49SE			N56E	72NW					N80W	80SE		
1574	SP	SA LS. & SH.	N84W	34SW												
1575	SP	THIN BED LS & SH	N87E	49SE												
1576	SP	SI LS.	N68E	34SE												
1577	SP	SI LS.	N80W	27SE												
1578	SP	SA LS. & SH.	N50E	34SE												
1579	SP	SA LS. & SH.	N66E	36SE												
1580	SP	GREEN SH	N54E	56NW												
1581	SP	SA LS. & SH.	N89E	53SE												
1582	SP	SA LS.	N67E	59SE												
1583	SP	SA LS. & SH.	N71E	62SE												
1584	SP	SA LS. & SH.	N61E	70SE												
1585	SP	SA LS.	N61E	84NW												
1586	SP	SI LS.	N89W	68SE												
1587	SP	SI LS.	N33E	79NW												
1588	SP	SA LS. & SH.	N52E	39SE												
1589	SP	SI LS.	N71E	74SE												
1590	SP	SA LS. & SH.	N55E	46SE												
1591	SP	SA LS. & SH.	N89W	53SE												
1592	SP	SA LS.	N61E	36SE												
1593	SP	SA LS. & SH.	N49E	45SE												
1594	SP	SA LS.	N41E	31SE												
1595	SP	SA LS.	N18E	44SE												
1596	SP	SA LS.	N27E	17SE			N34E	78NW								
1597	SP	CALC SH.	N51E	56SE			N53E	70NW								
1598	SP	THICK BED SH.	N68E	48SE												
1599	SP	SI LS.	N51E	84NW												
1600	SP	THICK BED SH.	N54E	74SE												
1601	SP	SA LS. & SH.	N57E	63SE												

Station	Quad	Lithology	BEDDING		Axial Surface		Cleavage		IL	Amp.	SLICKENSIDES		Joint		CROSS BED	
			Strike	Dip	DIP2	STRIKE	Strike	Dip2	Angle	(m)	Plunge3	Trend3	Strike 2	Dip3	Plunge4	Trend4
1602	SP	SA LS. & SH.	N86E	80SE												
1603	SP	SA LS. & SH.	N50E	49SE												
1604	SP	CALC SH.	N61E	41SE												
1605	SP	THICK BED SH.	N76E	53SE												
1606	SP	CALC SH.	N61E	51SE												
1607	SP	SA LS. & SH.	N42E	60SE												
1608	SP	SA LS. & SH.	N53E	39SE												
1609	SP	SA LS.	N60E	72SE												
1610	SP	THICK BED SH.	N84E	43SE												
1611	SP	THIN BED LS & SH	N86E	42SE												
1612	SP	CALC SH. & bl ls.	N54E	44SE												
1613	SP	CLAYEY SILTST.	N71W	30SE												
1614	SP	CALC SH.	N51E	40SE												
1615	SP	CALC SH.	N60E	42SE												
1616	SP	CALC SH.	N58E	48SE												
1617	SP	CALC SH.	N71E	38SE												
1618	B	SA LS. & SH.	N59E	79SE	10SE	N36E	N52E	10NW			10SE	N50E			9SE	N50E
1619	B	QZ. SS	N48E	11NW												
1620	B	QZ. SS	N78E	29NW												
1621	SP	QZ. SS	N30E	37NW												
1622	SP	QZ. SS	N62E	28NW												
1623	SP	QZ. SS	N21E	21SE												
1624	SP	RED SS	N31E	36NW												
1625	SP	SA LS.	N51E	32SE												
1626	SP	SA LS. & SH.	N60E	16NW												
1627	SP	CALC SH.	N0E	0SE												
1628	B	SA LS. & SH.	N31E	12SE												
1629	B	RED SS	N49E	38SE												
1630	SP	SA LS. & SH.	N65E	80NW	19SE	N53E	N38E	69SE	30							
1631	SP	SA LS.	N52E	71SE												
1632	SP	SA LS.	N36E	75SE												
1633	SP	SA LS.	N50E	51SE			N42E	63NW					N48W	78SW		
1634	SP	SA LS. & SH.	N73E	28SE			N46E	56NW								
1635	SP	SA LS.	N40E	46NW	8SW	N40E			60	2						
1636	SP	SA LS.	N56E	69SE												
1637	SP	SA LS.	N51E	71SE												
1638	SP	SA LS.	N60E	70NW												
1639	SP	QZ. SS	N21E	56SE												
1640	SP	SA LS. & SH.	N61E	53SE												
1641	SP	OMB FOSSIL LS	N49E	71NW												

Station	Quad	Lithology	BEDDING		Axial Surface		Cleavage		IL	Amp.	SLICKENSIDES		Joint		CROSS BED	
			Strike	Dip	DIP2	STRIKE	Strike	Dip2	Angle	(m)	Plunge3	Trend3	Strike 2	Dip3	Plunge4	Trend4
1642	SP	OMB FOSSIL LS	N38E	79SE												
1643	SP	OMB FOSSIL LS	N56E	59SE												
1644	SP	OMB FOSSIL LS	N41E	51SE												
1645	SP	RED MUDSTONE	N45E	37SE			N67E	58NW								
1646	SP	RED SS	N52E	47SE												
1647	SP	RED MUDSTONE/QZ SS	N85E	25SE												
1648	SP	SA LS.	N69E	85SE												
1649	SP	SA LS.	N61E	37SE												
1650	SP	SA LS.	N64E	55SE												
1651	SP	SA LS.	N61E	21NW												
1652	SP	SA LS.	N49E	83SE			N28E	56SE					N35W	5SE		
1653	SP	SA LS. & SH.	N37E	30SE												
1654	SP	QZ. SS	N77E	77NW												
1655	M	CALC SH.	N38E	79SE												
1656	B	SA LS. & SH.	N74E	17SE												
1657	M	SA SH.	N15E	48SE												
1658	M	SA SH.	N0E	0SE												
1659	SP	SA LS.	N69E	54NW												
1660	SP	SA LS. & SH.	N61E	79NW			N41E	22SE								
1661	SP	SA LS. & SH.	N63E	64SE												
1662	SP	SA LS.	N61E	41SE			N71E	47NW								
1663	SP	SA LS.	N59E	45NW												
1664	SP	SA LS.	N40E	58SE												
1665	SP	SA LS.	N39E	36SE												
1666	SP	SA LS.	N0E	0SE												
1667	SP	SA LS.	N54E	72NW												
1668	SP	SA LS.	N56E	60NW												
1669	SP	SA LS.	N55E	49SE												
1670	SP	SA LS.	N69E	42SE												
1671	SP	SA LS. & SH.	N81E	41NW												
1672	SP	SA LS. & SH.	N60E	49SE												
1673	SP	SA LS.	N79E	52SE												
1674	SP	SA LS.	N5W	9SE												
1675	SP	SA LS.	N80W	49SE												
1676	SP	SA LS.	N29E	12NW												
1677	SP	SA LS.	N0E	0SE												
1678	SP	SA LS.	N70E	40SE												
1679	SP	SA LS.	N51E	50SE												
1680	SP	SA LS.	N70E	35SE												
1681	SP	SA LS.	N59E	39NW												

Station	Quad	Lithology	BEDDING		Axial Surface		Cleavage		IL	Amp.	SLICKENSIDES		Joint		CROSS BED	
			Strike	Dip	DIP2	STRIKE	Strike	Dip2	Angle	(m)	Plunge3	Trend3	Strike 2	Dip3	Plunge4	Trend4
1682	SP	RED MUDSTONE/QZ SS	N72E	41SE												
1683	SP	SA LS.	N74E	52SE												
1684	SP	SA LS.	N81E	45NW												
1685	SP	SA LS. & SH.	N51E	66SE												
1686	SP	SA LS. & SH.	N44E	51SE	18SW	N47E	N46E	78NW					N15E	68NW		
1687	SP	SA LS.	N71E	46NW												
1688	SP	SA LS.	N60E	71SE												
1689	SP	SA LS.	N58E	82NW												
1690	SP	SA LS. & SH.	N51E	58SE												
1691	SP	SA LS. & SH.	N65E	72SE												
1692	SP	SA LS.	N51E	60SE												
1693	SP	SA LS.	N53E	52NW												
1694	M	SA LS.	N39E	49SE												
1695	SP	SI LS.	N51E	32SE												
1696	SP	SA LS. & SH.	N51E	64SE												
1697	SP	SA LS. & SH.	N88W	12SE												
1698	SP	SA LS.	N79E	24NW												
1699	SP	DOLOMITE	N43E	29SE												
1700	SP	DOLOMITE	N52E	31SE												
1701	SP	DOLOMITE	N48E	31SE												
1702	SP	NODULAR LS OL	N54E	90SE												
1703	SP	NODULAR LS OL	N58E	68NW												
1704	SP	NODULAR LS OL	N52E	48SE												
1705	M	NOD. LS/DOLOMITE	N33E	17SE												
1706	SP	NODULAR LS /WHITE LS	N51E	37SE												
1707	SP	DOLOMITE	N47E	31SE	16NW	N48E	N41E	78SE	60	1						
1708	SP	CALC SH.	N71E	46SE			N65E	71NW								
1709	SP	QZ. SS	N21E	31NW												
1710	SP	RED MUDSTONE/QZ SS	N49E	21NW												
1711	SP	QZ. SS	N45E	86NW												
1712	SP	RED MUDSTONE/QZ SS	N76E	31NW			N32E	86NW					N41W	86NE		
1713	M	RED MUDSTONE/QZ SS	N54E	41SE			N61E	72NW					N61E	41NW		
1714	M	FOSSILIFEROUS LS.	N39E	24SE			N51E	66NW								
	M															
	M															
	M															
	M															
	M															
	M															
	M															
	M															

VITA

John Garrett Bultman was born in Augusta, GA on November 21, 1977 to Gerald and Judy Bultman. At two years of age he and his family moved to Lilburn, Georgia (now surburban Atlanta). At the age of five John was hit by a car traveling 80 km.p.h on a highway and was thrown in the air over three lanes and landed near a guard rail. He broke one leg, one collarbone, a couple of ribs, and had fifty-six stitches in his head and spent a couple of weeks in the hospital. At the seven years of age he and his family moved to Greeneville, TN (ironically very near this study area) and remained there untill he was fourteen. He and his family then moved to Gulfport, MS where he lived till he was eighteen. John is very interested in music and moved to Hattiesburg, MS to attend the University of Southern Mississippi. He was music major for 3 years, sang in Carnegie Hall, Lincoln Center, Riverside Church, and toured with a rock band before abruptly changing his major to geology due to a very influential now deceased professor, Dr. Chris Cameron. He received a Bachelor of Science degree in Geology in 2001, and began work at Aquaterra Engineering in Jackson, MS. John entered the graduate program in geology at the University of Tennessee-Knoxville in January, 2003 and graduated with his Master of Science degree focused on Structural Geology and Tectonics in the fall of 2005.